1-1-2018

Biomarkers to Localize Seizure from Electrocorticography to Neurons Level

Bahareh Elahian

BIOMARKERS TO LOCALIZE SEIZURE FROM ELECTROCORTICOGRAPHY TO NEURONAL LEVEL

by

Bahareh Elahian

A Dissertation

Submitted in Partial Fulfillment of the

Requirements for the Degree of

Doctor of Philosophy

Major: Engineering

The University of Memphis

May 2018

To Mom and Dad for your true, unconditional and never-ending love and support.

Acknowledgements

I started my PhD in 2015 with a big passion to find a method to assist patients with *seizure and epilepsy*. Today, I feel I have come a long way since I started my journey three years ago, but I am surely nowhere near the end of it. In this journey there are many people who provided me their support each in their own way. To all of you, I am deeply thankful.

First, I want to thank my adviser, **Dr. Mohammed Yeasin—**a gifted scientist and leader—for his continuous support and invaluable mentoring. I have learned more than science and engineering from my advisor. He taught me how to encounter obstacles not only in research but also in real life. He was a nurturing advisor whom I consulted when I felt despair, and left his office with optimism and a smile. I am very grateful for having the chance to be his student. His special advice to me was, "To be successful, you have to be at the right time, at the right place, with the right information." I thank **Dr. Joon Kang** at Johns Hopkins Hospital who made it possible for me to work in such a great environment where I was surrounded by experts. I am very grateful for her guidance every step of the way. I am also grateful to work with **Dr. Shennan Weiss** in Thomas Jefferson Hospital as part of my internship. Dr Weiss taught me to hard work and assisted me to resolve the concepts of neuroscience as a goal of my PhD research. I will never forget those moments when he was reminding me: "Bahar, think like a neuroscientist!" I am thankful for his thoughtful feedback.

I thank my officemates at CVPIA for being such good friends and helping me whenever I needed it: Pouya Bashivan, Rakib Al-Fahad, Anam Iftekhar, Shajun Alam, Faruk Ahmed. I want to extend a special thanks to my friend in the Electrical and Computer Engineering Department, Hasti Shabani, who was like my sister. I could trust her in any aspect and share with her all my feelings. Ankita Mohapatra, who was also my roommate for one and half year. I will never forget those good memories we made together. Babak Noroozi, Saleha Khatun for making our department such a friendly and exciting place to work in. I of course

thank my parents who always provided me their support and encouragement. Hope to see them soon.

Abstract

Elahian, Bahareh. PhD. The University of Memphis. March, 2018. Biomarkers to localize seizure from electrocorticography to neurons level. Advisor: Mohammed Yeasin, PhD.

Epilepsy—a disorder that is far more common than is widely realized—results in high morbidity and even mortality. It is defined semiologically in part, but it is a disorder caused by the disturbed synchronization of natural brain oscillations. The current standard treatment is implanting intracranial electrodes that are continuously connected to an acquisition system while the patient waits in an Epilepsy Monitoring Unit (EMU) until the patient has a seizure. Given enough seizures, this information can be taken to the operating room. Then, the electrodes, which had shown pathologic activity, are marked and surgical resection of the determined pathologic areas follows. This entire process can take up to a month in any given patient and results in considerable patient and system costs. It is known that there are electrophysiologic markers that happen between seizures or interictally. However, the question of whether those markers can define the seizure onset zone (SOZ) adequately enough to perform resection has not been resolved completely yet. The purpose of this work is to explore those electrophysiologic biomarkers and define the methods to both detect them reliably and compare them to previously determined SOZ. First, high frequency oscillations (HFO)—a now heavily explored interictal electrophysiologic biomarker—are investigated via a pre-worked detector; its role in SOZ determination is considered in the context of both old (interictal epileptiform discharges) and new (phase-amplitude coupling) biomarkers. Further, work is explored for automating the localization process via a machine learning algorithm to automatically classify the SOZ and non-SOZ. We also compared the rate of HFO in/out of SOZ and the resection area in four different epochs: at night, awake time, preictal, and ictal. Seizures initiate when most or all neurons in epileptic regions start to fire synchronously. Evidence obtained from the entorhinal cortex (EC) in animal models of epileptiform synchronization show that low-voltage fast (LVF) onset seizures are initiated by synchronous

inhibitory events. We sought to establish whether the increased firing of inhibitory interneurons occurs at the onset of spontaneous LVF seizures in patients with mesial-temporal lobe epilepsy, and whether the increased firing of excitatory neurons follows this.

Table of Contents

List of Tables

List of Figures

Chapter 1

Introduction

A seizure is an excessive discharge of electrical activity within the brain that leads to a change in movement, sensation, experience, or consciousness. Seizures have various effects on the body depending on where in the brain they start and where they spread. Not all seizures are epileptic fits. Epilepsy is characterized by unprovoked seizures due to the engagement of the central nervous system. On the other hand, non-epileptic seizure disorders could be caused by several measurements: stroke, head injuries, brain infections, congenital birth effects, birth-related brain injuries, tumor and other space occupying lesions. Some epilepsy patients are drug-resistant; in this case, their physicians normally recommend that they go through surgery. During surgery, the part of the brain that shows seizure activity will be removed. Surgical resection of the seizure focus is an effective treatment for select patients with medically intractable focal epilepsy.

Success of the surgery depends on the precise localization and resection of the epileptogenic seizure onset zone. Accurate seizure onset localization is crucial for both the clinical management and for understanding the mechanism of epilepsy. Currently, the localization of the seizure onset relies heavily on visual analysis of scalp electroencephalo-graphic (EEG) or intracranial electrocorticographic (ECoG) recordings in low-frequency bands.

Surgical resection of the seizure focus is an effective treatment for patients with medically intractable focal epilepsy. The success of the surgery depends on the precise localization and complete resection of the epileptogenic seizure onset zone (SOZ). Accurate localization of the SOZ is crucial for both the clinical management and understanding of the mechanism of epilepsy. Currently, localization of the seizure onset relies on visual analysis of

scalp electroencephalographic (EEG) or intracranial electrocorticographic (ECoG) recordings in low-frequency bands.

Patients with focal lesions—identified by magnetic resonance imaging (MRI) of the brain—can often undergo surgery following favorable scalp EEG findings without intracranial EEG recordings (Spencer 2002). However, scalp EEG recordings may be inadequate for precise localization of the SOZ in many patients; in such an event, intracranial recordings are necessary. The intracranial ictal EEG recordings provide information about seizure onset and propagation. To determine the SOZ, epileptologists typically inspect the ictal ECoG recordings visually and look for signatures such as low-voltage fast activity and rhythmic spiking from individual electrodes at the time of seizure onset (Niedermeyer and Silva 2005). Considering the large number of implanted electrodes (typically 50 to 200 contacts), identifying the seizure onset by visual inspection of the ictal ECoG recordings is often time-consuming and requires expertise (Bulacio et al. 2012; Widdess-Walsh et al. 2007). Furthermore, visual inspection of the ictal ECoG recordings to identify the SOZ can result in a poor surgical outcome (Bulacio et al. 2012). A study involving 414 patients who underwent intracranial electrode placement reported that visual inspection of the ictal ECoG recordings resulted in complete seizure freedom in 61%, 47%, and 42% of patients at one, three, and ten years after surgery, respectively (Bulacio et al. 2012).

There is a need to identify reliable biomarkers that can accurately localize the extent of the ictal epileptogenic zone, thereby assisting and improving visual identification of the SOZ. On the other hand, epileptic seizures are traditionally characterized by the ultimate expression of monolithic, hypersynchronous neuronal activity arising from unbalanced runaway excitation or inhibition. Neuronal spiking activity during limbic seizure initiation and spread is highly heterogeneous, thereby suggesting complex interactions among different types of neurons. The transition from the pre-ictal to ictal state in focal epileptic disorders has

commonly been considered the result of the excessive synchronization of excitatory neuronal networks caused by the weakening of synaptic inhibition (Merricks et al. 2015; AYALA et al. 1973); however, this concept, though "logically obvious," is not supported by any firm experimental evidence. Rather, studies performed in animal models of epilepsy or of epileptiform synchronization have shown that focal seizures—particularly those characterized by a low voltage fast (LVF) onset—are paradoxically initiated by the synchronous activity of inhibitory cells (for further review, see: (Avoli et al. 2016)). The LVF seizure onset, which consists of EEG activity in the beta-gamma range at times heralded by a spike, is the most frequent onset pattern recorded from the mesial temporal lobe neocortex in focal epileptic disorders (Velasco et al. 2000; Perucca, Dubeau, and Gotman 2014). In addition, LVF onset seizures in patients with mesial temporal lobe epilepsy are associated with distinct patterns of hippocampal sclerosis. The surgery, in this case, can end in failure due to the involvement of temporal and extra-temporal neocortical networks (Memarian et al. 2015; Ogren, Bragin, et al. 2009). Data obtained in vitro from brain slices or from the isolated guinea pig preparation have demonstrated that the onset of LVF seizure-like discharges, induced by amino acid or low doses of bicuculline, coincides in the entorhinal cortex (EC) or hippocampus with robust inhibitory events in principal, excitatory neurons, along with sustained interneuron activity (Curtis and Avoli 2015; Lopantsev and Avoli 1998; Žiburkus1 et al. 2006; Gnatkovsky et al. 2008; Uva et al. 2015). In line with this evidence, optogenetic stimulation of the parvalbumin- or somatostatin-positive interneurons can initiate LVF seizure-like discharges similar to those occurring spontaneously (Shiri et al. 2016; A. Bragin et al. 1999). Experimentally, LVF onset seizures are also recorded in *status epilepticus*-induced models of mesial temporal lobe epilepsy [16-20]. Single-unit recordings obtained in vivo from the hippocampus of these epileptic animals have shown that seizure onset correlates with an arrest of the principal neurons firing together with an increased interneuron discharge

(Grasse, Karunakaran, and Moxon 2013; Toyoda et al. 2015). Since the specific imbalance between the excitation and inhibition at LVF onset has only been identified in pharmacological and optogenetic models, the role of this mechanism in the generation of spontaneous LVF seizures in humans with epilepsy remains unclear. Prior in vivo extracellular recordings of action potentials during spontaneous neocortical seizures with LVF onset in humans has demonstrated both highly heterogeneous ensemble activity (Truccolo et al. 2011) and suppressed firing, followed by a slowly propagating wave of increased neuronal firing (C. a. Schevon et al. 2012). Hence, in this study, we analyzed the microelectrode recordings of local field potentials (LFP), high-frequency oscillations and action potentials in human mesial temporal structures during spontaneous LVF onset seizures. A neurophysiological signature of LVF activity is an increase in ripple rates with minimal changes in the fast ripple rate (Shiri et al. 2016; Levesque et al. 2012). To investigate excitatory/inhibitory balance during LVF activity, we utilized single unit analysis to discriminate the action potentials generated by putative excitatory neurons from those generated by putative inhibitory neurons.

The first aim of this study was to develop and evaluate a method to identify the SOZ using a machine learning approach based on biomarkers extracted from features of the ECoG signal to identify SOZ. In addition, we differentiated those channels with the seizure activity from those that did not show seizure activity. Second, we aimed to study the difference in HFO rates as a biomarker for seizure onset on three different time domains and then correlate them with the reported seizure onset zone, resected area, and the outcome of surgery. Third, through our research, we explored whether there is an imbalance in the neuron level between the inhibitory and excitatory neurons at the LVF onset of spontaneous limbic seizures in humans.

1.1 Research Aims

The goal of the interdisciplinary research was to develop a unified framework to precisely localize seizures in humans. In particular, we have: (**1)** developed a novel biomarker to identify and classify SOZ and non-SOZ electrodes; (**2)** identified and evaluated HFO and FHFO rates in different time epochs to correlate the result with reported SOZ from neurosurgeons, resected area, and outcome of surgery; (**3)** studied neurons from microelectrodes in humans to investigate the difference between the inhibitory and excitatory neurons in LVF seizure onsets. We pursued these objectives via the following aims:

Aim 1: Robust biomarker to classify SOZ and non-SOZ.

The study of high-frequency oscillations (HFOs) and interictal HFOs to localize the brain area where spontaneous seizures initiate (i.e., the SOZ) is of a large clinical interest). HFOs can be detected at the microscopic and macroscopic scale recording. Advances in empirical evidence and theories present opportunities to better understand the nature and role of these signals in characterizing and modeling SOZ. In addition, the types and origin of seizure vary across the population. Statistically, all areas of the brain are equally likely to be the origin of seizure since there is no single correspondence between the HFOs and types of seizure. In addition, the presence of artifacts, spikes, and noise makes it very hard to identify SOZs through visual inspection, even for an expert. Also, it takes a long time (~10 hours to visually mark HFOs in a 10-channel 10-min recording) to examine data recorded over several days to identify the SOZ visually. To plan the surgery, at least two neurologists must agree on their determination of the resection area. To address the issues, as mentioned earlier, we propose to develop a multivariate approach to find robust neuro-biomarkers that are invariant to technical variations and consistent across the population over long hours of recording. The primary goal is to develop a decision support system to identify candidate SOZs to help inspect the recordings online, reduce the planning time of surgery, and improve surgical

outcome by accurately localizing the SOZs despite the presence of artifacts and individual variations. The interaction between different electroencephalography (EEG) frequency bands has been widely investigated in normal and pathologic brain activity. We are interested in understanding whether one frequency band modulates the activity of a different frequency band on seizure onset. We studied the phase lock value (PLV) obtained from phase-amplitude coupling (PAC) between high gamma (80-150 Hz) and lower frequency (4-30 Hz) as a biomarker to robustly predict the SOZ from intracranial EEG.

Aim 1.1: Machine learning approach to classify SOZ and non-SOZ channels: We adopted a machine learning approach that uses features derived from the PLV values to classify electrodes with and without seizure activities. We also wish to render a model to save time and effort to localize SOZs while the epileptologists perform the visual inspection. This approach should allow the detection of true SOZs in cases where expert judgment fails.

Even though the machine and the model may look proper, all the proposed methods should be evaluated subjectively and objectively. We will ask neurologists to cross-validate our results (notably, clinical discussion is a very costly and lengthy process).

Aim 1.2: Evaluation of the results with the outcome of surgery and visually identified SOZ: Further, we compare our results with the epileptologists gold standard methods and the outcome of seizure surgery. The goal is to employ most of the criteria that epileptologists consider to identify SOZ and develop an automatic and fast model to classify SOZ and non-SOZ electrodes.

Aim 2: Study the rate of HFO and FHFO in different epochs of time and compare this rate with reported SOZ and resected areas.

We studied the difference of HFO /FHFO in different epochs that included the following: the night before seizure, resting state before seizure (we will refer to it as “awake period”), pre-ictal and ictal. The aim of this analysis is to find the rate of HFO/ FHFO in

which the epoch is more correlated with SOZ, the resected area, and finally with surgical outcome. In this study, HFO/ FHFO detection is not a patient base.

Aim 2.1: Automated algorithm to find HFO and FHFO

To detect the HFO/FHFO, we developed an algorithm that is not in the patient base and does not require any tuning for HFO/FHFO detection. For this detection, we will reject the artifact and spike waveform prior to the HFO/FHFO final result.

Aim 3: Imbalance in the neurons level at the LVF seizure onset of human neuronal spiking activity during limbic seizure initiation and spread is highly heterogeneous. Thus, this suggests complex interactions among different types of neurons. During spontaneous low-voltage fast (LVF) onset seizures in animal models of mesial temporal lobe epilepsy (MTLE), the firing rate of inhibitory interneurons increases, while the firing rate of the principle neurons decreases and then rebounds. We asked whether spontaneous focal seizures in patients also exhibit similar changes in putative excitatory and inhibitory firing during LVF activity.

Overall, our research focused on developing novel approaches toward finding biomarkers and evaluating the results with the real surgery outcome to determine the SOZ precisely; however, at the end, we studied the possible causes of seizures in neuron level for a very typical MTLE seizure onset type (LVF). The outcome of this research assists experts' judgment to identify SOZ.

Aim 3.1: Spike sorting

To be able to answer the question as to whether inhibitory neurons start firing prior to excitatory neurons, we first need to detect action potentials and second to separate them from each other. In this study, we used Waveclus software to detect the action potentials. Next, we used K-mean clustering to separate the putative neurons into two well-known groups: inhibitory and excitatory interneurons. At the end, we double-checked whether we could

successfully separate them and whether or not they were categorized correctly. As we know from animal models, inhibitory neurons are phase locked with LVF activity, which is not the case for excitatory neurons. We will check whether our putative interneurons follow the same concept.

1.2 Broader Impacts

The studies described here reflect an interdisciplinary blend of engineering and neuroscience. The outcomes of these studies will enable neurosurgeons to identify SOZ and obtain the Engle I outcome of surgery both quicker and more accurately.

1.3 Novelty

In our research, one of the key innovations was to find a new biomarker based on the features extracted from *PLV* and using *Machine learning approaches* to classify the SOZ and non-SOZ channels.

The second innovative aspect of our approach was *the finding that spontaneous low-voltage fast limbic seizures in humans exhibit a specific excitatory-inhibitory imbalance at seizure onset.* Intracellular recordings during low-voltage fast (LVF) onset seizures from the entorhinal cortex in animal models of mesial-temporal lobe epilepsy have demonstrated that these seizures are initiated by a synchronous inhibitory event. We proved that spontaneous limbic seizures in patients with medically refractory mesial-temporal lobe epilepsy also exhibited increased firing of inhibitory interneurons at onset.

1.4 Significance

An accurate biomarker to automatically identify SOZ and non-SOZ electrodes:

Recently, researchers have proposed the high frequency oscillation (HFO; gamma: 40-100 Hz, ripples: 100-200 Hz, and fast ripples: 250-500 Hz) of neural activities as an indicator of the seizure-generating site (G. A. Worrell et al. 2004; Engel and da Silva 2012; J. Jacobs et

al. 2012; Julia Jacobs et al. 2010; Jirsch et al. 2006). It has also been demonstrated that HFO carries information distinct from that provided by low-frequency discharges (G. A. Worrell et al. 2004; Engel and da Silva 2012; J. Jacobs et al. 2012; Julia Jacobs et al. 2010; Jirsch et al. 2006). Further, ripples have been found to coexist with various background EEG patterns (Melani et al. 2013). In addition, surgical resection of the areas generating ripples and fast ripples coexisting with flat background EEG activity has been found to significantly correlate with a seizure-free outcome (Kerber et al. 2014). Moreover, the resection of areas generating ripples with a continuously oscillating background EEG pattern showed no positive correlation with post-surgical outcome (Kerber et al. 2014). It has been shown that HFOs are also present in intracranial EEG recording from normal brain regions and even in non-epileptic subjects (Blanco et al. 2011). The presence of these physiologic events complicates the use of HFOs as biomarkers in epilepsy.

In light of these limitations, some studies have looked at the interactions between different rhythms to localize the seizure onset (Catalina Alvarado-Rojas et al. 2014; C. Alvarado-Rojas et al. 2011). Specifically, cross frequency coupling (CFC) in the form of modulation has been explored as a predictive feature of seizures. Phase-amplitude coupling (PAC) occurs when the amplitude of a faster rhythm is coupled to the phase of a slower rhythm. Phase locking value (PLV) has been used to calculate the phase synchrony between two frequency bands (Mormann et al. 2005). Recently, CFC of ictal ECoG recordings was shown to characterize SOZ successfully (Shennan A Weiss et al. 2013; Shennan Aibel Weiss et al. 2016; R T Canolty et al. 2006). In particular, it has been shown that PAC between the phase of low-frequency and amplitude of high frequency oscillations was more useful for the localization of an epileptic focus than the amplitude of high gamma alone (Shennan A Weiss et al. 2013). By employing microelectrode array recording, Weiss et al. calculated PLV and phase locking high gamma (PLHG) measures to identify the SOZ. By adapting a threshold on PLHG, Weiss

et al. (Shennan A Weiss et al. 2013) could differentiate the core seizure territory (SOZ) from the surrounding penumbra. We obtained the *Phase locking Value (PLV)* of ictal ECoG recordings using standard intracranial electrode arrays. Therefore, we hypothesized that PAC between the amplitude of high frequency (80-150 Hz) and phase of low frequency (4-30 Hz), recorded from ECoG data immediately before and after seizure onset, could be used as a biomarker to identify SOZ.

Unbalance of excitatory and inhibitory influences leading to seizure generation:

It is widely accepted that the development of epileptiform activity results from a shift in the balance between excitation and inhibition (Dichter and Ayala 1987; Tasker and Dudek 1991). One of the few treatment options available to patients with pharmacoresistant focal epilepsy is to identify the brain area from which seizures arise and remove it. As the risks to the patient from such a procedure are substantial, it is necessary to define the epileptogenic zone as accurately as possible (Rosenow and Hans Luders 2001). Key localizing information should be available from subdural EEG recordings, but animal studies suggest that there may be a major pitfall in how EEG recordings are interpreted. Studies of epileptiform propagation in mouse brain slices clearly show territories ahead of the ictal wavefront where there are very large amplitude excitatory and inhibitory conductances, with little postsynaptic recruitment (Trevelyan et al. 2006; Trevelyan, Sussillo, and Yuste 2007; Trevelyan 2009). Similar patterns have also been recorded in vivo in animals following focal injection of $GABA_A$ antagonists (Avoli et al. 2016; Schwartz and Bonhoeffer 2001). The ictal wavefront generates huge feedforward excitation, yet a rapid feedforward inhibition provides a powerful restraint. We hypothesized, therefore, that if such a restraint is also present in naturally occurring (clinical) epilepsy, there should exist a 'penumbra' around the ictal activity where there are large amplitude EEG signals, reflecting feedforward synaptic currents, but with little actual local recruitment of neurons. It will be important to identify some of the sites where

large EEG signals do not correspond to local firing, because this may confound how we localize seizures.

To examine this hypothesis, it is necessary to map out actual firing patterns over spatially extended territories during seizures and contrast these with the spread of postsynaptic currents away from the ictal focus. This has recently become possible following the development of microelectrode arrays (MEAs) suitable for use in humans (Waziri et al. 2009; C. A. Schevon et al. 2009). Here, we have presented a series of MEA recordings to show the spatial pattern of Low Voltage Fast (LVF) activity at the onset of clinical seizures. We further characterize the activity patterns of inhibitory and excitatory neurons at different regions of the brain (entorhinal cortex, hippocampus, and amygdala), and we will compare the pattern of each group of neurons ipsilateral and contralateral to SOZ.

Chapter 2

Research Context

Epilepsy is one of the most common neurologic diseases, with a 1% prevalence in the population. Approximately one-third of the newly diagnosed cases will become medically refractory epilepsy (MRE) (Asadi-Pooya et al. 2016). Temporal lobe epilepsy (TLE) is the most frequent type of focal refractory epilepsy, accounting for two thirds of localization-related epilepsies (Kelvin et al. 2007). Surgical resection of MRE aims to reduce the frequency and intensity of seizures, thereby reducing neurological disease and antiepileptic drug toxicity, and lastly, the potential curing of the patient. Preoperative evaluation involves a team of neurologists, neurosurgeons, neuropsychologists, radiologists, technicians, nursing, and ancillary staff and requires structural and functional imaging, prolonged video-EEG monitoring, and neuropsychological assessment. Contemporary advances in imaging, apart from electrophysiologic localization techniques, have enabled more patients to benefit from respective surgery. A randomized controlled trial (RCT) studied the seizure outcome of epilepsy surgery in MRE TLE and showed it to be more efficacious compared to prolonged antiepileptic drug (AED) therapy (Wiebe and B 2001). Some studies have shown that the excess mortality associated with MRE is eliminated in patients who are seizure-free after surgery (Sperling Michael R. 2015).

2.1 Definition and impact of temporal lobe epilepsy (TLE)

According to the International League Against Epilepsy (ILAE), an epileptic seizure is a paroxysm originating from abnormal, excessive, or synchronous neuronal activity in the brain (Fisher et al. 2014). Epilepsy is a disorder of the brain defined by an enduring predilection to generating seizures and the cognitive, psychological, and social consequences of the disease. Further, epilepsy itself increases the risk of accidents and sudden unexpected death (SUDEP) (Novak et al. 2015). The definition of epilepsy details the manifestation of at least two non-provoked electrographic seizures. Epilepsy is a broad category of symptom complexes arising from disordered brain functions that may be secondary to a variety of pathologic processes.

In TLE, the most common pattern, the seizures begin at the mesial or neocortical temporal lobe structures.

2.2 Temporal lobe epilepsy surgery

2.2.1 History of epilepsy surgery

The history of epilepsy surgery is believed to have started in the 19th century in London, England, when Victor Horsley operated on a 22-year-old man with focal motor seizures caused by a depressed skull fracture (Eadie 2005). This created an interest in the possibility of surgical resection by removing what was probably thought to be a seizure-generating brain. In particular, this helped researchers discern the role of the temporal lobe as a critical localization of MRE. The pioneering work of Jasper and Penfield in Montreal, Canada, in addition to that of Bailey and Gibbs in Boston, USA, led the anterior temporal lobe (ATL) resection (Penfield and Jasper 1954).

2.2.2 Indications for epilepsy surgery candidacy

Clearly, the seizures need to be resistant to medical therapy. MRE has now been defined as the failure of adequate trials of two tolerated and appropriately chosen and used AED schedules (whether as monotherapies or in combination) to achieve continual freedom from seizures (Leppik 2010). Subjects with resistant epilepsy might be better served at centers for 16 comprehensive evaluations and presurgical work-up. Next, the clinical diagnosis should be focal epilepsy. Although a higher age (over 50 years) is not a contraindication for TLE surgery, it has been shown in several reports that seizure outcome is more favorable in younger patients (Yun et al. 2006; Srikijvilaikul et al. 2011). For patients older than 50, the risks for surgical and neurological complications are, as expected, rather higher (Marks 2002). While normal intelligence is not a prerequisite for surgical inclusion, cognitive disability raises the chance of multifocal and multilobar epileptogenicity; however, it has been revealed that patients with a low IQ can be helped with surgery, in particular, those with

lesion-positive TLE, although the seizure outcome at the lowest IQ level was not found to be helpful. In order to make final recommendations, the cognitive effects of epilepsy surgery and psychosocial outcome in this latter group of patients should be studied further in detail (Smith and Puka 2016). Patients with long-lasting psychiatric diseases are usually not excluded from surgical evaluation, but preoperative counselling with a psychiatrist familiar with epilepsy surgery is compulsory. Conversely, surgery would be precluded for patients with active psychosis, depression, or a significant personality disorder because of the inability of the patients to cooperate in the evaluation and difficulty in post-operative rehabilitation.

2.2.3 Preoperative evaluation

To achieve a seizure-free state with no side effects, a patient's epilepsy must be thoroughly characterized prior to surgery. This presurgical evaluation involves identifying the epileptogenic zone (EZ)—the area of the cortex that can generate epileptic seizures—and that if removed, would stop the seizure activity (Rosenow and Hans Luders 2001). However, it is not possible to definitively identify the EZ in advance of surgery. It is only possible to estimate the tissue boundaries of this area using a variety of diagnostic tools including EEG and neuroimaging techniques.

The EEG aids in locating the seizure onset zone (SOZ), the cortical region from which seizure generation can objectively be measured. A neurologist using standard visual analysis of the raw EEG, which may include both scalp and intracranial recordings, identifies seizure onset and offset times. SOZs are defined electrographically as the electrode(s) with the earliest seizure activity. The SOZ and EZ do not necessarily overlap; clinical results have demonstrated both positive and negative results in relation to seizure freedom following the removal of SOZs. It is hypothesized that the EZ is a combination of the SOZ and a potential seizure onset zone (see Figure 2-1), as tissue areas in unresected potential SOZs have been shown to trigger seizures post-epilepsy surgery (Lüders et al. 2006).

Neuroimaging techniques are used to detect abnormalities of the brain both in structure and function. Magnetic resonance imaging (MRI) is the preoperative imaging of choice for the discovery of morphological brain abnormalities or lesions (Figure 2-2). Such abnormalities, including tissue scaring (sclerosis), vascular, and developmental malformations, and tumors, are investigated to determine their involvement in the seizure activity. Similarly, positron emission tomography (PET) is a technique that measures the cellular activity in the brain. Areas of the brain with abnormal levels, high or low, may also point to the EZ (Werz and Pita 2010). While brain malformations may aid in the identification of the EZ, a larger number of patients present with unrelated brain irregularities or none at all.

It is critical to identify the exact cortical region responsible for seizure generation, not only to allow for a positive surgical outcome, but also to prevent postoperative neurological deficits. Eloquent cortex describes brain tissue that, if removed, will result in a functional deficit, which can rang from paralysis, a loss in sensory processing, and cognitive deficits. As a result, there is a fine balance in maximizing the excision of the EZ while minimizing that of the eloquent cortex during epilepsy surgery.

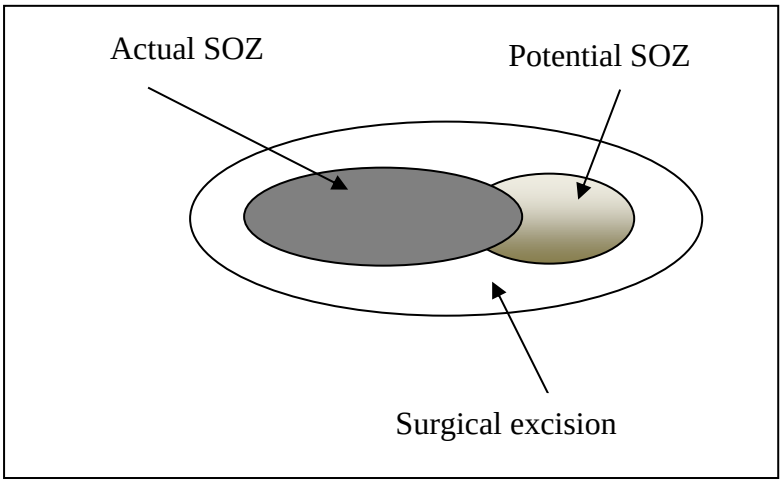

Figure 2.1. The epileptogenic zone. The diagram shows the actual and potential SOZ, along with the surgical resection area. Since the resection includes both SOZs, the outcome of this surgery is a seizure-free case [60].

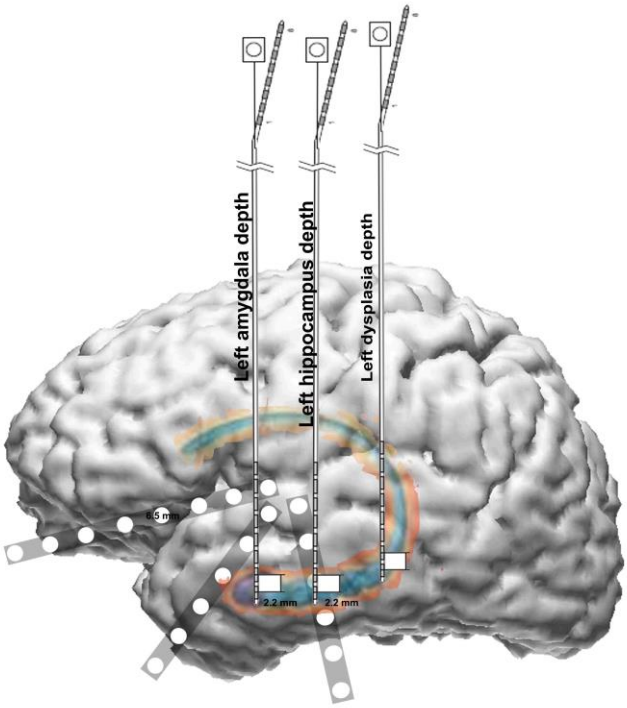

a)

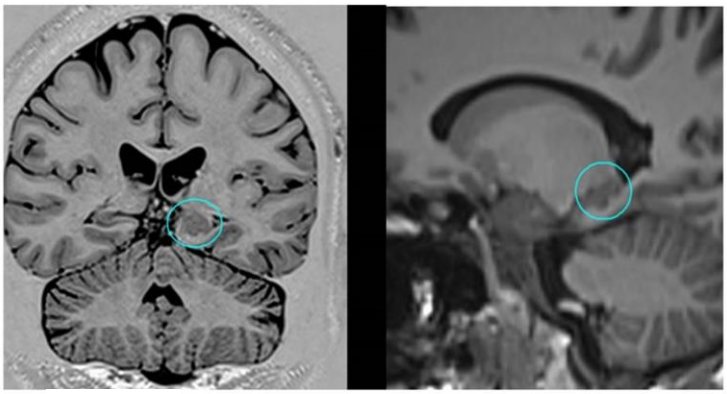

b)

Figure 2.2. Typical imaging finding from generalized tonic-clonic seizure (GTCs). The patient is a 38-year-old male who experienced his first seizure when he was 16 (from Johns Hopkins Hospital 2017).

a) Location of depth in the hippocampus and grids on cortex;

b) 3T MRI shows apparent thickening of the dorsal left perihippocampal gyrus (circles).

2.3 Invasive EEG evaluation

2.3.1 Indications

In a large fraction of TLE patients, the MRIs suggest unilateral MTS and concordant interictal and ictal scalp-EEG recordings, functional imaging, and clinical findings; hence,

allowing straightforward surgical treatment. When non-invasive studies remain in disagreement or inconclusive regarding localization of SOZ, this indicates video-EEG with intracranial EEG electrodes. In general, the use of invasive EEG occurs for non-lesional focal epilepsy (as determined by the aforementioned protocols), lesional but disagreeing scalp-EEG or other non-invasive findings, bitemporal or frontotemporal, rare occurrences in TLE, and the demarcation of the eloquent areas (language/motor/memory) with an array of contacts (Rosenow and Hans Luders 2001). The main advantages of IEEG contacts and evaluation are improved spatial resolution and the ability to record higher bandwidth, which are filtered and attenuated in surface EEG. iEEG also creates the prospect of interrogating the deep anatomies, such as basal and mesial temporal structures, or even the thalamus. Conversely, the disadvantage of subdural EEG contacts is their incomplete coverage of the whole brain; with intracerebral depth contacts, this area is even more limited. If the actual SOZ is outside of the area covered by the electrodes, the electrodes are measuring seizure spread instead of the initial focus. Van Loo described a failure rate of 2%–53% in localizing the SOZ with the invasive EEG methods used in their studies (Van Loo, Pieter et al. 2011). The additional costs and possible complications related to the invasive procedures should always be taken into account when the intracranial EEG evaluations with individual patients are considered. Costs per case range between 75,000 and 250,000 dollars (in 2016-2017).

2.3.2 Intracranial electrodes

Subdural strip contacts are the devices most commonly used in invasive preoperative EEG assessment of TLE patients. The strip electrodes consist of 4-10 platinum or stainless steel contacts in a single row, which can be positioned directly on the cortex into the subdural space through burr holes. Assignment of the contacts is individually customized according to the hypothesis of the SOZ suggested by phase 1 monitoring. The subdural strips and grids are most often placed bilaterally, covering the basal and temporal lateral lobes as well as a part of

the frontal lobe, including the orbitofrontal cortex (Figure 2-3). Naturally, the ideal setting varies among centers conferring to their conventional practice and indication for iEEG. DBS-like or depth contacts (Figure 2-2) can be valuable in patients with MTLE to define the side of SOZ. Subdural electrodes are 20% less sensitive than depth electrodes when used to detect seizures starting in the hippocampus. When the subtemporal subdural electrode covers the parahippocampal area medially to the collateral sulcus, the seizures are with a high degree of localized precision, which is consistent with the consequences from depth electrodes recording (Eisenschenk et al. 2001). Correct implantation of depth contacts necessitates a stereotactic device using the occipital approach, implanting one electrode on each side along the axis of the hippocampus and lastly entering the amygdala, or two electrodes through the lateral temporal cortex to the hippocampus and amygdala. The practice of depth electrodes increases the risk of intracerebral hemorrhage because it is more invasive than subdural implantation. A grid array consists of multiple electrodes fixed in a flexible sheet of silicone, which can be implanted in an open craniotomy to cover large areas of the cortex. To localize the SOZ, it can also be used to demarcate so-called eloquent areas by cortical stimulation. Grid electrodes are principally used to assess patients with extra-temporal epilepsy.

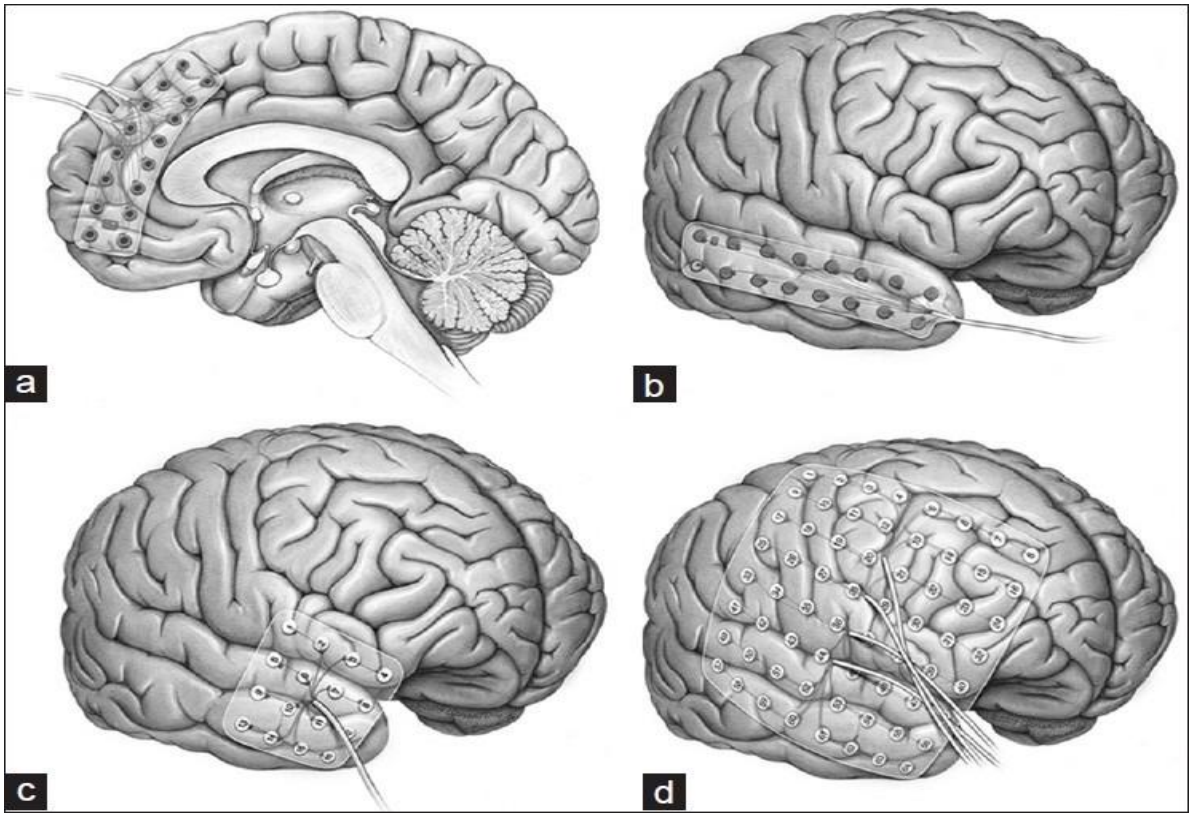

Figure 2..3. The spatial placement, coverage, and number of implanted iEEG electrodes are dictated by the size and location of the SOZ, as identified during the pre-surgical planning phase. a: 2x8 electrode grid within the interhemispheric space; b: 2x8 electrode gr grid on the temporal lobe; c: 4x4 grid over the frontal and temporal lobes; d: 8x8 grid over the frontal lobe (Voorhies and Cohen-Gadol 2013).

2.3.3 Complications

The amount of patients necessitating iEEG evaluation in epilepsy centers is decreasing due to development of non-invasive methods. There remains a subgroup of patients for whom iEEG evaluation is needed, and the risks and benefits must be weighed for each patient. Several retrospective series of complications related to invasive evaluation have been reported, and the rate of major adverse events causing permanent deficits appears to be low (Önal et al. 2003). The most common complications, as with most surgical procedures, are infections and hemorrhage. Invasive monitoring with grid electrodes is associated with more significant problems (Noe et al. 2014; Van Gompel et al. 2008). In three of these articles, reported deaths have been mainly associated with uncontrollable brain edema. Most of the complications

were, however, transient, and their occurrence was associated (e.g., with the larger and greater number of grids and a longer duration of evaluation and older age of the patient). Subdural grid implantation seems to be better tolerated in children than in adults (Van Gompel et al. 2008). Researchers have suggested that the greater plasticity of children's brain tissue and veins, as well as a greater tolerance for foreign bodies, could explain the lower rate of complications in pediatric populations (Noe et al. 2014).

2.3.4 Strategies for operative treatment

Since the pioneering work by neurosurgeons Penfield, Bailey and Falconer on TLE surgery, many modifications of customized and anatomical temporal lobe resections have been adopted. The median length of resection from the temporal tip was 5.5 cm in the nondominant lateral temporal cortex (range 2–6.5 cm), 4.5 cm on the dominant side (range 2–6 cm), and 3 cm of the hippocampus (range 1–3.5 27 cm) (Rosenow and Hans Luders 2001; Wiebe and B 2001). It is hoped that resection of the SOZ leads to seizure control, seizure freedom, or successful surgery followed by no negative impact on mental capacity, and no effect on postsurgical memory. In several studies, classical anterior temporal lobe resection, including amygdalohippocampectomy vs. selective amygdalohippocampectomy (SAH), has been evaluated to determine its impact on the seizure outcome. Most of the retrospective analyses have concluded that these different strategies for surgical approaches result in equally good seizure outcomes (Hu et al. 2013)(Staba et al. 2002). There are reports of worse outcomes with pediatric patients undergoing SAH, which casts into doubt the existence of purely mesial juvenile TLE (Mansouri et al. 2015). The impact of the extent of mesial or neocortical resection in TLE on the seizure outcome is controversial. Some studies show better seizure outcomes with extensive resection of the hippocampus or the entorhinal cortex (Al-Otaibi et al. 2012). All larger resection volume has been associated with improved seizure control (Gump, Skjei, and Karkare 2013); however, no benefits have been observed

regarding the relationship between more extensive resections and seizure control (Jehi, Wyllie, and Devinsky 2015). It has been reported that a greater resection of the hippocampus may predict a better outcome; however, this was not associated with the extent of resection of the lateral temporal gyri (Joo et al. 2005). There is a considerably greater disparity among epilepsy centers in terms of the extent and types of resection in temporal lobe surgery for epilepsy. Also, neither more selective types of resection nor a larger extent of resection have been proven to achieve a better seizure outcome. For decades, many epilepsy centers have used intraoperative electrocorticography (ECoG) to define the extent of both mesial and lateral temporal lobe resections. However, the use of intraoperative ECoG as a guide for surgery to achieve better seizure outcome is controversial. The presence of spikes outside the boundaries of neocortical temporal resection areas, as guided by ECoG, have not correlated with outcome (Krendl, Lurger, and Baumgartner 2008). The recorded post-resection epileptic discharge did not correlate with the outcome, and neither did recorded post-resection discharge predict clinical seizures (Schwartz et al. 2000). Intraoperative hippocampal ECoG has also been used in guiding the custom resection of the hippocampus, which may potentially allow the functionally important hippocampus to be left behind. McKhann et al. found that hippocampal ECoG predicted how much of the hippocampus should be removed to maximize seizure-free outcome (McKhann et al. 2000). Intraoperative ECoG has also been used in predicting seizure outcome in selective amygdalohippocampectomies. ECoG has also been used to guide the extent of resection for removing lesions associated with temporal lobe epilepsy. The critical question is whether to remove only the lesion or to perform more aggressive resection to achieve better seizure control. In their series of 61 patients with temporal lobe cavernomas, Van Gompel et al. recently demonstrated that the use of intraoperative ECoG was associated with larger resection and an improved seizure outcome (Van Gompel et al. 2008).

2.3.5 Seizure outcome of surgery

The most widely utilized classification system for postoperative seizure outcome has been adapted from Engel (Table 1) (Durnford et al. 2011). However, the category of patients free of disabling seizures (Class I) does not separate those patients with postoperative auras, and the outcome measure '≥ 50% seizure reduction' is missing from the classification, which is typically used in antiepileptic drug trials (=Engel IVA). Taking these issues into account, the International League Against Epilepsy (ILAE) issued a commission report proposing a new outcome classification 29 (Table 2), which also counts seizure days rather than total number of postoperative seizures

Chapter 3

Electrophysiologic Biomarkers of Seizure Onset

3.1 Interictal Biomarkers

Epileptic seizures serve as the gold standard for SOZ localization during the invasive monitoring session for patients undergoing evaluation for respective surgery. So-called ictal EEG are suboptimal in terms of cost, risk, time, and morbidity; however, the EEG is not without sporadic markers of epileptogenicity between ictal (seizure) events. The most obvious events are interictal spikes or IEDs, High Frequency Oscillations (HFO), and more recently, phase-amplitude coupling (PAC) events (a Bragin et al. 1995; A. Bragin et al. 2002). IEDs and HFO have been more heavily investigated than PAC but these interictal biomarkers are not currently used in clinical practice in the United States. Unfortunately, clinical acquisition does not provide adequate spectral bandwidth to acquire these events, therefore data must be collected using special equipment with capability of high frequency sampling. Notably, these events cannot be captured on scalp EEG (G. a. Worrell et al. 2012).

3.1.1 What is High Frequency Oscillation (HFO)?

Over the last decade, High Frequency Oscillations have been studied extensively as a promising interictal electrophysiologic biomarker of seizure activity and onset in humans, in animals, and in vivo. Studies have shown that HFOs might be useful in identifying SOZ, and may even have utility in distinguishing pathologic from non-pathologic seizures and the prediction of the temporal patterns of onset (temporal prediction in addition to spatial) (Varatharajah et al. 2017). HFO is defined as an electrophysiologically detectable oscillation with a central frequency between 30-600Hz. EEG bands are conventionally characterized as slow at less than 1Hz, delta between 1 and 4 Hz, theta between 4 and 8Hz, alpha between 8 and 13Hz, beta between 13 and 30Hz, gamma above this, and ripple above that. There is some loose convention with bands above 30Hz as being low gamma at 30-60Hz, high gamma at 60-100Hz, ripple from 100-250Hz, and fast ripple up to 600Hz. The high frequency

oscillations are essentially all those above 30Hz. They are transient, possessing multiple ‘turns’ that are sinusoidal (See Figure 3-1). These events occur on the order of a few dozen milliseconds and occur spontaneously in the hippocampus, primarily during slow wave sleep, and can also be seen in the neocortex (Gloss, Nolan, and Staba 2015; Grenier, Timofeev, and Steriade 2001; Matsumoto et al. 2013). Recently, there has been a discussion on differences between real and not-real HFO (Benar et al. 2010; Amiri et al. 2015). Amiri et al. discussed how filtering can introduce false HFOs (Amiri et al. 2015). They reported a multivariate method (Support Vector Machine) to classify the real and False HFOs from the raw and unfiltered signal; Benar et al. advocated that a real HFO is expected to be detected in the raw signal by visual inspection; otherwise, it would be discarded (Benar et al. 2010). In addition, they have suggested analyzing the time-frequency representation of HFOs to define whether an HFO is real or false. Based on their approach, a transient event and an oscillation have a different signature; a real HFO is represented by an isolated peak in the time-frequency plot (restricted in frequency, an “island”) located in the frequency band of 80-500 Hz, while a transient event generates an elongated blob that is extended in frequency. At the HFO detection stage, the oscillatory component of a real HFO satisfied criteria on energy and duration, while that of a spurious HFO did not, which leads to its rejection as an HFO (Chaibi et al. 2014).

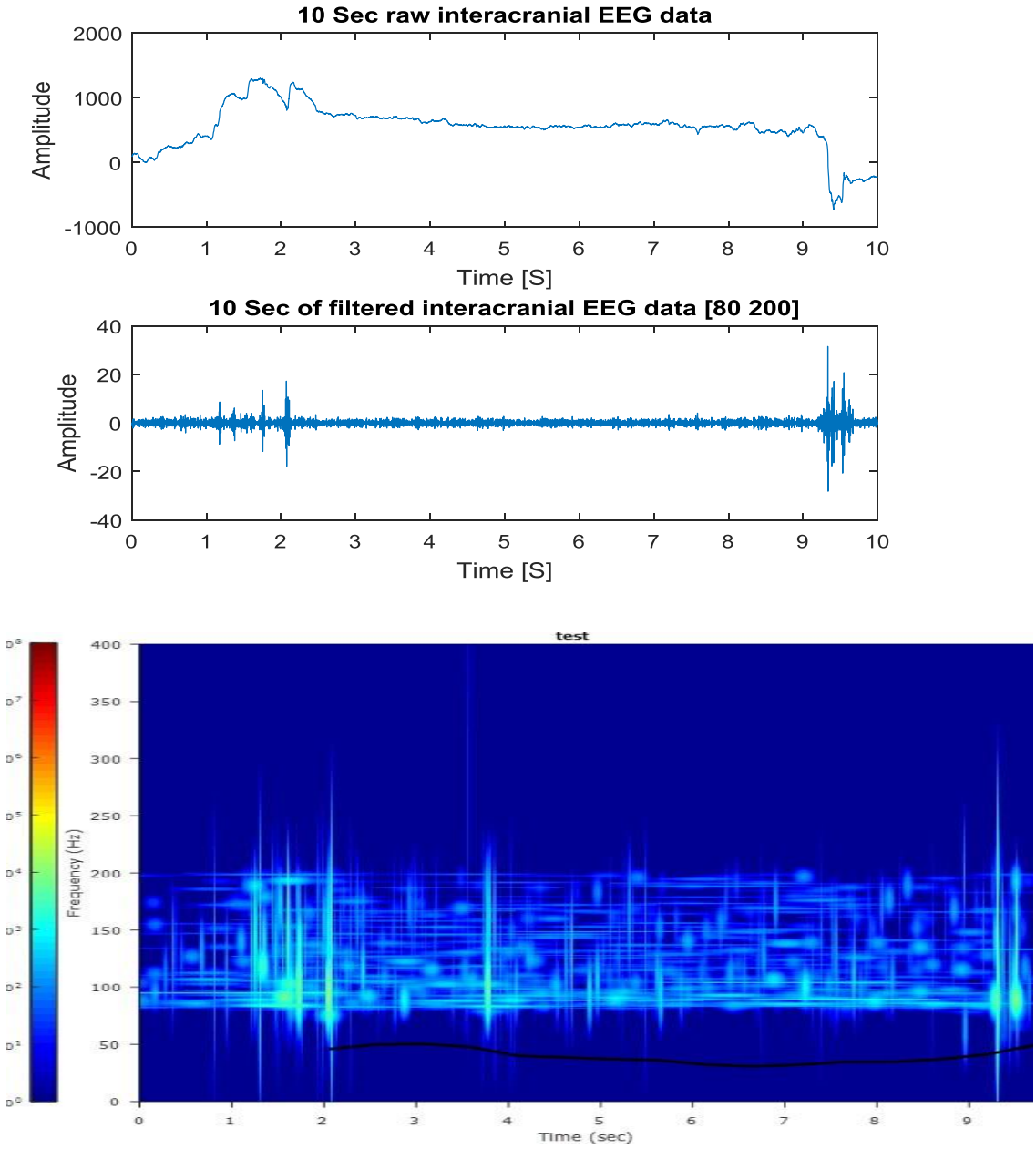

Figure 3.1. Demonstration of High Frequency Oscillations (HFO). First panel shows the raw interacranial EEG data, middle panel illustrates the filtered signal in high gamma band, and the bottom panel illustrates the matching pursuit illustration for the same channel and same epoch. As depicted in the last panel, HFO can be visually identified in time-frequency domain.

3.1.1.1 Cellular mechanism of HFOs

Of course, the details on the mechanisms of HFOs comes from animal experimentation and in vitro paradigms (Ylinen et al. 1995; Menendez de la Prida and Trevelyan 2011). In a normal mammalian brain, the local inhibitory network of cells is key in the development of HFOs. CA1 sharp-wave ripple complexes and during ripple HFOs and task-evoked fast ripple HFOs,

interneurons, which in the hippocampus are basket cells and in the neocortex fast spiking cells, fire regularly during HFO extracellular recording (J Csicsvari et al. 1999; Klausberger et al. 2003; Ylinen et al. 1995). GABA is thought to be the prime neuromodulatory molecule that controls the dynamics of this event, thereby governing the inhibitory postsynaptic potentials imposed on the principal cells. In the hippocampus, this role is on the pyramidal cells. In the neocortex, this is played out by intrinsic burst fast bursting cells. According to Buzsaki, this provides precise temporal windows, which regulate firing and coordinate excitatory synaptic transmission on postsynaptic targets (Ylinen et al. 1995; Singer 1999). This interaction between pyramidal cells in physiologic situations is observed in the encoding of information, motor integration, and memory consolidation processes. In the epileptic brain of mammals, however, the dynamics are different. In the hippocampus, a fast HFO (ripple range) is believed to signify brief bursts of population spikes generated from a cluster of synapsed pathological neurons (Staba et al. 2004; A. Bragin, Wilson, and Engel 2007). Some other investigations have shown a burst of population spikes for ripple HFO events in the dentate gyrus, which is an area that usually does not generate ripple range HFOs, which led that team to call such HFOs ‘pathological’. This definition is somewhat fluid, but was said to include population spikes within the ripple and fast ripple bands, and, as observed in the hippocampus (A. Bragin, Wilson, and Engel 2007; Engel et al. 2009). The in vitro work generally agrees with this finding, which shows that the recurrent excitatory network in CA3 can generate patterns that synchronize with population spikes. Dentate and hippocampus experiments further characterized pathological HFOs after the suppression of GABA receptors (Foffani et al. 2007). Another study found increases in principal cells spiking with reduced interneuron firing that coincided with dentate pilocarpine epilepsy models (A. Bragin, Benassi, and Kheiri, Farshad, Jerome 2011). Principal cells in certain instances, along with interneurons, could explain the pathological HFOs in the high ripple range; however, in some patients, there is little evidence of any fast ripple firing when controlling for electrode

placement (Staba 2012; Ylinen et al. 1995). In Chapter 5, we further explain the contribution of ripples and fast ripples in SOZ.

3.1.1.2 Recording, Detection using Macro- and Micro-electrodes

Brain activity comprises a broad range of temporal interactions generated within the local and distal networks of neurons. Hence, these interactions can be parsed at many different time-scales separated by several orders of magnitude. At the most global level, shifts in voltage or direct current have been observed over minutes and hours of recording. Buried within this signal, there are oscillations of neuronal networks, which themselves range from infra-slow, slow-wave, and delta frequency rhythms generated by thalamocortical circuits (0.1-4 Hz, i.e., cycles per second). For example, during the deep sleep phases, delta waves are more dominant. Fast oscillations in the gamma and ripple frequencies (30-600 Hz) emerge from local synchronization of neurons in the hippocampus or the neocortex. Finally, at the millisecond level of the LFP, one can detect individual waveforms of 600-6000 Hz activity corresponding to action potentials fired by neurons, which can further be assigned to specific single cells (we talk in detail about this issue in Chapter 6). Action potentials emerge from the sum of synaptic interactions within a single neuron, whereas slow waves are the result of reciprocal projections between cortical and sub-cortical neurons in the thalamus and the basal ganglia. Both the local and the distal connections modulate the activity of neuronal networks, and are hence important in putting together the big picture (Le Van Quyen and Bragin 2007). The organization of the big picture—the brain—can be described in terms of a ‘small-world network’, forming local and distant connections with all other nodes. Altogether, the connected nodes form a network with a micro- and macro-level structure, both locally segregated and globally distributed, reflected in its coordinated fast and slow activities. These activities can be captured at the same time when recorded with both micro and macro electrodes having different biophysical properties, as shown in Figure 3-2. The

two contact types have different sizes, and hence conduct current with impedances that measure voltage change generated across micro- or macro- neuronal circuits.

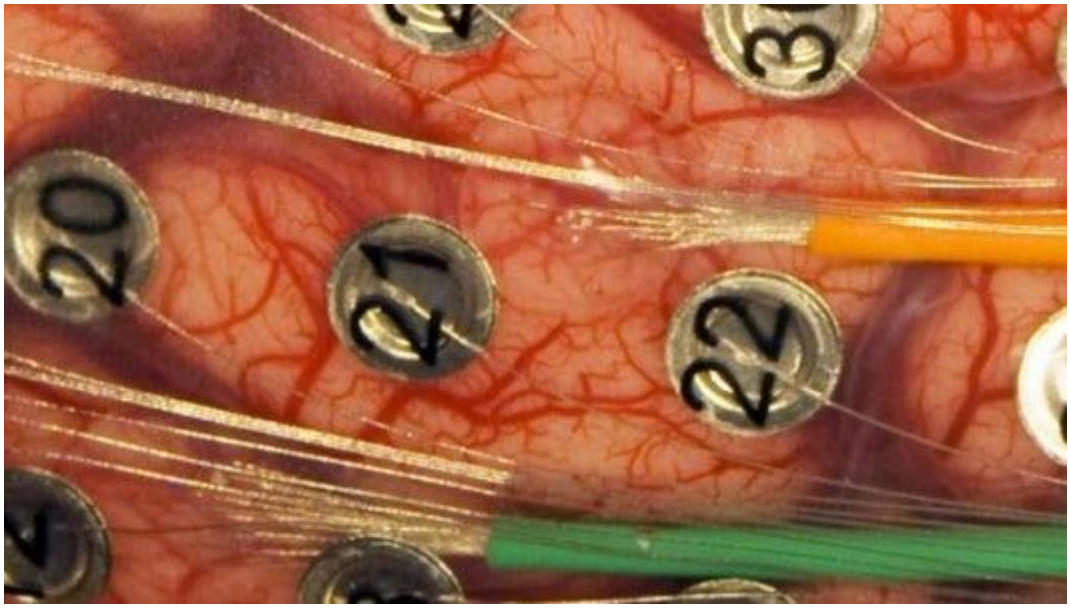

Figure 3.2. Simultaneous data recording from micro- and macro-scale electrodes. https://newatlas.com/brain-microelectrodes/12141/

Microelectrodes, which are typically 40 μm in diameter, probe the LFP changes and action potentials of neurons located as far away as 100-200 μm from the contact site. The amplitude of single neuron spiking decays exponentially with distance; therefore, action potentials can only be reliably detected above the level of electrical noise for neurons in the close vicinity of ~50 μm radius from the electrode (Buzsáki 2004). LFP, on the other hand, is not quite as influenced by the brief discharges of neuronal spiking themselves due to the longer-lasting extracellular currents that spiking produces. Micro-electrodes offer a high resolution view of specific neuronal assemblies, but cannot capture origins of a wider network activity. These transmembrane currents are the strongest around neuronal cell bodies and synapses where the action potentials are generated and travel along the somatodendritic tree, thus creating a field of current flow. When whole populations of neurons spike in unison and are arranged in layers with their projections aligned in one axis, a strong composite field of transmembrane current emerges parallel to the somatodendritic axis with a source in the

cell body layer (Nunez and Srinivasan 2006). LFP is the extracellular indirect measure of this current thought to originate within 250 μm from the recording electrode. However, the extent of LFP and its spread through brain tissue can be much greater depending on the geometry of neuronal network architecture, strength, and synchrony of network activity (Kajikawa and Schroeder 2011). The questions raised here are: How far does the LFP spread? Alternatively, what specific contributions to the field of transmembrane current remain to be elucidated? On top of the ion currents that drive membrane depolarization, there are more physiological processes that shape the local field, such as action potentials fired synchronously by many neurons, calcium spikes lasting 10-100ms, fluctuations in the membrane potential, membrane hyperpolarization (e.g., following action potentials, and other sources of current mediated through gap junctions) (Buzsáki and Wang 2012; Nunez and Srinivasan 2006). These will affect not only LFP but also the 'aggregate' field of the cortical surface ECoG and the scalp EEG signals. Taking all of the above-mentioned factors together, it is clear that the task of choosing the appropriate size of windows to look at our big picture is a challenging one.

A reductionist approach can be taken to this problem by investigating the minimum volume of brain tissue that is sufficient for the coordinated activity of neuronal networks. High frequency oscillations spanning gamma (30-120 Hz), ripple (120-250 Hz) and fast ripple (250-600 Hz) bands are the fastest known examples of coordinated network firing, which is especially important in intracranial recordings from epileptic brains (G. a. Worrell et al. 2012). The fast ripple oscillations, which are characteristic of ictal and interictal epileptiform discharges, are confined to sub-millimeter volumes of brain tissue and can be generated in vitro in populations of 1000-2000 neurons. Such cell counts occupy a field with a radius of ~200 μm—a proposed critical volume for coordinated network activity—which roughly corresponds to the size of the microelectrode. This suggests that microelectrodes are capable of sampling the action potential firing and LFP oscillations of specific neuronal ensembles, at least in the fast ripple frequencies.

Both electrode types would still register oscillations in the lower LFP spectrum from the more widely distributed network oscillations, which are often observed on several adjacent macro-contact points.

Considering all these concepts, neuronal activity is generated locally but mediates interactions across widespread network connections formed both within and across brain structures, much like the thalamocortical slow waves. Even though the optimal strategy to sample the broad spectrum of brain network oscillations is not yet known, the need for large-scale sampling technologies is generally recognized. Other techniques for capturing action potentials involving arrays (a bundle of 8 micro-electrodes) that span specific cortical layers or subregions have also been used in combination with LFP, ECoG and EEG recordings (Le Van Quyen and Bragin 2007). Such large-scale recordings that employ complementary technologies are key to elucidating the big picture of the brain's oscillating clockwork. In subsequent parts of this subsection, there is a review of the existing and future technical solutions to the large-scale human intracranial recordings.

Table 3.1. Engle Classification of prospective outcome [106].

Class I	Free of disabling seizures. A. Completely Seizure free since surgery. B. Non-disabling simple partial seizures since surgery C. Some disabling seizures after surgery but free of disabling seizures at least for 2 years. D. Generalized convulsions with anti-seizure drugs discontinuation only.
Class II	Rare Disabling seizures "Almost seizure-free" A. Initially free of disabling seizures but has rare seizures now. B. Rare disabling seizure since surgery. C. More than rare disabling seizures since surgery, but rare seizures at least for last 2 years. D. Nocturnal seizures only.
Class IIII	Worthwhile improvement A. |Worthwhile seizure reduction. B. Prolonged seizure-free intervals amounting to greater than half the follow-up period, but not <2 years.
Class IV	No worthwhile improvement A. Significant seizure outcome. B. No appreciable changes. C. Seizures worse.

Table 3.2 IALE proposal for new classification of outcome with respect to epileptic seizures [78].

Outcome classification	**Definition**
1	Completely seizure-free, no auras
2	Only auras, no other seizures
3	One to three seizures days per year; ± auras
4	Four seizures days per year to 50% reduction of baseline seizure days; ± auras
5	Less than 50% reduction of baseline seizure days
6	More than 100% increase of baseline seizures days ; ± auras

Chapter 4

Interracial phase-amplitude coupling localizes epileptogenic tissue in temporal lobe epilepsy

Epilepsy is a chronic disease defined by recurrent seizures (Leppik 2010). Approximately 1/3 of patients are not amenable to conservative treatment but can be evaluated for surgical resection of the pathologic brain tissue after failing enough anti-epileptic drugs (AEDs). The purpose of this surgery is to remove the seizure onset zone (SOZ), defined as the area of cortex from which the seizures originate (Banerjee, Filippi, and Allen Hauser 2009; Geertsema et al. 2015). The gold standard method for the evaluation of SOZ is ictal recording from intracranial electroencephalogram (iEEG) and synchronized video (Geertsema et al. 2015; Kim et al. 2012). In this process, patients are implanted with multiple electrode arrays and monitored in the EMU. During this time, a great deal of interictal data is also recorded but is of less use to the clinical teams. Among the many electrophysiologic biomarkers being investigated (G. a. Worrell et al. 2012; Kim et al. 2012), phase-amplitude coupling is one which has emerged as a reasonable promising marker to be used in seizure prediction (Catalina Alvarado-Rojas et al. 2014) and detection (Kohtaroh Edakawa, Takufumi Yanagisawa, Haruhiko Kishima, Satoru Oshino, Hui Ming Khoo, Maki Kobayashi, and Yoshimine 2016). Interictal evaluations have largely involved cognitive or behavioral testing (Kucewicz et al. 2014, 2015) and have made assumptions that any electrodes in the seizure onset zone are of little consequence for analysis. The aim of this study is to investigate the role of phase-amplitude coupling to distinguish between electrodes in SOZ and non-SOZ.

4.1 Phase Amplitude Coupling

Greater insights into the neuronal mechanisms of large population behavior and the brain oscillations emanating therein during the interictal period could not only improve seizure onset localization and seizure prediction, but also help improve information surrounding the

pathophysiology of seizure initiation in the brain (Catalina Alvarado-Rojas et al. 2014). High-frequency activity including gamma oscillations and ripples (up to 500Hz) have been associated with epileptiform activity in human epilepsies (R T Canolty et al. 2006; Julia Jacobs et al. 2016; Shennan A Weiss et al. 2016).

The cortex has natural brain rhythms that span over five scales of magnitude (Buzsaki 2006). Also, there is a logarithmic inverse relationship between power and frequency, known as power-law, where power drops off from low frequencies to high resulting in a 1/f relationship. This is a signature of scale-free systems (Buzsaki 2006), where higher frequencies are modulated by lower frequencies (in phase-phase or phase-amplitude coupled scenarios), larger networks are recruited by lower frequencies (Buzsáki 2004). There is evidence for these dynamics both physiologically and pathologically (Vanhatalo et al. 2004). In the temporal lobe, PAC between theta phase and high gamma amplitude is largely observed (R T Canolty et al. 2006; Ryan T. Canolty et al. 2012). In different anatomical areas, theta-gamma is not generally expected to be the relevant cross-frequency coupling of oscillations. Beta-gamma between thalamus and motor cortex or alpha-gamma (Osipova, Hermes, and Jensen 2008). The relevant cross-coupling has also been shown to be state dependent. In particular, Slow Wave Sleep has been shown as relevant for cross-frequency coupling. Edakawa recently showed that seizures can be detected using PAC when utilizing beta and high gamma as an adjunct to ictal biomarkers (Kohtaroh Edakawa, Takufumi Yanagisawa, Haruhiko Kishima, Satoru Oshino, Hui Ming Khoo, Maki Kobayashi, and Yoshimine 2016). Their work alluded to the possibility of interictal periods where PAC values increase and may generate false-positives in differentiating the ictal from the interictal state, but whether long periods of interictal time could be used to differentiate SOZ from non-SOZ was not a question explored. Moreover, few studies have sought to obtain the best frequency range and best state in interictal time to determine the seizure onset zone or even whether the seizure onset zone can be determined using PAC as an interictal biomarker.

Coupling between slow potentials and HFA as a phenomenon is being actively studied in many diseases and in normal physiologic states. How this phenomenon relates to epilepsy is very much an open question, and insights can be gained into cortical network excitability (Catalina Alvarado-Rojas et al. 2014). It has been shown that slow oscillations are able to trigger and group HFA. The coupling between Berger bands and HFA has been termed *nested oscillations*, and may be a significant signature of cortical activation and perhaps a novel biomarker in epilepsy (Guirgis et al. 2015; Ibrahim et al. 2014; Maris, van Vugt, and Kahana 2011). Previous studies in iEEG have identified PAC of HFA (40-180Hz) being modulated by theta or delta (0.5-9Hz) (Catalina Alvarado-Rojas et al. 2014). These observations helped develop a notion to study in detail the physiology of PAC in patients with medically refractory focal epilepsy.

The main aim of this study was to develop and evaluate a method for identification of the SOZ using a machine learning approach based on biomarkers extracted from the PLV of ictal ECoG recordings obtained using standard intracranial electrode arrays. We hypothesized that PAC between the amplitude of high frequency (80-150 Hz) and a phase of low frequency (4-30 Hz), when recorded from ECoG data immediately before and after seizure onset, could be used as a biomarker to identify SOZ. Also, we demonstrated that the features extracted from the PLV could automatically classify SOZ and non-SOZ electrodes.

4.2 Methods

4.2.1 Patient population

This was a retrospective study of 18 patients with epilepsy who underwent a Phase II epilepsy surgery evaluation with intracranial electrodes at Le Bonheur Children's Hospital in Memphis, Tennessee. The patients were evaluated between August 2013 and July 2015 (Table 4-1). Eight patients who had no resection after their Phase II evaluation or had less than six months follow-up were excluded, leaving 10 patients (7 males, ages 23.0 ± 9.0

[mean ± SD] years) (Table 1). All patients had a diagnosis of medically intractable epilepsy and underwent pre-surgical evaluation including scalp video-EEG monitoring and MRI of the brain. Seven patients had temporal lobe seizures and three patients had extra-temporal epileptogenicity. Four patients with temporal lobe epilepsy underwent Phase II evaluation because they had a normal MRI of the brain. Three patients with possible mesial temporal sclerosis (i.e., Patients 1, 4, and 5) needed a Phase II evaluation for localization of the seizure focus. Patient 4 had left mesial temporal sclerosis in addition to left thalamic and generalized white matter volume loss. MRI of the brain in patients 1 and 5 showed reduced hippocampal size without an associated increased signal, and their scalp EEG features did not reveal a clear temporal lobe onset of seizures. Three patients with extra-temporal lobe epilepsy (Patients 2, 9, and 10) also had findings necessitating a Phase II evaluation. Patient 2 had a suspected non-lesional dominant frontal lobe focus, Patient 9 had tuberous sclerosis complex with multiple tubers; patient 10 had a prior resection in addition to the seizure origin being close to the visual cortex.

Subdural grid and strip electrodes (4.5 mm diameter; 10 mm inter-electrode distance; PMT Corporation, Chanhassen, MN, USA) were surgically implanted to cover the probable epileptogenic area and, if necessary, to study the relation between the epileptogenic area and functional cortex. The postsurgical follow-up periods ranged from 6 to 28 months.

4.2.2 Visual identification of SOZ and surgical outcome

The recorded ECoG data were independently assessed offline by two board certified epileptologists (James Weless and Basanagoud Mudigoudar, Nuerologists in Le Bonheur hospital) to clinically delineate the SOZs corresponding to each of the 21 seizure instances in all patients (603 electrodes total). The SOZ was determined by the epileptologists based on the visual inspection of ECoG at ictal onset and during early spread. In patients with multiple seizure foci, the visually identified SOZ (vSOZ) comprised a set of all electrodes responsible for all of the captured seizures. All patients underwent epilepsy surgery. The resection area

was prospectively determined based on the vSOZ electrodes from the ictal ECoG recordings. When necessary, the SOZ for resection could be modified in relation to the eloquent cortex location that was identified by cortical stimulation mapping. Since this study was performed retrospectively, the results of this study were not used to guide the surgical decisions.

Engel classification was used to classify the seizure outcome. The outcome was Engel Class I in six patients, Class III in one patient, and Class IV in three patients (Table 4-1). We simplified the seizure outcome into the following two groups for our analysis: Group I comprised the six Engels Class I patients who were completely seizure-free without auras for at least six months following surgery; Group II comprised the four non-seizure-free patients who all had improved seizure control, but were not seizure free.

4.2.3 ECoG recording, PLV calculation, and extraction of features

Subdural ECoG recordings were acquired using a standard clinical video EEG system (XLTEK, Natus Medical Inc., Pleasanton, CA, USA) with two additional subdural electrodes over brain regions without active discharges used as ground and reference electrodes. The ECoG data were recorded at 1 kHz after bandpass-filtering at 0.1-300 Hz. We used a bipolar montage with two pairs of adjacent electrodes after excluding those with artifacts.

Table 4.1 Patients' demographic and clinical data. CPS: Complex partial seizures; FCD: focal cortical dysplasia; FL: frontal lobe; PL: parietal lobe; TL: temporal lobe; OL: occipital lobe.

Patient	Age (yr)/ Gender	Pathology	MRI	EEE (yrs)	Seizure type	Seizure focus	Seizure instances	Num. Elec. (Grid/Strip)	Follow-up (months)	Engel Class
1	27/F	Hippocampal sclerosis & micro-dysgenesis of amygdala	Decreased volume of the left hippocampus	10	CPS	Left TL	1	48/16	13	I
2	27/M	FCD, Type 1A	Normal	21	CPS	Left FL	2	80/18	8	I
3	20/M	FCD & microdysgenesis	Normal	13	CPS	Left TL	2	40/20	14	I

Patient	Age (yr)/ Gender	Pathology	MRI	EEE (yrs)	Seizure type	Seizure focus	Seizure instances	Num. Elec. (Grid/Strip)	Follow-up (months)	Engel Class
4	40/M	Hippocampal sclerosis	Left thalamic & hippocampal volume loss, & white matter volume loss	36	CPS	Left TL	2	40/14	16	I
5	19/F	Hippocampal sclerosis	Left hippocampal volume loss	6	CPS	Left TL	3	48/12	5	I
6	21/M	FCD, Type 2A	Normal	10	CPS	Right TL	1	32/24	26	I
7	27/M	Gliosis, chronic inflammation, reactive changes	Normal	8	CPS	Left TL	3	41/30	14	IV
8	20/F	FCD, Type 2A	Normal	3	CPS	Left TL	3	32/20	28	IV
9	5/M	Cortical dysplasia/tuber	Multiple cortical tubers	2.6	CPS & myoclonic tonic seizures	Right PL	1	32	6	III
10	17/M	FCD	Prior right Occipital resection	15	Simple partial seizures & CPS	Right OL	3	32/24	9	IV

Our analysis is based on the PLV, which is a measure of cross-frequency coupling of phase synchronization (Lachaux et al. 1999). It has been demonstrated that the PLV between the phase of low frequency (4-30 HZ) and the phase of the Hilbert transform of high gamma frequency (80-150 HZ) correlated strongly with multi-unit firing bursts within the core territory of the seizure; thus, it has been proposed as a reliable biomarker for identifying the SOZ (Shennan A Weiss et al. 2013; Penny et al. 2008). PLV was calculated as:

$$PLV = \left| \frac{1}{N} \sum_{n=1}^{N} \exp\left(i(\varphi_{4-30}[n] - \varphi_{a_{80-150}}[n])\right) \right| \qquad (1)$$

where φ_{4-30} is the instantaneous phase of the ECoG signal in the 4-30 Hz frequency band (calculated using the Hilbert transform), a_{80-150} is the instantaneous amplitude of the high gamma frequency band 80-150 Hz calculated from the Hilbert transform of ECoG signal, and

$\varphi_{a_{80-150}}$ is calculated from a second Hilbert transform and represents the instantaneous phase of a_{80-150}.

After applying a notch filter at 60 Hz and 120 Hz on the ECoG data, we calculated PLV during two time intervals: (1) a five-minute inter-ictal time window, and (2) a five-minute pre- and post-ictal time window with the midpoint at the ictal onset identified visually by two epileptologists. During the baseline period, patients were instructed to be at rest with eyes open while they were awake without any sign of drowsiness. By visually inspecting the ECoG signal during the baseline period, we selected 60-second time segments without eye blink and interictal epileptiform discharges or excess slow waves. Then, we calculated the mean (μ_b) and standard deviation (σ_b) of the PLV during this 60-second baseline and used these values in our feature extraction algorithm. After calculating PLV in the five-minute pre- and post-ictal time window, we used features extracted from the value of PLV in a 30-to-10-second time window before the seizure onset in our algorithm. We also used the values of PLV from seizure-onset to seizure-offset as a feature in our algorithm. The seizure-offset was visually identified by two epileptologists (JW and BM).

Previous studies reported that high frequency oscillations in high gamma and other frequency bands during several seconds prior to clinical seizure onset can identify the SOZ (Fujiwara et al. 2012; Ochi et al. 2007). We also observed that the PLV (between the amplitude of high gamma and phase of lower rhythms) was enhanced prior to clinical seizure onset in the vSOZ electrodes. In agreement with Weiss et al. (Shennan A Weiss et al. 2013), we also observed enhancement of the PLV in some vSOZ electrodes. Furthermore, we found that enhancement of the PLV in a 30-sec-to-10-sec pre-ictal period can efficiently separate vSOZ electrodes from non-vSOZ electrodes. By investigating different features extracted from PLV before and after ictal onset, we found that a combination of four features extracted

from pre-ictal PLV and one feature extracted from PLV after ictal onset can optimally identify vSOZ.

Our algorithm for identifying the SOZ was based on the five features described below. The first four features were extracted based on the value of PLV in a 30-to-10-second time window before the seizure onset. The last feature was calculated based on the value of PLV from seizure onset to seizure offset.

1. PLV positive: This feature was assigned to "1" if the PLV would exceed a threshold of "$\mu_b + 6 \times \sigma_b$", where μ_b and σ_b are the mean and standard deviation of PLV in 60-second time intervals during the baseline, respectively.
2. *Duration of PLV positive*: Duration of PLV signal exceeding a threshold at $\mu_b + 6 \times \sigma_b$
3. *PLV peak*: maximum value of PLV.
4. *PLV mean:* average value of PLV.
5. *PLV power:* The power of the PLV signal during seizure onset until the end of seizure which was calculated as $\frac{1}{N+1}\sum_{t=0}^{N} PLV(t)^2$ where $t = 0$ is the seizure onset time and $t = N$ is the seizure offset time.

These features were selected based on our investigation of the values of PLV in resected and non-resected electrodes in seizure-free patients (Figure 4-2). In addition, Malinowska et al. (Malinowska et al. 2015) used similar features based on HFO to identify SOZ electrodes..

Figure 4-2 shows the PLV of resected and non-resected electrodes in seizure-free patients. As shown in this figure, the value of PLV before seizure onset was generally larger in resected electrodes than in non-resected electrodes. In seizure-free patients, the peak and power of PLV after seizure onset were larger in resected electrodes than in non-resected

electrodes. Figure 4-2-c shows the average of PLV across all seizure instances in seizure-free patients (Patients 1-6). As shown in this figure, both the peak and mean power of PLV were larger in the resected electrodes than in the non-resected electrodes. We used these characteristics of the PLV to extract the above five features for identification of the SOZ electrodes. We named the identified SOZ electrode aSOZ (i.e., algorithm-positive SOZ), according to our algorithm.

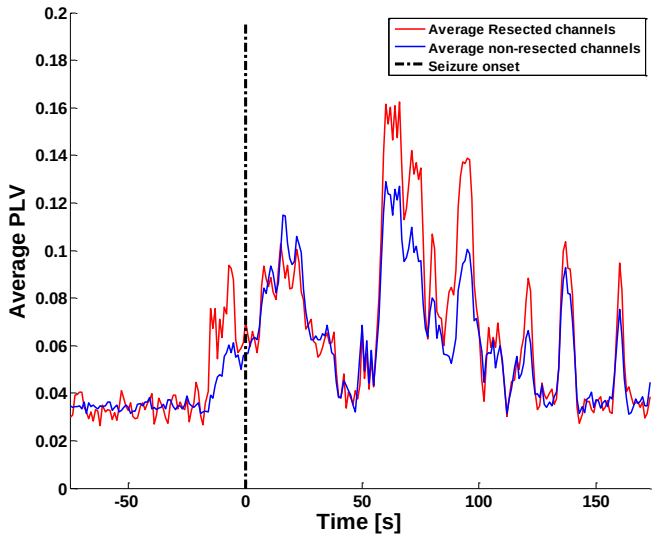

(a)

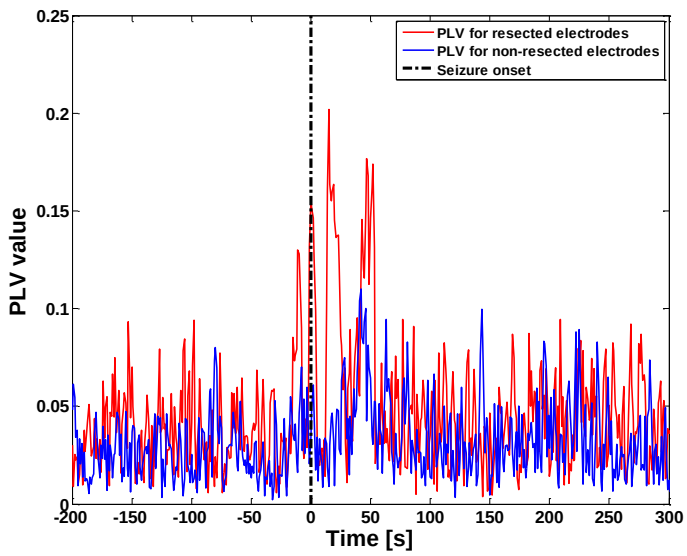

(b)

Figure 4.1. Comparison of the average values of PLV across resected and non-resected electrodes in seizure free patients. (a) Average PLV across resected (red) and non-resected (blue) electrodes in Patient 1 are shown. (b) Average PLV was calculated across all resected (red) and non-resected (blue) electrodes in all seizure-free patients. Time zero represents seizure onset.

4.2.4 Classification of SOZ electrodes

In seizure-free patients, the resected area (RA) comprised the SOZ, and all electrodes outside of the RA were not SOZ. In our machine learning approach, we classified the subdural electrodes in seizure-free patients into two classes: resected electrodes in Class 1 and non-resected electrodes in Class 2. We trained and cross-validated a logistic regression classifier to classify each electrode in seizure-free patients into two classes. The logistic regression has been used in previous studies to differentiate interictal and ictal HFOs and to classify the patterns in the brain recordings (Mirowski et al. 2009; Okanishi et al. 2014; Freedman 2009). In seizure-free patients, we defined electrodes in Class 1 as aSOZ and the rest of electrodes as non-aSOZ (Class 2). There were 140 resected electrodes (Class 1) and 252 non-resected electrodes (Class 2) in seizure-free patients. We calculated five aforementioned features, extracted from the PLV in all electrodes in seizure-free patients and trained and cross-validated the logistic regression classifier based on these features. We implemented the logistic regression using L1 regularization and a grid search for the regularization parameters within a logarithmic range of $10^{-2} – 10^{3}$, and then validated the classifier using a 10-fold cross-validation approach. We performed receiver operating characteristic (ROC) analysis to evaluate performance of the classifier in seizure-free patients. Finally, we tested the performance of the trained logistic regression classifier to identify aSOZ electrodes in non-seizure-free patients (211 electrodes in Patients 7-10).

4.2.5. Correlation between seizure outcome and resection of aSOZ electrodes

We calculated the seizure outcome as:

$$Seizure\ outcome = \frac{number\ of\ seizures\ before\ surgery - number\ of\ seizures\ after\ surgery}{number\ of\ seizures\ before\ surgery}$$

where the number of seizures represents the average number of seizures per month pre- and post-operatively. Then, we calculated the correlation between the seizure outcome and the number of non-resected aSOZ electrodes in non-seizure-free patients.

4.3 Results

Clinical data were reviewed and analyzed for 10 patients who underwent resection following a Phase II evaluation during the study period. The demographics of the patients along with characteristics of their epilepsy, pathology, and outcome are presented in Table 4-1. Six patients had temporal lobe seizures and four patients had extra-temporal lobe seizures. Their follow-up duration ranged from six to 28 months.

Figure 4-3 shows the PLV values in a seizure-free patient (Patient 1) and a non-seizure-free patient (Patient 6). As shown in this figure, PLV was positive in some electrodes before seizure onset. We considered an electrode as PLV-positive if the PLV of that electrode during 30 to 10 seconds before seizure onset was larger than the threshold at "$\mu_b + 6 \times \sigma_b$", where μ_b and σ_b are, respectively, the mean and standard deviation of PLV in a 60-second time interval during the baseline.

(a)

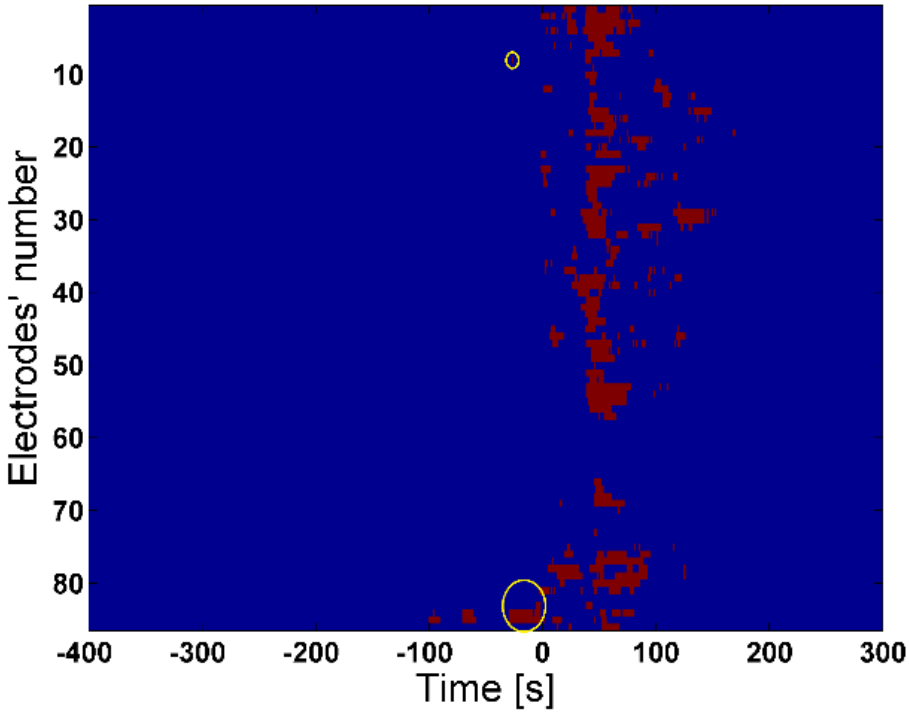

(b)

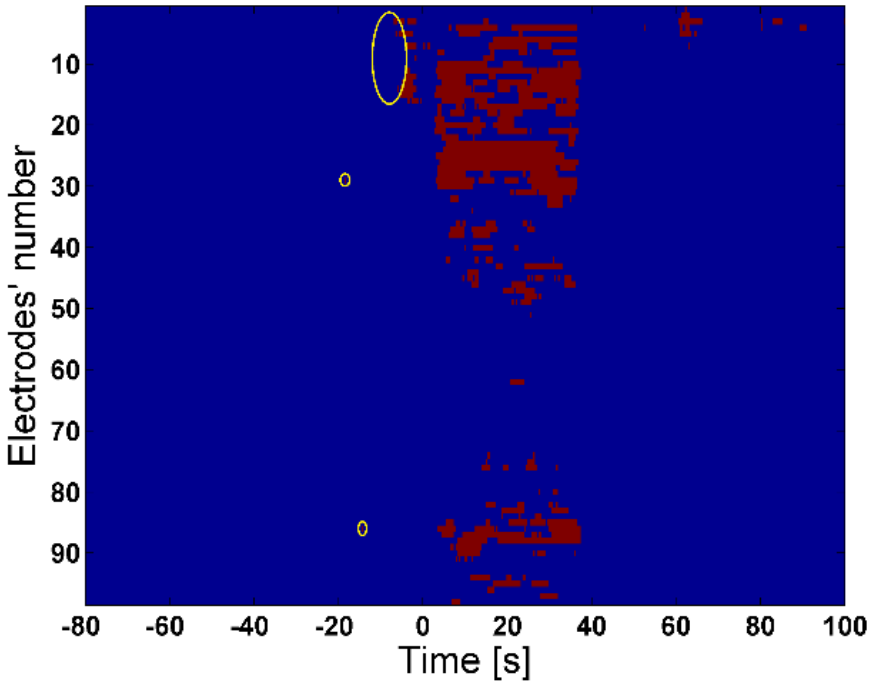

Figure 4.2. PLV for a seizure episode in (a) a seizure-free patient (Patient 1), and (b) a non- seizure-free patient (Patient 6). Time point zero corresponds to seizure onset. Early PLV-positive before seizure onset in both patients is noticeable and marked with yellow ellipse. In (a), two PLV-positive electrodes (i.e., electrodes #84 and 85 correspond to the strip electrodes PST1 and PST2) were resected. In (b), the electrodes, which had early

PLV-positivity have not been completely removed (yellow circles show PLV activity 10 sec before onset in electrodes LFT 3, 4, 5, 14, 29, and 18 sec before the onset in AST 1).

Figure 4-4 shows the locations of SOZ electrodes and the resected areas in all patients. Our algorithm identified 54 aSOZ electrodes in six seizure-free patients; 52 of those electrodes (96%) were within the resected area (Table 4-2). All aSOZ electrodes were within the resected area in five of the six seizure-free patients; no false positive SOZ electrodes were found in these patients. In the remaining seizure-free patient (Patient 6), the proposed algorithm found eight aSOZ electrodes: six within the resected area; two were false positive and located outside the resected area (Table 4-2). Forty-seven electrodes were identified visually (by the two epileptologists) as vSOZ in seizure-free patients; our algorithm detected 28 of those electrodes as aSOZ. The ROC curve of the proposed classifier in seizure-free patients is plotted in Figure 4-a. The areas under the ROC curve were 69%. The accuracy and precision of the classifier were 83% and 90%, respectively.

Our algorithm identified 62 aSOZ electrodes in non-seizure-free patients (Patients 7-10), with 43 (69%) of the electrodes located within the resected area and 19 (31%) outside of the resected area (Table 4-2). Forty electrodes were identified visually (by the two epileptologists) as vSOZ in non-seizure-free patients; our algorithm detected 20 of those electrodes as aSOZ. It is noteworthy that nine electrodes in non-seizure-free patients were aSOZ while these electrodes were not vSOZ and they were outside of the resected area.

After comparing the seizure frequency before and after surgery in non-seizure-free patients, we found that Patients 7, 8, and 10, who were Engle Class IV and had higher postsurgical seizure frequency compared to Patient 9 who was Engle Class III. It is notable that Patient 9 had the smallest number of non-resected aSOZ electrodes among the non-seizure free patients. Patient 8 had up to three seizures per month before surgery and her seizure frequency was decreased to one or two seizures per month after surgery. In Patient 8, our algorithm identified four aSOZ electrodes outside of the resected area; two of those

electrodes were vSOZ but not resected due to an overlap with eloquent cortex. Patient 10 had up to four seizures per day before surgery and improved to less than three seizures per week after surgery. Our algorithm identified six electrodes outside of the resected area in this patient, three of which were visually detected by the epileptologist, but not resected.

Figure 4-4-b illustrates the correlation between the number of aSOZ electrodes beyond the resected area and the seizure outcome in four non-seizure free patients. As shown in this figure, poorer seizure outcomes correspond to a larger number of non-resected aSOZ electrodes.

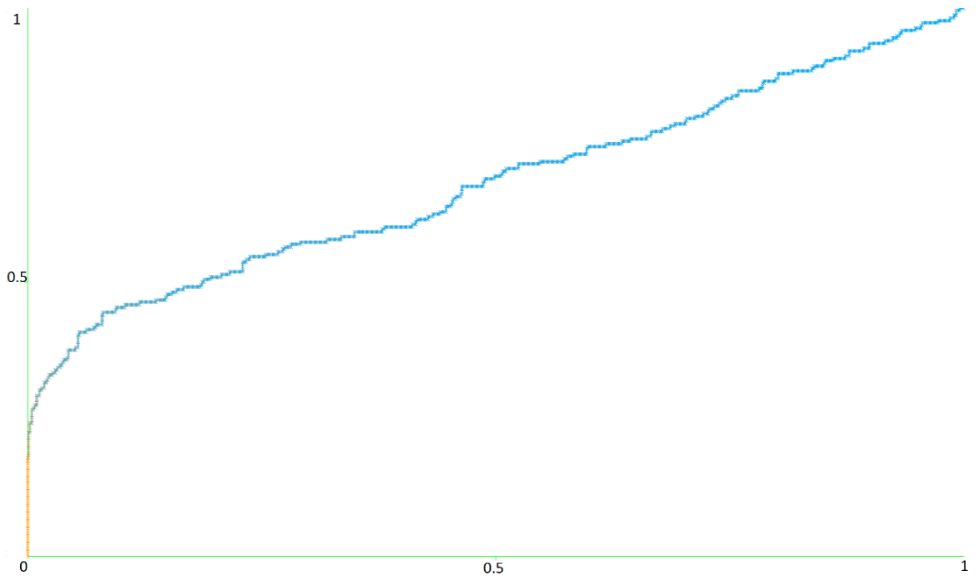

Figure 4.3. Evaluation of the performance of the proposed method. (a) The ROC curve of the proposed classifier in seizure-free patients.

(a)

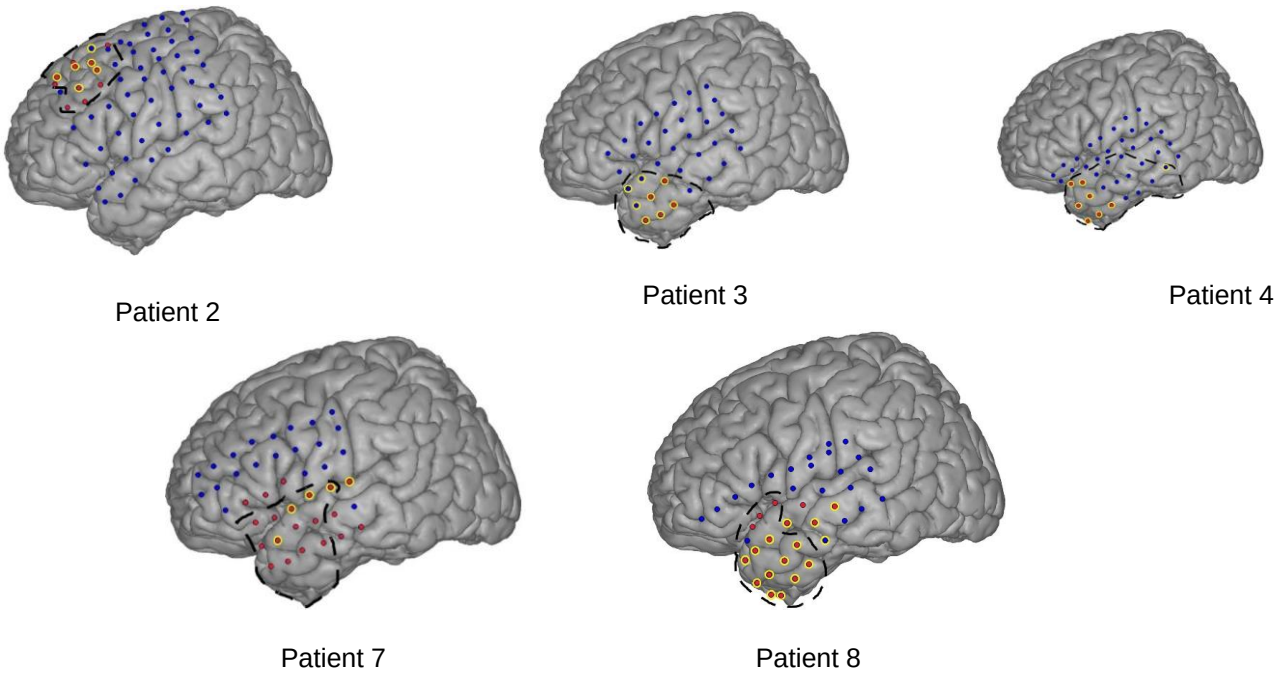

(b)

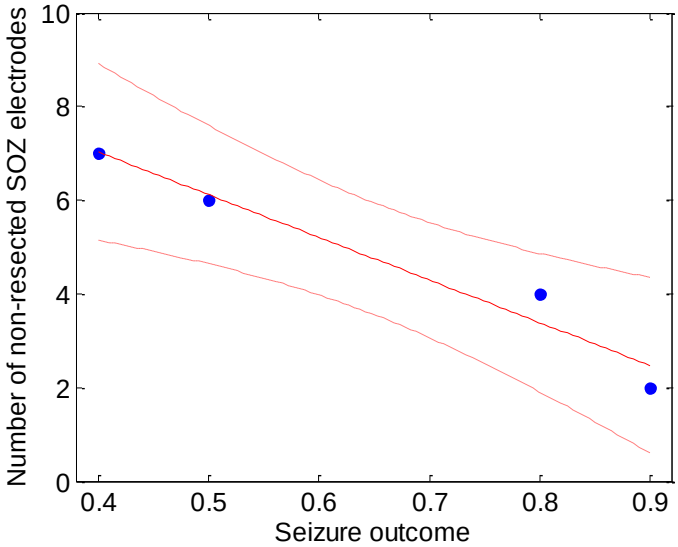

(c)

Figure 4.4. Evaluation of the performance of the proposed method. (b) Locations of the subdural electrodes—after normalization to the Montreal Neurological Institute (MNI) coordinate system—are shown on top of the cortical surface in three seizure-free (top) and two non-seizure-free (bottom) patients. Solid dots in red color represent SOZ electrodes identified by our algorithm. Yellow circles represent SOZ electrodes identified visually by epileptologists. The broken black line shows the resected area. (c) Correlation between the numbers

of identified SOZ electrodes by the proposed method beyond the resected area and the seizure outcome in four non-seizure-free patients. A poor seizure outcome correlates with a larger number of non-resected SOZs.

Table 4.2 Comparison of resected electrodes, SOZ electrodes identified by our algorithm, and visually identified SOZ electrodes by epileptologists in seizure-free patients.

Patients	**Electrodes**	**Resected Electrodes**	**Identified as SOZ by our algorithm**	**Visually detected by epileptologists**
1	Label	TG 1:6, 9:12, 17:20, 25:27 TP 1:6 AST 1:4 PST 1:4	PST 1, 2, 3	PST 1-2
	number	31	3	2
2	Label	LF 33:35, 42:44, 49:52, 57:60 LPIH 3,4	LF 33: 35, 42, 43, 49, 50, 51, 52, 57, 60	LF 42,43,50,51,57,59
	number	16	11	6
3	Label	LFT 2:5, 10:12, 18,19, TP 1:6, AST 1:4	LFT 2:4, 11:12, TP 2:6	LFT 2:4, 10:13, 18:20, TP 1:3, AST 1:3
	number	19	10	16
4	Label	LT 1:7,9:14, 17:21, TP 1:6, AST 1:4, PST 1:4	LT 1:3, 9,10, 17,18, PST 2, 3	LT 1:3, 7, 9,10, 17, 18, TP 1:4, AST 1:3, PST 1:4
	number	32	9	19
5	Label	LT 1:3, 9, 10, 17, 18, 25, 26 ATP 1:4 AST 1:4	LT 1, 2 ,9 ,17,25 ATP 1:4 AST 1:4	AST 1,2
	number	17	13	2
6	Label	RTG 1:3, 9:12, 17:20, 25:29 RAST 1:4 RPST 1,2 RTP 1:4	RTG 1,9 RAST 1,2 RPST 3,4 RTP 1,2	RAST 1,2
	number	26	8	2

Table 4.3 Comparison of resected electrodes, SOZ electrodes identified by our algorithm, and visually identified SOZ electrodes by epileptologists in non-seizure-free patients.

Patients	Electrodes	Resected Electrodes	Identified as SOZ by our algorithm but not resected	Identified as SOZ by our algorithm and resected	Visually detected by epileptologists
7	Label	LFT 4:6,11:14, 19:23 AST 1:4	LFT 3,7,8, 15, 24, 27:29	LFT 4:6,11:14, 19:23 AST 1,2	LFT 12, 21:24, AST1,2
	number	16	8	14	7
8	Label	LT 1:4, 9:12, 17:19,25:28 AST1:4	LT 13,14, 20, 21	LT 1:4, 9:12, 17,26,27,28, AST 1:4	LT 1:5, 9:14, 17:20, AST 1:3, PST 3,4
	number	19	4	16	20
9	Label	RPG 13:15, 21:24, 29:32	RPG 27, 28	RP 14, 22, 31, 32	RPG14, 21, 22, 23, 27, 28, 29
	number	11	2	4	7
10	Label	ROG 20, 21, 28, 29, 30 IIH 3,4, SIH 3,4	ROG 2,10,11,12,19, 27	ROG 28,29,30, SIH 2,3,4 IIH 1,2	ROG 11,12,19,20, 21, 28
	number	9	6	8	6

4.4 Discussion

The results of this study revealed that the PLV between the amplitude of high gamma and the phase of lower frequency of ictal ECoG recordings can identify SOZ electrodes. Previous studies have investigated the application of PAC and PLV using different combinations of frequency bands to characterize ictal and interictal states (Cohen 2008; Weiss Shennan et al. 2015; Kohtaroh Edakawa, Takufumi Yanagisawa, Haruhiko Kishima, Satoru Oshino, Hui Ming Khoo, Maki Kobayashi, and Yoshimine 2016). The results of these studies demonstrated that coupling between frequency bands of ECoG is useful for detection of seizure onset. Some studies reported that coupling between different frequency bands allow characterization of the seizures and mechanisms of the epileptiform discharges, and suggested that the spatial distribution of coupling can be useful in surgical decision-making

(Weiss Shennan et al. 2015). Although previous studies reported the significance of amplitude of high gamma in seizure detection (J. Jacobs et al. 2012; Höller et al. 2015; Ochi et al. 2007; Ferastraoaru et al. 2016), the results of some recent studies demonstrated that PAC characterizes epileptiform activity more accurately than the amplitude of high gamma frequencies (Shennan A Weiss et al. 2013; Ibrahim et al. 2014). In this study, we applied PAC to distinguish SOZ and non-SOZ electrodes using ictal ECoG recordings.

As shown in Figure 4-4, the aSOZ electrodes in non-seizure-free patients were both within and outside of the resected area. The fact that our algorithm identified that some aSOZ electrodes within the resected area in all non-seizure-free patients may correspond to the improvement of seizure in these patients after surgery. On the other hand, some aSOZ electrodes were outside the resected area in all non-seizure-free patients, and we hypothesis that the failure to resect the area underneath of these electrodes resulted in a non-seizure-free status in these patients. It is noteworthy that most of the non-resected vSOZ electrodes in non-seizure-free patients were also aSOZ. Since these electrodes were overlapping or adjacent to the eloquent cortex, a decision was made not to resect those electrodes, even though there was concern that they were involved in seizure onset. As listed in Table 4-3, one electrode in Patient 7 (i.e., LFT 24), three electrodes in Patient 8 (i.e., LT13, LT14, and LT 20), two electrodes in Patient 9 (i.e., RPG27 and RPG28), and three electrodes in Patient 10 (i.e., ROG11, ROG12, and ROG 19) were detected visually by epileptologists and identified as aSOZ; however, these electrodes were not resected. Post-operation, these electrodes have been confirmed by neurologists that are inside the language/vision or the memory part of the cortex.

Some aSOZ electrodes were outside the resected area in non-seizure-free patients, though we cannot specify those electrodes as true positive or false positive. However, the following findings indicate that those electrodes are most likely true positive: (1) The non-resected aSOZ electrodes were close to the resected area. This may correspond to the fact that

seizure intensity reflects the degree of its consecutive development and engagement from an original epileptogenic core area to the secondary or adjacent areas (Ikeda et al. 1999); (2) in seizure-free patients, using the same method applied in non-seizure-free patients, only two out of 54 aSOZ electrodes were outside of the resected area; and (3) we found a correlation between the number of non-resected aSOZ electrodes and the seizure outcome (Figure 4-4-c).

4.5 Conclusion

We developed and evaluated a method to identify SOZ in patients with epilepsy using ictal ECoG recordings. To this end, we extracted five features based on the phase coupling between the higher frequency (80-150 Hz) and lower frequency (4- 30 Hz) rhythms. We identified SOZ electrodes using a machine learning approach based on the logistic regression classifier. We found that almost all (more than 96%) of the aSOZ electrodes were within the resected area in seizure-free patients. Furthermore, the proposed algorithm found 31% of aSOZ electrodes outside of the resected area in non-seizure-free patients. We also demonstrated that the seizure outcome in non-seizure-free patients correlated with the number of non-resected aSOZ electrodes. The approach in this study could assist in identification of the SOZ and, as such, may enhance the standard clinical procedure of visual inspection. This has the potential to improve seizure-free outcomes, and we believe it should be included in the surgical decision-making process when intracranial electrodes are utilized. Further study using a larger number of patients would confirm our findings.

Chapter 5

High Frequency Oscillations in different epochs

Summary:

For the past two decades, research for any potential biomarkers for seizure onset has been fueled by the introduction of interictal high-frequency oscillations (HFOs, 80–500 Hz) (Urrestarazu et al. 2007; Staba et al. 2002). These brief oscillations visible on intracranial EEG (iEEG) are considered strongly bound to the seizure onset zone (SOZ) (Julia Jacobs et al. 2008; Crépon et al. 2010) and many researchers suggested that they can be correlated with surgical outcome (Haegelen et al. 2013; van 't Klooster et al. 2015). However, not all HFOs are pathological. In spite of the current researches as to whether fast ripples (FR, 250- 500Hz) seem to always be pathological (Menendez de la Prida, Staba, and Dian 2015), ripples (80-250Hz) are more involved in physiological processes (Alkawadri et al. 2014).

5.1 Contributions to High Frequency Oscillations

By recording directly from the human brain, we get a unique opportunity to investigate the correlation of neurans with brain functions. These cognitive phenomena are supposed to be orchestrated by broadband cortical and subcortical neuronal networks coordinated into synchronous oscillations over a wide spectrum of frequencies (Buzsaki 2006). High frequency oscillations (HFOs) extend beyond the boundary of gamma band activity and have recently been the focus of both animal and human studies in the case of neurophysiology of cognition and epilepsy (G. a. Worrell et al. 2012).

In spite of all researches, little is known about the physiological and pathological role of HFOs out of the gamma band. These ultra-fast neuronal oscillations, were primarily recorded in rodent hippocampus as part of their sharp-wave ripple complexes, known as 'ripples'. Ripples are short discharges of synchronized firing of neuronal ensembles, mainly occurring during states of rest and sleep (Buzsaki, Horvath, and Urioste 1992).It is been said that in sleep, ripples have been correlated with the activity of neurons in specific hippocampal

regions that were active during preceding behavior in rats. Human HFOs which are faster than the ripples, called ‘fast ripples’ (250–500 Hz), were initially correlated with pathological network activity in seizure (A. Bragin et al. 1999; Staba et al. 2002). Subsequently, interictal gamma (G. A. Worrell et al. 2004) and ripple (G. A. Worrell et al. 2008) were also reported to be elevated in the SOZ in patients with focal epilepsy (Gregory a Worrell and Gotman 2011), (Foster and Wilson 2006). In addition, fast ripple oscillations in some studies have been associated with normal physiological functions (Baker, Gabriel, and Lemon 2003; Barth 2003). Hence, the frequency of an HFO does not seem to be a reliable biomarker whether it is pathological or physiological. Nonetheless, as HFOs are raised in a focal epileptogenic brain, there is a potential that they could be used as a clinical biomarker (Staba 2010; Gregory a Worrell and Gotman 2011). It is also been reported that the rate of HFO in SOZ is higher than in other areas during interracial periods and more frequent during slow-wave sleep compared to wakefulness (Staba et al. 2004).

The most researches identifying HFOs is based on human identification (Haegelen et al. 2013; Kerber et al. 2014; Van Diessen et al. 2013; Julia Jacobs et al. 2010). This requires specially trained personnel and is very labor intensive, taking an hour to review 10 min of data from a single channel (Rina Zelmann et al. 2009). The feasibility of translating HFO biomarkers into clinical practice is quite low unless automated methods are employed (G. a. Worrell et al. 2012).

A significant challenge in the clinical use of HFOs is the difficulty in identifying them in intracranial EEG recording; since they are brief (<100 ms), low amplitude, uncommon (occurring <0.1 % of the time in channel,) and require significant data processing. The well-studied means of identifying HFOs is based on human identification (Haegelen et al. 2013; Kerber et al. 2014; Van Diessen et al. 2013; Julia Jacobs et al. 2010). This requires specially trained personnel and is very labor intensive, taking an hour to review 10 min of data from a

single biomarker into clinical practice and is quite low, unless automated methods are employed (G. a. Worrell et al. 2012; Gliske et al. 2016).

The main goal of the current study is to provide a reliable algorithm capable of identifying HFOs (including ripples and fast ripples) in long-term intracranial EEG data without any per-patient tuning or operator intervention. We also investigated the correlation of the rate of HFO in four distinct epochs, including sleep, awake, pre-ictal and ictal time, and the SOZ, and also compare it to the resection area and the outcome of surgery.

5.2 Method

5.2.1 Patient population and data

We selected consecutive patients with medication refractory who underwent continuous intracerebral (depth, strip and grid electrodes) EEG recordings at the Johns Hopkins Hospital between June 2012 and April 2014 for seizure foci identification and potential surgical treatment. We considered those recording just from patients: (1) diagnosed with mesial temporal or neocortical onset seizures, (2) with at least 12 h of interictal activity before the first seizure, during clinical monitoring, (3) at least 2 minutes of the ictal event. Based on clinical requirements, various combinations of penetrating depth electrodes and subdural electrode grids were surgically implanted for prolonged seizure monitoring. Data were continuously acquired at 10 kHz from up to 128 channels (Digital Lynx, Neuralynx Inc.) and stored as a custom format for compression (Malinowska et al. 2015). Considering all the restrictions for this study, we analyzed 6 patients and 12 episodes of seizure (2 per patient); 3 of the patients were seizure free. Table 5-1 summarized patients' information. As mentioned before, we used two episodes of seizure for each patient.

Table 5.1 Patient population information. Abbreviations: RAD: Right Amygdalar Depth, RHD: Right Hippocampal Depth .LHD: Left Hippocamal Depth : RBT: Right Basal Temporal LAD: Left Amygdalar Depth.RTG: Right Temporal Grid, FTG: Fronto Temporal Grid .PBS: Posterior Basal Strip, ABS: Anterior Basal Strip, LOG: Left Occipital Grid, SOD: Superior Occipital Depth, MOG: Middle Occipital Grid, IOD: Inferior Occipital Depth, IOG: Inferior Occipital Grid.

Patient	SOZ	Resected	Outcome of surgery
1	RAD16, RHD,RBT1-3	RTG 17, 18, 25, 26, 33, 34, 41, 42, 49, 50, 57, 58, RBT 1-3, 7-9, RAD, RHD	Seizure Free
2	LHD1-6,LAD1-6	LHD1-6,LAD1-6	Seizure Free
3	LAD, LHD	FTG grid: 49-54, 57-62; strips ABS, PBS, LAD 1-8, LHD 1-8	Seizure Free
4	ABT1-3, MBT1-2, PBT1-3, PHD1-3	FTG 33-35, 41-44, 49-52, 57-60, MBT, ABT, PBT (resection did not include FTG 36 because this was eloquent for language based on cortical stimulation)	Not Seizure-Free
5	LOG16-18,IOG1-10,MOD3-5,IOD3-6	LOG16-17 ,18, IOG 4-5, 9-10, MOG 3-6, can't tell which SOD, IOD electrodes	Not Seizure-Free
6	TPS1-6,TAS2-4,PSD2-8, PID2-8,LPGgrid	LPG grid: 49-53, 57-61, PSD, PID (resection did not include TAS or TPS because these were eloquent language cortex based on cort stim)	Not Seizure-Free

5.2.2 Delta power at night

Periods of 12 h at night has been used for each patient to calculate the delta power. For this calculation, we used the night before the seizure happened. Those periods with continues high power were marked for HFO detection in sleep for each patient.

5.2.3 HFO detection

Periods of 10 minutes in deep sleep, awake, preictal, and ictal were divided into 2-minute segments and filtered at 80-200 HZ for ripples and 200-500 HZ for fast ripples, also called fast HFO (band-pass filter using two-way least squares FIR filtering, EEGLAB, Matlab). To detect ripples and fast ripples (HFOs), we applied an automated method based on (Shennan

Aibel Weiss et al. 2016; Julia Jacobs et al. 2009; R. Zelmann et al. 2010), which implements identification of HFOs based on the following criteria:

- The event must consist of at least four consecutive oscillations on filtered EEG.
- The peak-to-peak amplitude of four consecutive oscillations should be above 10 µv.
- The amplitude of the event should be at least two times higher than the amplitude of oscillations of the surrounding background.
- The duration of the event should be less than 100 ms.

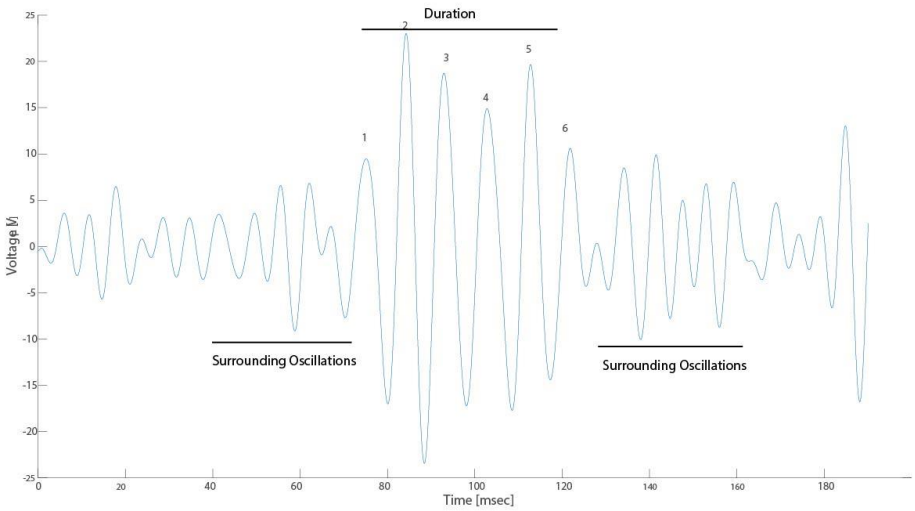

Figure 5.1. Example of an HFO pattern and characteristics.

As mentioned above, to detect the HFO, we used the other established algorithms and tried to remove the artifact and spike events from the detector. This removal was then checked by experts, and due to the high number of the HFO/FHFO events, a sample of them (50 events) were checked and subsequently confirmed the truth of rejection. Following this, we expanded the algorithm to the rest of the provided data.

In addition to the duration criteria for artifact, we set a cutoff frequency for high gamma to minimize contamination of the 60 Hz line noise and its first harmonic at 120 Hz. We also filtered data from 1-5 Hz, which is the frequency band for low theta and delta bands, these frequencies are not included in HFO analysis.

5.2.4 HFO rate comparison

5.2.4.1 Comparison between sleep, awake, preictal, ictal periods

HFO rate during sleep, awake and preictal periods was calculated as the average rate over 5 2-min segments. Duration of 10 minutes of awake data has chosen randomly during the day and at least 1 hour prior to seizure. By checking the recorded video, we were assured that the patient was not at sleep stage. The neurologists considered a 10-minute preictal exactly 10 minutes before the marked seizure onset. To be consistent with the ictal period among all patients, due to inequality of seizure duration, we only considered the first 2-minute of the ictal period across all patients.

Figure 5-2 shows how the rate of HFO changes during different epochs. As illustrated, this rate at night is not higher than awake and preictal. However, the ictal period has the HFO rate in all channels. This fact is not a surprise due to seizure propagation to all channels.

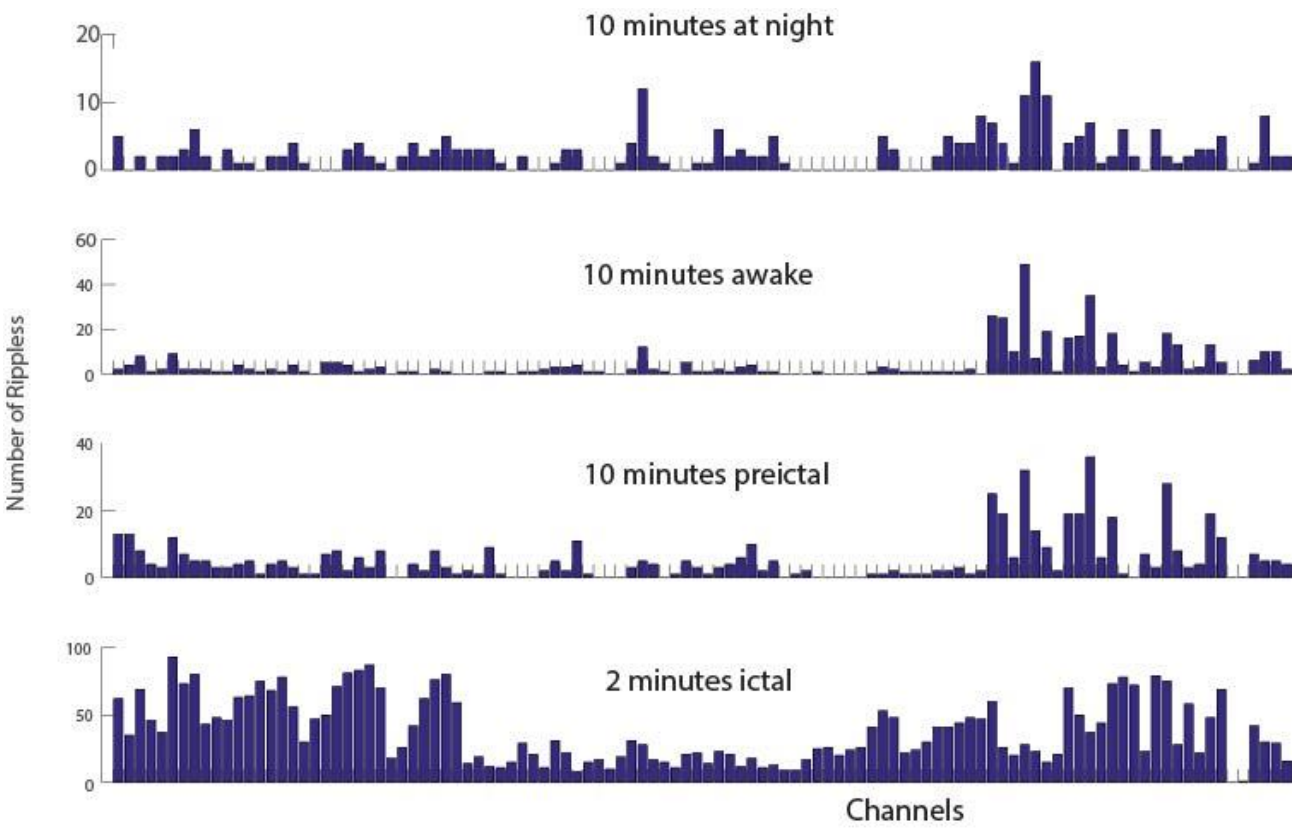

Figure 5.2. HFO rate in four distinct epoch including sleep, awake, preictal and ictal.

Like ripples, fast ripples do not have higher rate at night as compared to awake and preictal. As illustrated in Figure 5-3, for the same reason mentioned above, fast ripple at ictal time has the highest rate comparing to other three epochs.

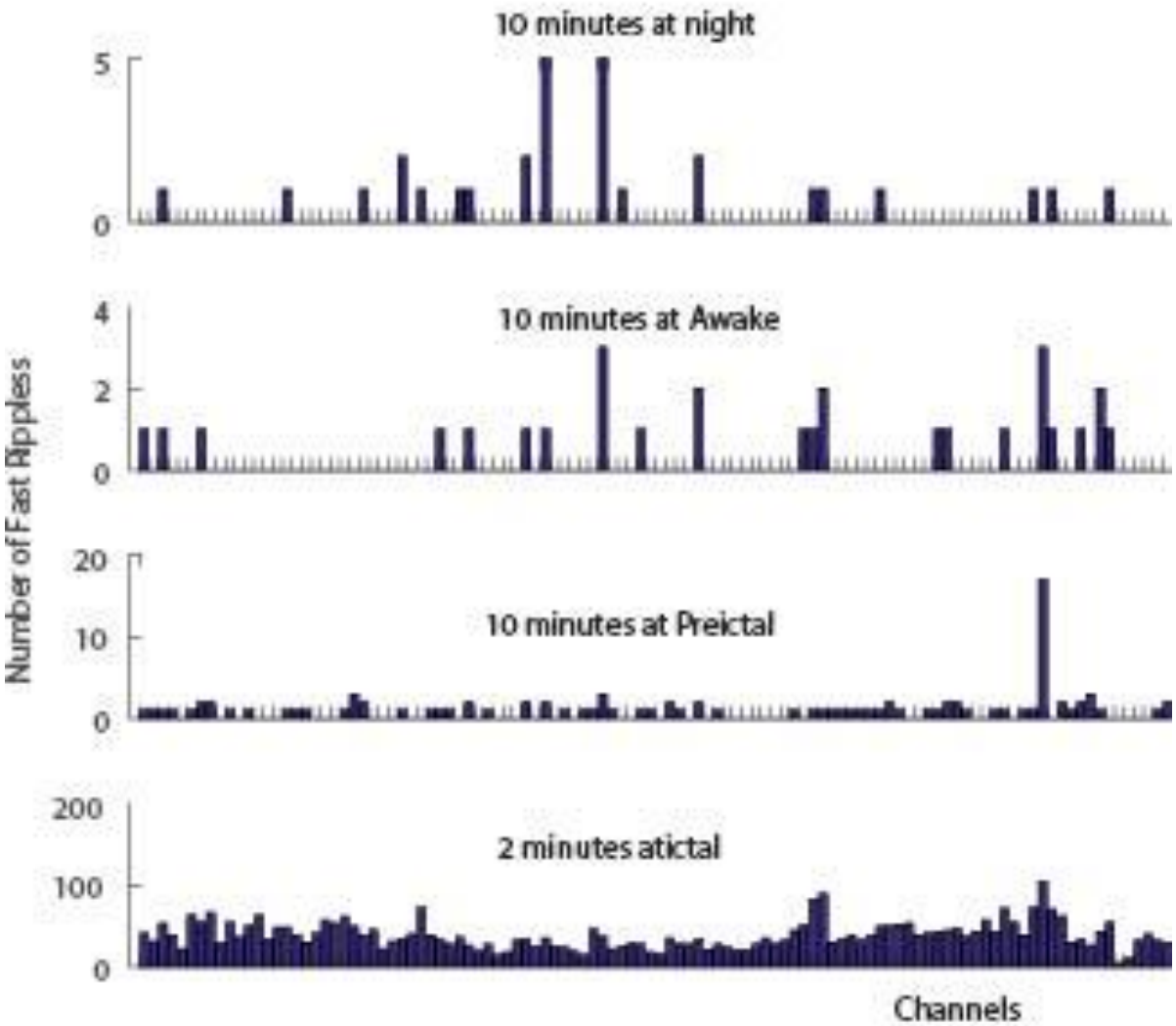

Figure 5.3. Number of fast ripples in 4 periods of sleep, awake, preictal and ictal.

Due to difference in the channel number per patient, we cannot average the ripples or fast ripples across the patients but the same pattern has observed fall 6 patients.

For each patient, we compared the rate of HFO in SOZ and resected area to the out of SOZ and resected area.

As we discussed in detail in Chapter 4, the resection area can be different from SOZ. While the patient is in EMU, he or she completes several tasks. Neurologists and engineers analyze the data and confirm the resection area in such a form that patient loss minimum or zero ability in language, auditory, vision, memory or motor sense after surgery. In fact, being seizure free with less resection area and best quality of life is a 'success' in surgery.
For this reason, and considering the aim of the current study, we only compared the HFO/ FHFO rate separately for the SOZ and resection area in different epoch. We found that, as expected, at ictal time, we had the highest HFOs and FHFOs as compared to other epochs. Since during seizure, due to propagation, more electrodes are involved in seizure, the high rate of HFO and FHFO is not dependent on in/out- SOZ or resected area.

As shown in Figure 5-4 through 5-6 and Table 5-1, in the ictal period, we have much more HFOs and FHFOs as compared to other epochs. Also, for each single period, the rate of HFOs/ FHFOs in resected or in SOZ are higher than out of resected or SOZ area. However, we could not find any significant differences between HFO/ FHFO at night compared to preictal or awake epoch. Table 5-1 shows all rates related to HFO and FHFO in four epochs including night, awake, preictal and ictal. These rates are the average of the events per minute in specific regions including the in/out SOZ and in/ out resected area. To check the significant difference between these rates for both events of HFO and FHFO, we used a chi-squared test. There are no significant diferences between the average rates of events in any cases. Figures 5-4 through 5-6, confirm the fact that there is no difference between the number of events in/out SOZ and resected area. Surprisingly, according to Table 5-2, the highest rate of HFO/FHFO is in ictal period, and contradictory of common believe, preictal period has the higher rates of events comparing to night in all cases. However, the difference is not significant, and we hope that by increasing the number of patients we can get a significant result. The difference in this study and the studies that believe at night we can see more HFO is that here we adapted algorithms to delete the artifacts.

Table 5.2 Rate of HFO and FHFO in/out of SOZ per minutes in four distinct epochs

Event	Area of interest	Night	Awake	Preictal	Ictal
HFO rate	**In SOZ**	0.5270	0.7517	0.8933	11.9732
	Out of SOZ	0.3480	0.3610	0.4851	6.0535
	In resected	0.5845	0.7227	0.9228	13.1946
	Out of resected	0.3665	0.4059	0.5263	5.6790
FHFO rate	**In SOZ**	0.2214	0.1853	0.2504	10.9523
	Out of SOZ	0.0782	0.0660	0.2504	10.9523
	In resected	0.2287	0.2201	0.2815	11.5899
	Out of resected	0.0775	0.0573	0.0860	4.9397

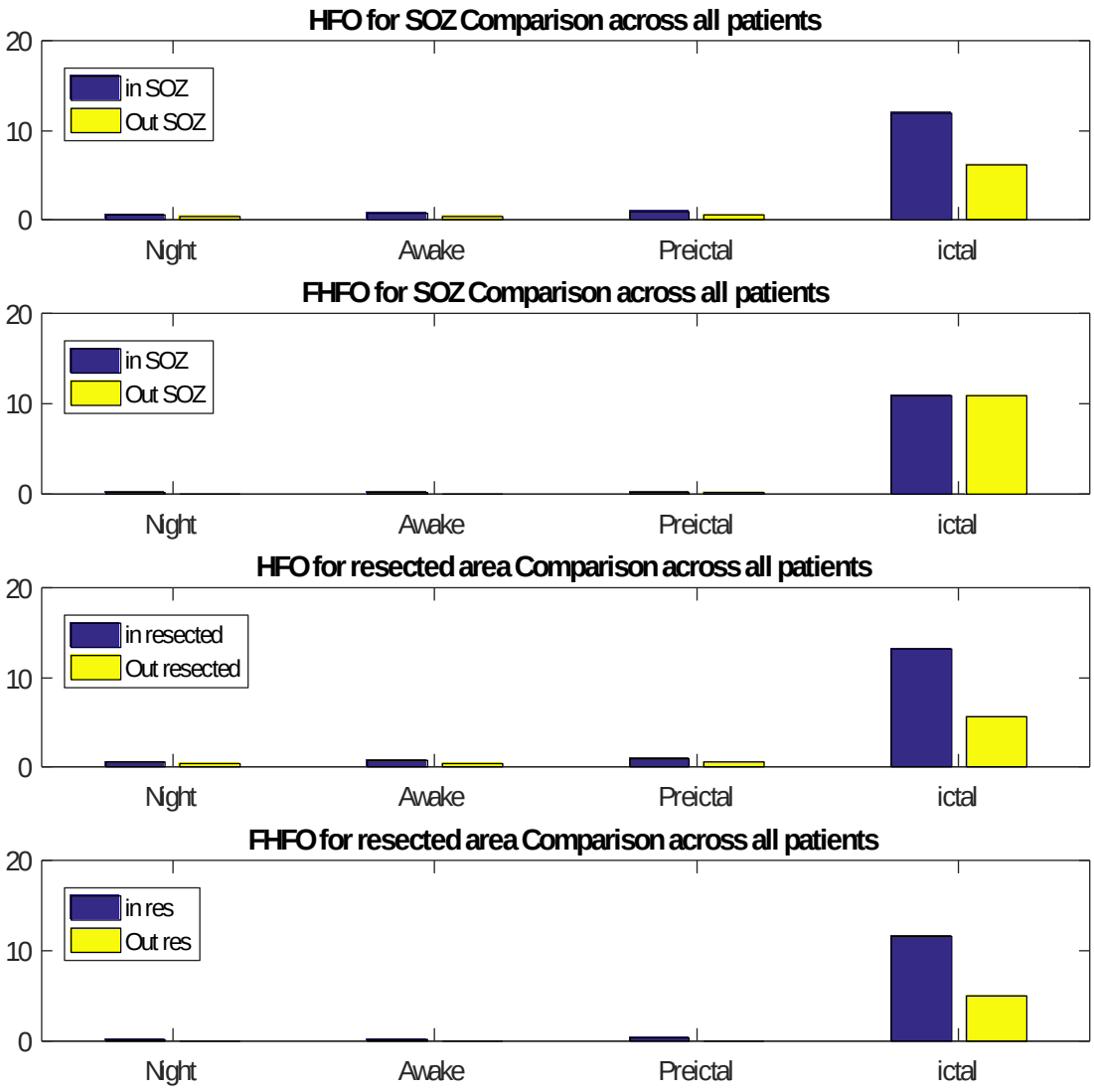

Figure 5.4. Comparison between HFO and FHFO for four epochs of time in/out SOZ and resection area for all patients.

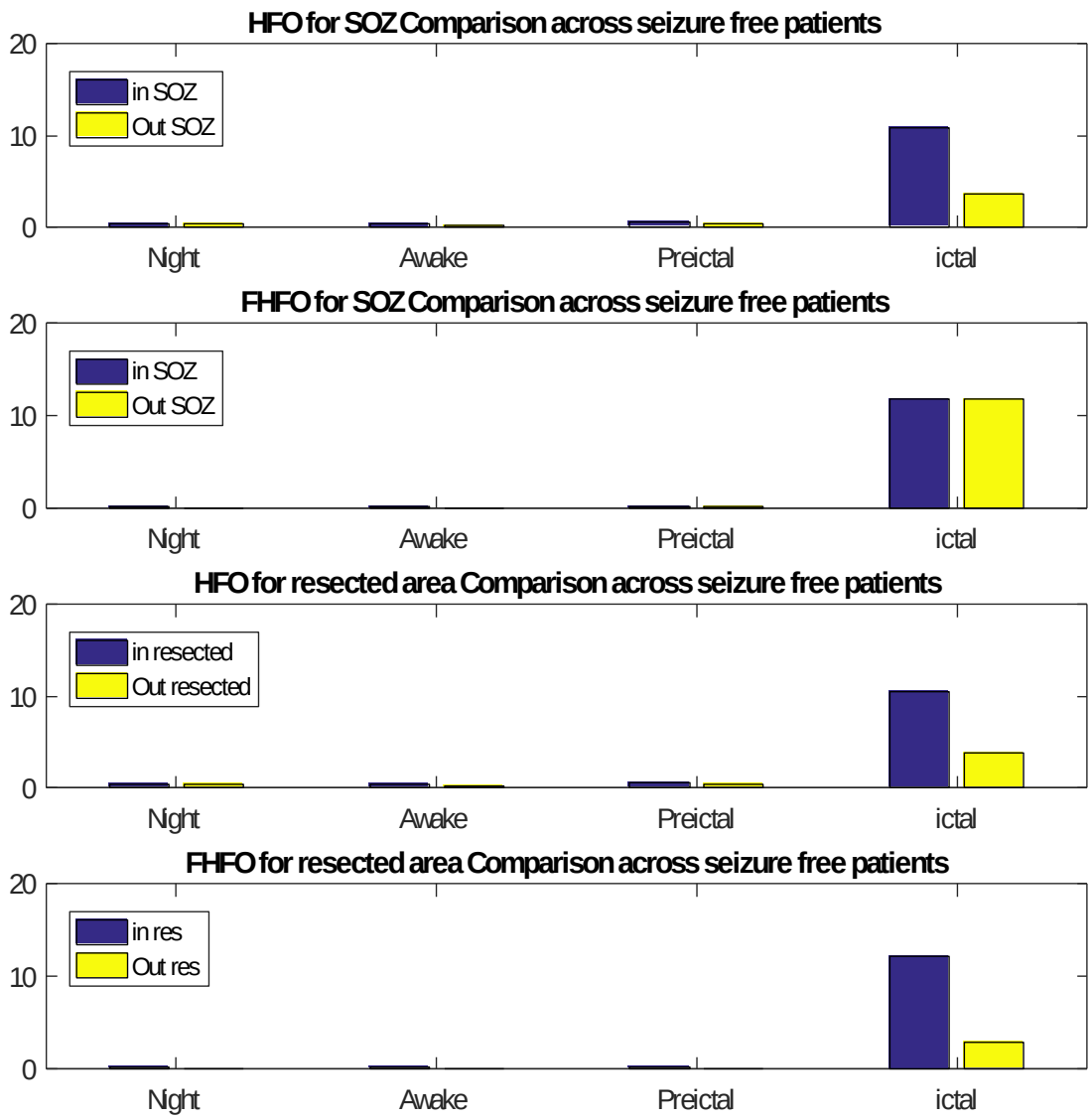

Figure 5.5. Comparison between HFO/ FHFO for four epoch of time in/out SOZ and resection area for seizure-free patients.

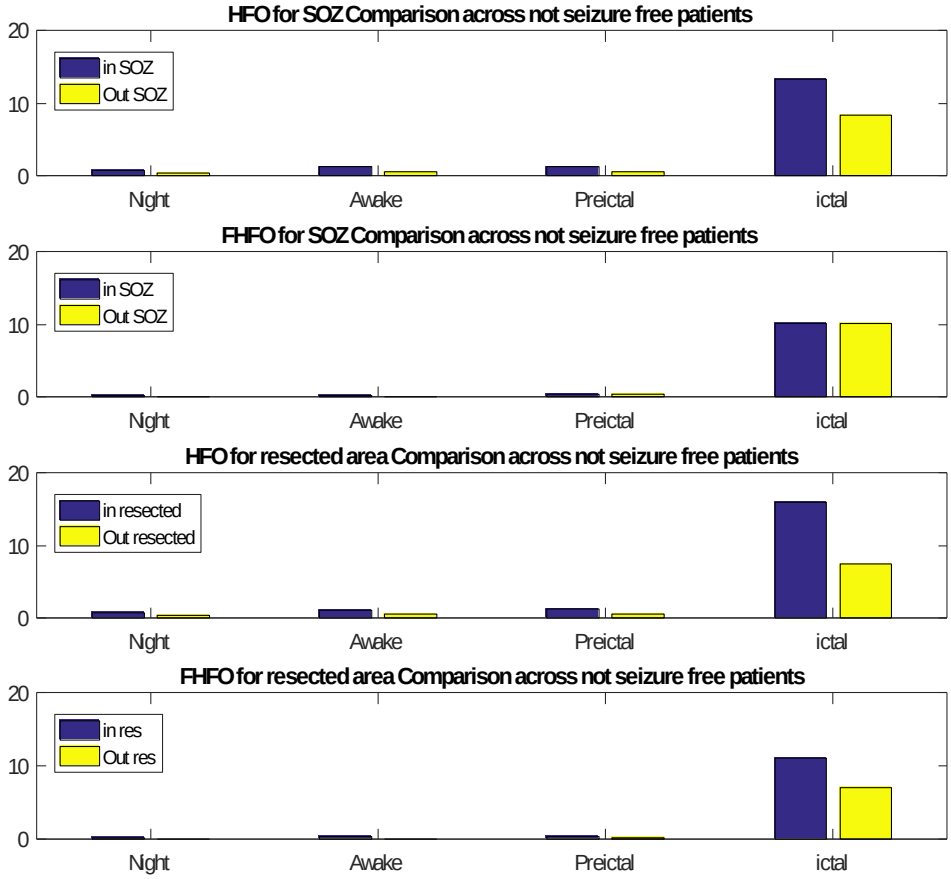

Figure 5.6. Comparison between HFO and FHFO for four epoch of time in/out SOZ and resection area for not seizure-free patients.

4.3 Conclusion:

Although in ictal time the rates of HFO and FHFO in/out- SOZ and resected areas are higher than sleep, awake and preictal stages, there is no significant difference between these rates between night and the rest of epochs. By these 6 patients and 12 episodes of seizures, we could not find any significant higher rate of HFO/FHFO at night than preictal. Contradictory to other studies, we proved that the rate of HFO/FHFO in preictal is more than night. So, at night, the rate of HFOs is not higher; indeed, they are easier to be detected in the absence of artifact. In this study we applied some artifact-removal methods, then we could show that, in 6 patients and 12 episodes of seizure, the rate of events at preictal I is higher than at night.

Chapter 6

Epileptiform Synchronization in neurons' level

6.1 Seizure-onset types

A new window for analyzing seizure onset patterns is opened when depth electrode recording introduced to the field. With interictal electrodes, it is not easy to perform a detailed analysis of seizure onsets. The reason is signals originating from deep sources, before reaching the scalp are attenuated. Not to mention the noise introduced by muscle artifacts further compounds the problem. This limitation induces a low reliability between independent observations when trying to detect regions of seizure onset and when classifying seizures are based on their onset pattern (Spencer et al. 1985).

However, two main seizure-onset have been identified by using depth electrodes implanted in the temporal and neocortical of patients with MTLE(A. Bragin et al. 2005; Ogren, Bragin, et al. 2009; Spencer, Kim, and Spencer 1992; Velasco et al. 2000). HYP seizures (Figure 6.2)—characterized by rhythmic low frequency (<2 Hz) high-amplitude spikes shapes which are followed by fast rhythms in the 10-20 Hz frequency range—mainly originate from the hippocampal regions and stay there, rarely spread to ipsilateral or contralateral to the seizure-onset zone (Velasco et al. 2000), (Spanedda, Cendes, and Gotman 1997; Spencer, Kim, and Spencer 1992).

The second type of seizure onset, known as LVF (Figure 6.3), is characterized by the rhythms in the range of beta gamma activity. Compared to HYP seizures, the site of source of LVF seizures is more diffuse and rapidly spread to ipsilateral and contralateral to SOZ and is often extrahippocampal (Spencer, Kim, and Spencer 1992). In other words, HYP ictal discharges can remain in the hippocampus for long periods without spreading to adjacent or eventually contralateral MT structures (Perucca, Dubeau, and Gotman 2014). However, before propagation this kind of seizure onset usually transition to another ictal seizure onset pattern, such as LVF (Velasco et al. 2000). The differences between the two seizure-onset

types emphasize that they may have some differences in their mechanisms and through the involvement of specific types of neurons. A sample of action potential with their corresponding different phases is illustrated in Figure 6.1.

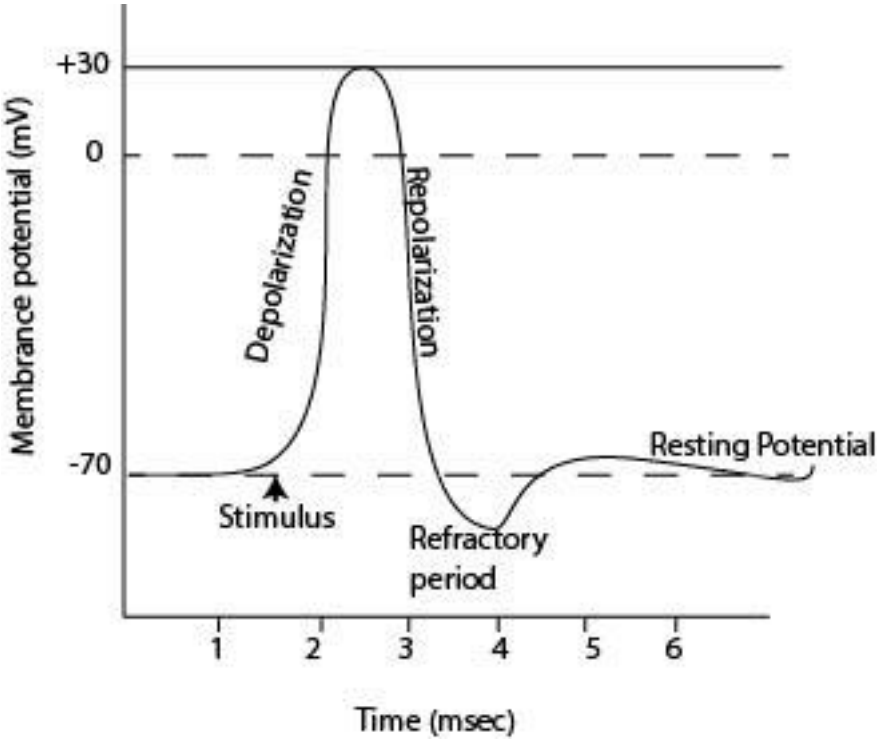

*Figure 6.5.*Schematic of action potential showing the various phases that occur as the voltage wave passes a point on a cell membrane.

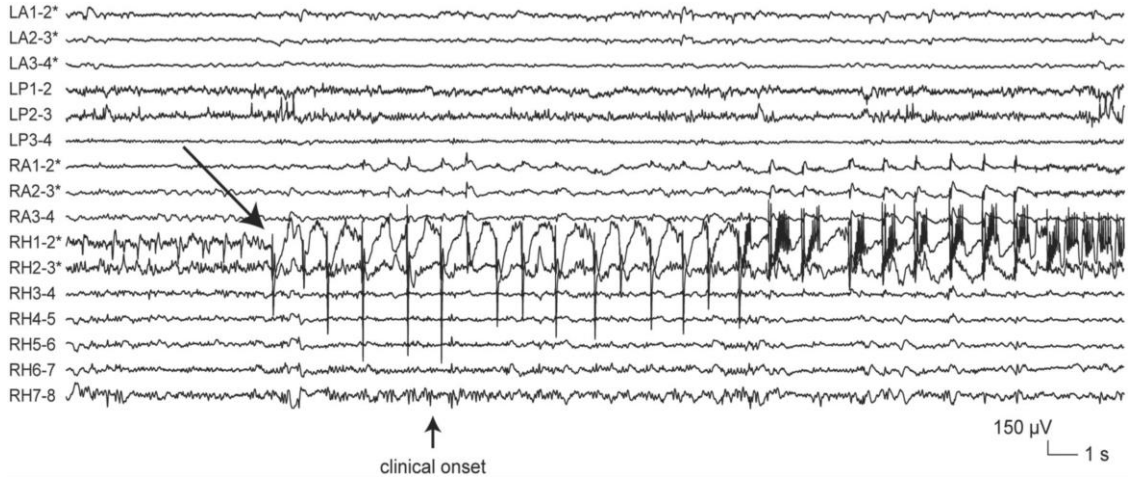

Figure 6.6. Hypersynchronous seizure onset. Low-frequency high-amplitude periodic spikes at seizure-onset. In this ictal intracranial EEG recording from a patient with bilateral mesial temporal atrophy/sclerosis, seizure-onset (arrow) consisted in the appearance of high-voltage spiking at 1 Hz, lasting for ~15 s at contacts RH1–2. Electrode targets: LA = left amygdala; LP = left posterior hippocampus; RA = right amygdala; RH = right

hippocampus. Asterisk indicates electrode contacts located in lesional/perilesional tissue. This recording is borrowed from Thomas Jefferson Hospital data archive.

6.2 Chronic models of MTLE

The clinical findings on seizure-onset types are aligned with the results obtained from animal models with MTLE. Bragin reported that a seizure event (SE) which induced by kainic acid in the hippocampus evoked both HYP and LVF seizures (A. Bragin et al. 2005) within a week after the injection. In the same study, they recorded the hippocampal and para-hippocampus data using depth electrodes and demonstrated that HYP seizures originated more from hippocampal structures ipsilateral to the injection site. The seizure-onset zone with LVF onsets, were located in both the hippocampus and EC and they spread to other brain regions. Surprisingly, when HYP propagates to other brain regions a transition to an LVF pattern was happened. (Levesque et al. 2012).These results confirm that LVF onset for seizures are more defuse than HYP seizures. Figure 6-3 illustrates an onset of seizure with HYP, which changed to LVF and then clinical bursts.

The analysis of HFOs occurring during the preictal and ictal periods has demonstrated a distinct pattern of HFO occurrence: fast ripples occur more in HYP onset of seizures, whereas they are rare during LVF seizures (A. Bragin et al. 2005; Levesque et al. 2012). On the other hand, an increase of ripple, occurs during LVF seizures (Levesque et al. 2012).

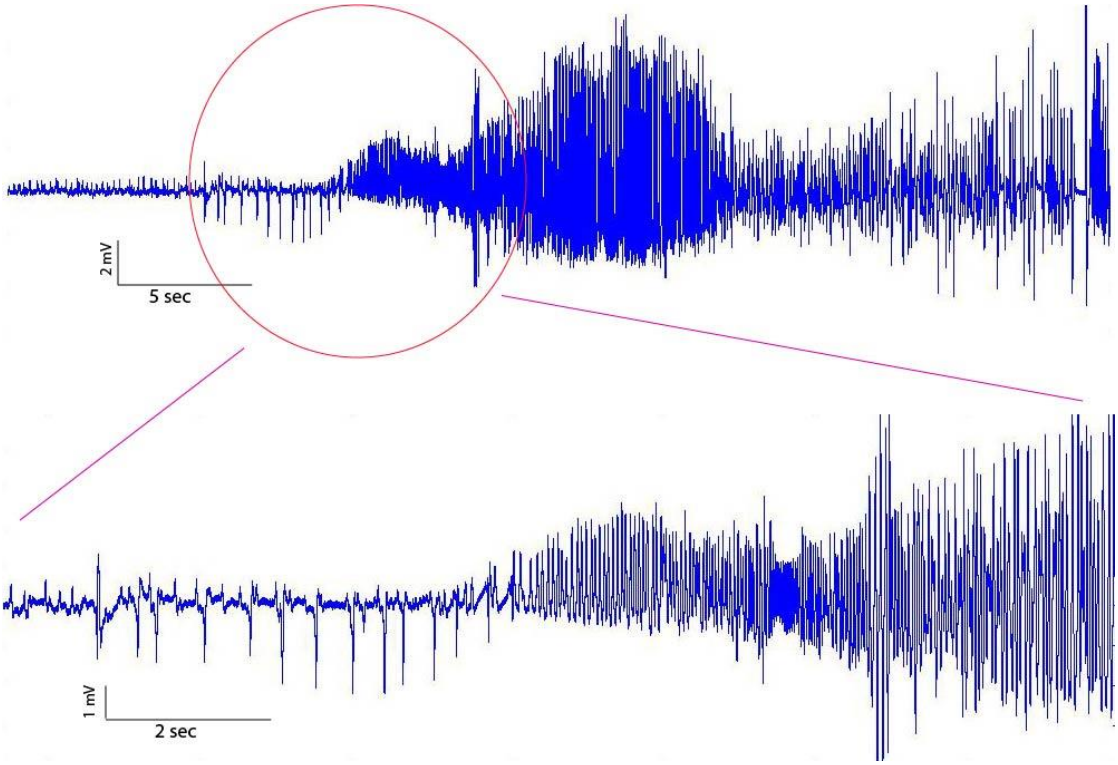

Figure 6.7. The onset of seizure, which started HYP and then changed to LVF before clinical bursts.

Furthermore, human studies have found that HFO power increases before or during the onset of some type of focal hippocampal seizures (Jirsch et al. 2006), (Khosravani et al. 2009), which is consistent with a spatially increase in power at the onset of focal seizures (Perucca, Dubeau, and Gotman 2014).

In this study, since we aimed to study the spread of seizure, we focused on those spontaneous seizures in humans that exhibited LVF at their onset. For such seizures, we investigated whether there is any imbalance between the inhibitory and excitatory neurons at the onset of seizure.

Figure 6.3 illustrates a sample of LVF seizure onset with a herald spike. The reason we demonstrated this particular recording here is to show that, in some cases LVF may start even before the herald spike. Due to this fact, a visual investigation is recommended for each single electrode. The top panel in Figure 6.3, shows a seizure with interictal recording, While the middle panel shows the zoomed in picture of LVF. To demonstrate the LVF onset before the herald spike better, the bottom panel shows the more zoomed picture of the herald spike.

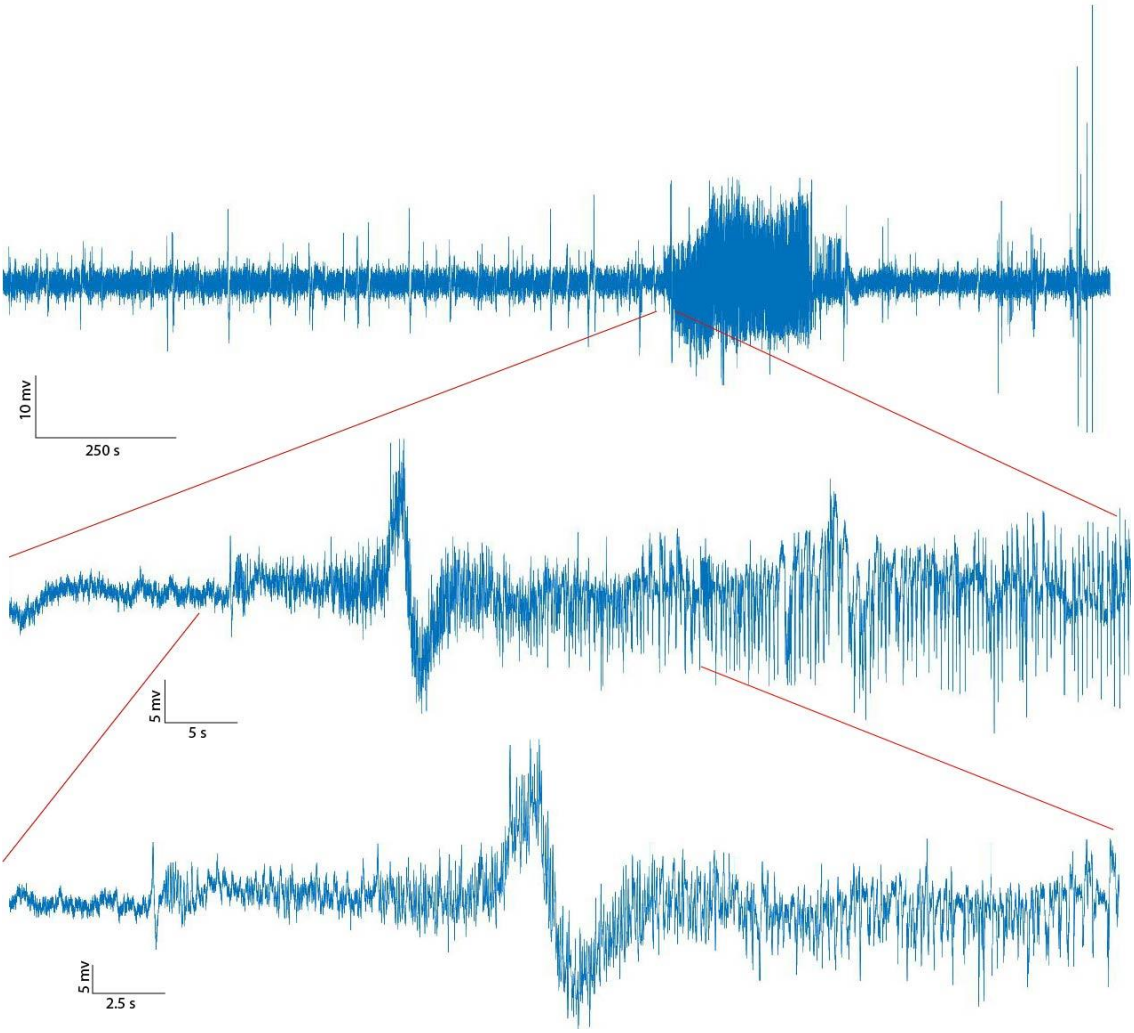

Figure 6.8. Herald spike in three different resolution. Top : seizure activity in microelectrode, middle: LVF herald spike and LVF activity, bottom: better visulalization of LVF before and after herald spike.

6.2 Methods

6.2.1 Patient population and data

We retrospectively analyzed data from five patients at either the University of California Los Angeles (UCLA) or Thomas Jefferson University (TJU) during seven spontaneous seizures at the time of intracranial monitoring using custom 24 and commercial Behnke-Fried combined macro- and micro-depth electrodes (Ad-Tech, Racine, WI), respectively. The electrodes were localized to anatomical regions, as described previously. The study was independently approved by the Institutional Review Boards of UCLA and TJU, and all patients provided consent. Only patients with mesial temporal lobe epilepsy or mesial temporal lobe epilepsy

plus other regions were included in the study. Only seizures exhibiting LVF activity at onset were selected for analysis.

Wide bandwidth (0.001–6 kHz) intracranial EEG (iEEG) and local field potentials were recorded from macro- and microelectrode contacts, respectively (40 ksamp/s; gain × 10,000) and amplified using an Atlas system (Neuralynx, Bozeman, MT, U.S.A.). In other experiments, wide bandwidth (0.001–6 kHz) local field potentials were recorded from microelectrodes using either a Cheetah recording system (Neuralynx, Bozeman, MT, U.S.A.) or a NeuroPort recording system (Blackrock, Salt Lake City, UT, U.S.A) (28-30 ksamp/s; gain x 10,000). In some of these experiments, wide bandwith iEEG was recorded using a Stellate (XLTEK, San Diego, CA, U.S.A) or a Nihon-Kohden 128-channel NK 1200 long-term monitoring system (Nihon-Kohden America, Foothill Ranch, CA, U.S.A.).

Patient population and related data regarding SOZ and outcome of surgery are summarized in

Table 6.1 Patient characteristics. Abbreviations MTL: mesial temporal lob sclerosis, ATL: Anterior temporal lobectomy.

Patient Age Sex	**Duration of Epilepsy**	**Scalp EEG**	**iEEG SOZ**	**Surgery**	**Outcome**
TJU049 39 F	3 yrs	Left temp oral	Left mesial temporal	Left ATL	Engel I @ 5 yrs
428 44 M	4 yrs	Left temp oral	Left mesial temporal	Left ATL	Engel I @ 4 yrs
439 48 F	18 yrs	Left temp oral	Right mesial temporal	Right ATL	Engel I @ 4 yrs
461 21 M	4 yrs	Left temp oral	Left mesial temporal	TBD	TBD
462 27 M	19 yrs	Left and right temp oral	Left temporal	Left Temporal Hippocampal Sparing	Engel III @1 yrs

6.3 Data Analysis

6.3.1 Extracting seizures from continuous LFP recordings

Custom software written in Matlab (Mathworks, Natick, MA) was used to inspect all continuous local field potential recordings for each ictal epoch. After determining the time of seizure onset, local field potential clips were produced. In all but one seizure, the clip

included a 3-minute preictal epoch. Aligned iEEG recordings were available for only a subset of the seizures.

6.3.2 Defining seizure onset patterns using local field potential recordings

The seizure onset zone (SOZ) and non-SOZ regions were classified based on visual inspection of the iEEG by a board certified clinician. The seizure onset pattern (LVF, hypersynchronous, repetitive spike and wave) and the time of seizure onset was assigned on the basis of visual inspection of the LFP by S.A.W and B.E (Perucca, Dubeau, and Gotman 2014; Shennan Aibel Weiss et al. 2016). The time of LVF onset and offset was determined based on computer-aided analysis of the LFP using normalized wavelet spectrograms by S.A.W and B.E.

6.3.3 Single unit characterization

We analyzed the mean action potential waveform of each single unit. From the mean form of each electrode, which includes all the spikes, we extracted the peak amplitude asymmetry, through to the following peak, and half width of half amplitude of the action potential. It is worth mentioning that, due to the variety of spikes even in one electrode, extracting these features is somehow impossible. Using these features, excitatory and inhibitory neurons were differentiated on the basis of K-mean clustering (Jozsef Csicsvari et al. 1998). This separation was done based on the previous knowledge that inhibitory neurons should have less half width, more amplitude asymmetry and less trough-to-peak than excitatory neurons (Librizzi et al. 2017). At this time, we may call the *putative* inhibitory and excitatory since we will do one more analysis at the end to make sure what we claimed are indeed inhibitory and excitatory.

Once the putative inhibitory and excitatory neurons were separated, we compared the mean action potential firing rate following smoothing using a Gaussian function with 100 msec kernel (Edelman and Goldberg 2003). The 100 msec came with experiment. We started with 200 msec kernel, but noticed that the spike rates were getting so smooth, and in some

cases we falsely missed low spike rate values. Contrary to animal models (Edelman and Goldberg 2003), a relatively long duration kernel was required due to a relatively sparse dataset. To compare the spike rates between epochs and define the epochs in which the firing rate reached its maximum, we used the smoothed spike rate derivations for each single unit. We applied Wilcoxon signed-rank test to compare these values before and after LVF onset for the SOZ and NSOZ, for each region (entorhinal cortex, hippocampus, amygdala), and separately for each set of neurons (inhibitory and excitatory).

6.3.4 Changes in waveform during LVF

To determine whether the waveforms of the putative excitatory and inhibitory neurons and the multi-unit action potentials were stable during the LVF epoch, we normalized each waveform and calculated the coefficients and score of the principal components ('princomp' command in Matlab) of all the action potential waveforms during the pre-ictal epoch. As we know, PC1 and PC2 show the most variation in the data. We plotted PC1 vs. PC2 to show whether the spikes are separable, and we could see two distinct groups. For each case (before LVF and During LVF), we had just one group. The results confirm that we had just one group that was inseparable during interracial before LVF onset and during LVF onset. We also plotted these two epochs on the same plot to show that—even before and after LVF—these groups were still close to each other. We next assessed the Mahalanobis distance (we explain more about this concept in Section 6.7) between the centroids identified using the scores of the first and second component of the pre- and post-LVF action potentials (Nadasdy et al. 2017; Merricks et al. 2015; Bower et al. 2017).

6.3.5 Identifying and quantifying ripples and fast ripples in the LFP recordings.

Ripples (80- 250) and fast ripples (250-600) were calculated as previously described (Shennan A Weiss et al. 2016). In brief, a Hilbert transform was used to calculate the instantaneous amplitude envelope of the power in the band-passed filtered EEG. The instantaneous amplitude time series was normalized and HFO events were detected when the

amplitude exceeded 3 SD for a minimum duration of 8 ms prior falling below 1.5 SD of the mean. Detections were confirmed by visual inspection. We compared ripple and fast ripple rates during the pre-LVF and LVF epochs using Wilcoxon signed-rank test in Matlab.

6.3.6 Phase relationships between action potentials and LVF oscillations.

The instantaneous phase of each LFP during the LVF epoch was calculated by applying a Hilbert transform to the band-pass filtered data (low LVF: 5-15 Hz, high LVF: 20-30 Hz). The Hilbert transform is defined as $y[t] = H(X[t]) = \frac{1}{\pi}\int_{-\infty}^{\infty}\frac{x[\tau]}{t-\tau}d\tau$ and results in the analytic signal $z[n] = a[n]\exp(i\theta[n])$, where $a[n]$ is the instantaneous amplitude of $y[t]$, and $i\theta[n]$ is the instantaneous phase.

We then used action potential timing t_{spike} to calculate the corresponding phase angles $\theta[t_{spike}]$ of each action potential with respect to the low voltage fast oscillations. We calculated the first trigonometric moment of these phase angles using the equation $m' = \sum exp^{i\varphi_{spike}} = R\ exp^{i\theta}$. The Rayleigh's Z-test for circular uniformity was calculated as $Z = nR^2A$. The probability that the null hypothesis holds was estimated as $p = exp^{-z^{33}}$.

6.4 Description of patients and seizures

We analyzed LFPs from 113 microelectrodes implanted in 5 patients during 7 spontaneous focal dyscognitive seizures with an LVF onset (Table 6.1). Not all microelectrodes record the unit data. That really depends on the neurosurgeons and how they implant the bundle of microelectrodes. This is why the number of units are different from the number of microelectrodes on the brain. Not to mention that capturing data from a single unit is really challenging and needs decades of experiments. In three of the patients, who were diagnosed with mesial temporal lobe epilepsy (MTLE), the seizures originated from mesial temporal structures; in these three patients, anteromesial temporal lobe resection resulted in a seizure-free outcome. The other two patients were diagnosed with MTLE+. One of the MTLE+

patients had a seizure originating from the mesial temporal lobe; the other patient had two temporal neocortical onset seizures, which propagated in less than one second to the ipsilateral mesial temporal lobe. The latter patient was treated with a lateral temporal lobe resection that spared the hippocampus and continued to experience seizures, although seizure frequency and severity was decreased. None of the patients exhibited both LVF onset seizures and hypersynchonous onset seizures that consisted of sharply contoured ictal discharges that evolve between 0.5-2.5 Hz. One of the goals of this research was to study how the seizure propagates. As we described in Section 6.1 through 6.3, those seizures that exhibit LVF at their onset are more defuse. They start from the entorhinal cortex but propagate rapidly to the hippocampus. Due to this fact, we focused on seizures with LVF at their onset.

6.5 Waveclus

To make a precise study of neuronal behavior, the first step is to appropriately classify the action potentials that were recorded from extracellular recordings. Many spike-sorting algorithms have been presented in the technical literatures (Susumu Takahashi, Anzai, and Sakurai 2003; S. Takahashi, Anzai, and Sakurai 2003; Adamos et al. 2010; Fee, Mitra, and Kleinfeld 1996). Wild et. al, (Wild et al. 2012) compared KlustaKwik (Harris et al. 2000) with Osort (Rutishauser, Schuman, and Mamelak 2006) and Waveclus (Quiroga, Nadasdy, and Ben-Shaul 2004). They concluded that in terms of accuracy Waveclus performs significantly better (P>0.01) for signals with a noise level of 0.15-0.30. In this study, we used Waveclus for spike sorting.

Waveclus is a software (plugin) based on Matlab. It is an unsupervised cluster cutting algorithm that is employed to detect and sort spikes from multiunit recordings. The method used in this software combines the wavelet transform to localize essential spike features with superparamagnetic clustering, which allows automatic classification of the data without

assumptions such as low variance or Gaussian distributions (Quiroga, Nadasdy, and Ben-Shaul 2004).

The spike detection method in this software has three steps:

1. Spikes are detected automatically by using a threshold for the amplitude. The threshold (*Thr*) was set to:

$$Thr = 4\,\sigma_n\,; \quad \sigma_n = median\,\{\frac{|x|}{0.6745}\}$$

   where x is the signal which is band-passed, σ_n is standard deviation of the noise in background. Since the standard deviation of the signal, such as high firing rates or large spike amplitude, can end to a very high threshold value, estimation based on median was been chosen.

   For each detected spike, 64 samples (for 30 KHz about 2.5 msec) were saved for further analysis. All spikes were aligned to their maximum at data point 20. To avoid spike misalignments due to low sampling, Cubic splines, were used to determine the spike-interpolated waveform of 256 samples.

2. For each of the spikes, the wavelet transform is calculated and the optimal coefficients for segregating the spike classes are automatically selected. Waveclus uses 64 wavelet coefficients for each spike and Haar wavelets. We know that each wavelet coefficient characterizes the spike shapes at different scales and times; however, the goal is to select a few coefficients that best separate the different spike classes. If there is more than one spike class per signal, we expect that coefficients have a multimodal distribution. Note that in Waveclus software the interest is not on any particular distribution of the data, but in deviation from normality as a sign of multimodal distribution.

3. The nominated wavelet coefficients will be the input of the superparametric clustering (SPC) algorithm; temperature is selected automatically and then the

clustering is performed. The Waveclus software was written in such a way that the temperature was variable from 0 to 0.2 in increments of 0.01. We discuss the temperature role very briefly here and refer to (Quiroga, Nadasdy, and Ben-Shaul 2004) for more information. The high temperatures correlate to a low probability that the neighboring points change the state together. That means many points may change their state completely independently from eachother. Therefore, they will be considered as seperate clusters but maybe only a few points in each, whereas low temperatures correspond to a higher probability of changing state together. Thus, many of points will change their state together and will therefore be considered as one cluster.

The first step and very critical issue before importing any data to Waveclus is to check the sampling frequency in a *set parameters.mat* file in the Waveclus package. Most of the microelectrodes are recording with a sampling rate of between 30 KHz -40 KHz. This parameter should be set accordingly.

Figure 6.4 illustrates a sample of spike sorting done for this project using Waveclus. As all of the clusters are shown in the second row and first from the left. Next, the sub-windows show the separated clusters. As explained before, the length of each sub-window is 64 and the peak of spikes are located at sample point 20. The last sub-window in this row (the first window from the right in the second panel) shows the artifacts. This sub-window was rejected for all the analysis in this study. The first window from the left in the third row shows the curve of temperature that can be changed. Normally, we would like to have a low temperature and more cluster size.

The other windows in the third row show the distribution of the spikes (interspike intervals) in each cluster. Having all this information, we just need to save all these clusters and their appropriate spikes in a Matlab format file. This can be done by clicking on “save clusters” bottom, on top of the window. The saved file in Matlab contains: (1) cluster class:

which is cluster membership in the first column and spike times in the second column, (2) spikes: which is the coordinate of shape of the spikes.

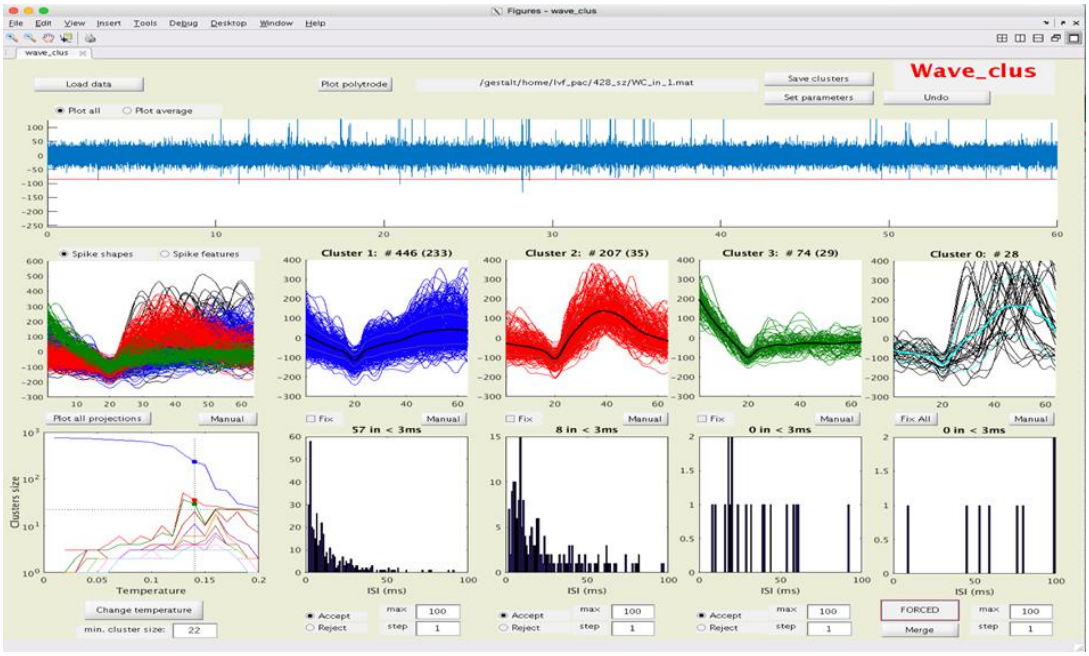

Figure 6.9. Illustration of a sample of spike sorting for this research using Waveclus.

6.6 Isolation and characterization of single units

To ensure quality control of single unit spike sorting, we quantified the number of false positive action potential detections on the bases of refractory period violations. We assumed an absolute refractory period of 1 ms, and a relative refractory period of 3 ms (Hill, Mehta, and Kleinfeld 2011). The final sorted single units exhibited no refractory period violations. To distinguish the putative excitatory from inhibitory units, we measured the peak amplitude asymmetry, half width, and trough-to-peak of the mean waveform for each single unit (LEvesque et al. 2016). These features are shown on a sample action potential in Figure 6.5, which borrowed from (Librizzi et al. 2017). Plotting these features revealed two distinct clusters of action potential morphologies. Spike trains containing action potentials with a shorter half-width, and trough-to-peak but larger peak amplitude asymmetry were classified as putative inhibitory interneurons (Figure 6.6); other spikes were classified as putative excitatory principal cells.

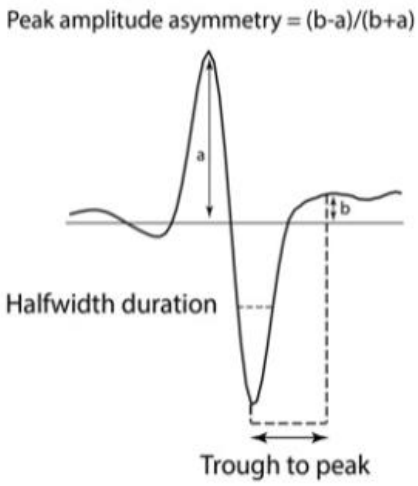

Figure 6.10. Illustration of three extracted features from an action potential borrowed from [163].

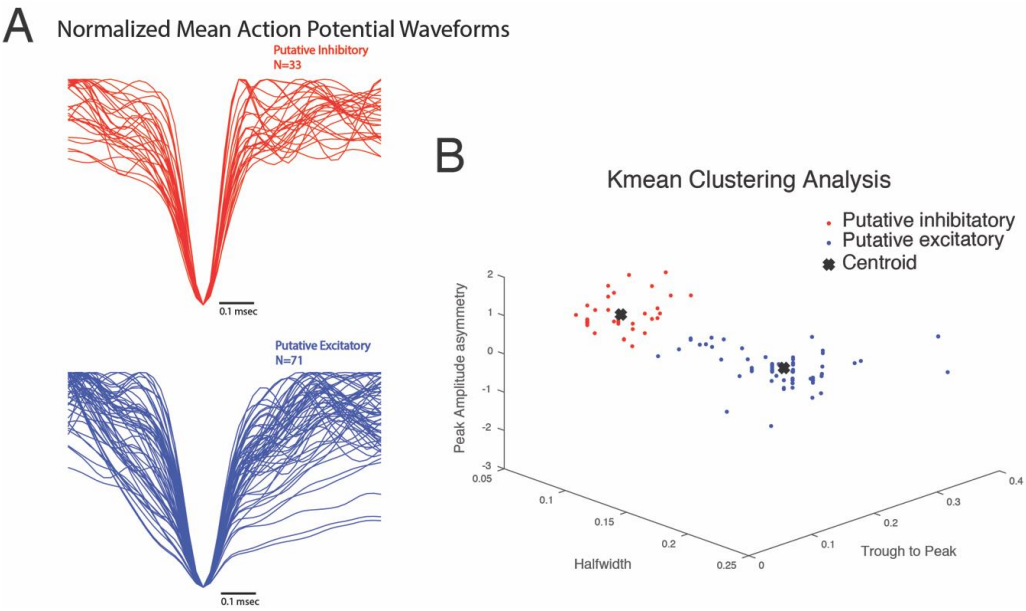

Figure 6.11 .Classification of exitatory and inhibitory neurons using kmean clustering. (A) Mean normalized waveforms of putative inhibitory and excitatory neurons isolated from microelectrodes during spontaneous LVF seizures in patients. (B) A three-dimensional plot of the extracted features: peak amplitude asymmetry, trough to peak and half width used to differentiate excitatory and inhibitory neurons based on K-means clustering.

Overall, we identified 50 excitatory neurons and 22 inhibitory neurons in the mesial temporal SOZ. We also identified 21 excitatory neurons and 11 inhibitory mesial temporal neurons contralateral to the SOZ. For patient 462 with MTLE+ and a neocortical seizure onset, we interpreted the ipsilateral mesial temporal structures as part of the seizure onset

zone because it was the site of rapid propagation and neocortical resection failed to result in seizure freedom.

Figure 6.7 illustrates how LVF appears in macro- and microelectrodes. These recordings are from the second episode of seizure for Patient 5. The data were from the UCLA dataset and the macro- and microelectrode recordings were already aligned. The first symbol of LVF is the herald or sentinel spike. The change in power of the signal in time-frequency plot is very clear at the beginning of the herald spike. As demonstrated in this figure, during LVF onset in spontaneous limbic seizures in humans, the firing rate of inhibitory neurons increases first, followed by a rebound in the firing rate of excitatory neurons.

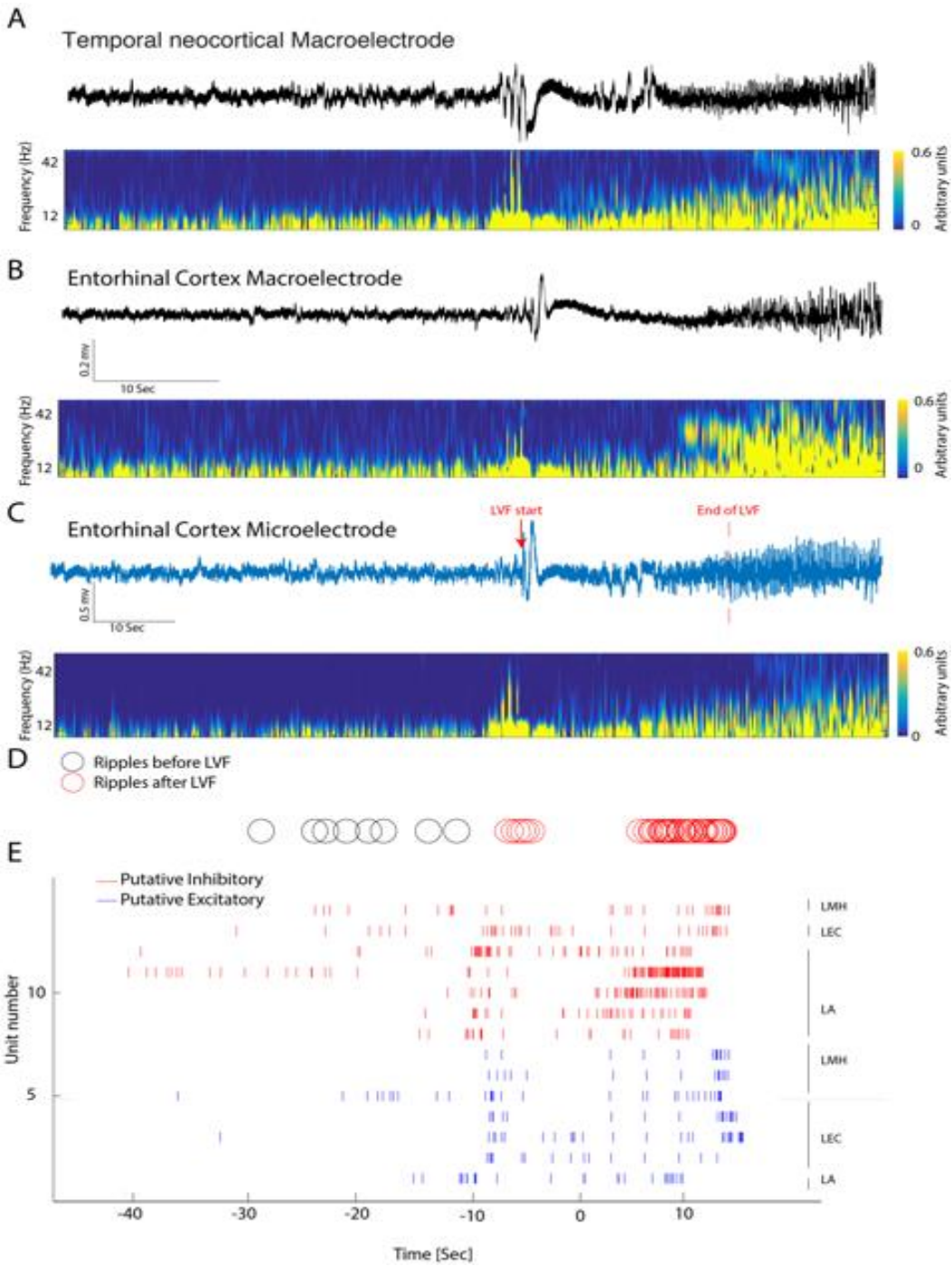

Figure 6.12 .LVF onset in macro- micro electodes aligned with raster plot and ripples. (A) Intracranial EEG recorded with macroelectrodes in the left temporal neocortex (top) and left entorhinal cortex (bottom) during a spontaneous LVF seizure in patient 462 with MTLE+. (B) Aligned LFP recorded from microelectrodes in the left entorhinal cortex indicating the beginning and end of LVF. (C) Aligned raster plot of spiking activity of excitatory and inhibitory neurons prior to and during seizure onset. Abbreviations (LEC: Left Entorhinal Cortex, RMH: Right Medial Hippocampus, LMH: Left Medial Hippocampus, RA: Right Amygdala, LA: Left Amygdala).

We next examined whether the action potential waveforms of the putative excitatory and inhibitory neurons exhibited an altered morphology during the LVF seizure-onset epoch. We found that none of the excitatory or inhibitory neurons included in this study exhibited a statistically significant change in morphology as quantified with the squared Mahalanobis distance ($p<0.01$, Figure 6.10). The Mahalanobis distance is a unitless quantity (similar to a z-score) describing the number of standard deviations between two waveforms, weighted by the variance in each dimension; decreasing distance is associated with increasing similarity between waveforms (Matlab Statistics and Machine Learning Toolbox 'mahal'). Since the action potential sorting process reduces the variability of waveform morphology, we also investigated whether the action potential waveform morphology of multi-unit activity (MUA) was altered during LVF seizure onset. Also, MUA waveform morphology did not change during LVF onset as quantified with the squared Mahalanobis distance. We did not sort any spike for multi-unit action potential detection. We detected them using a threshold of 5.92 × median of the absolute deviation of the signal (Merricks et al. 2015).

To demonstrate the distribution of scores, we randomly chose one of the units and calculated the PCA (Figure 6.9).

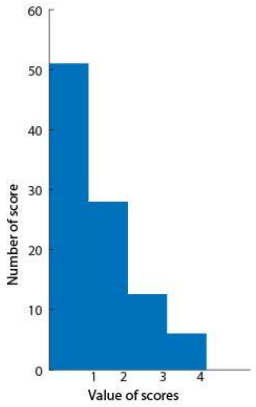

Figure 6.13. Distribution of score on randomly selected unit

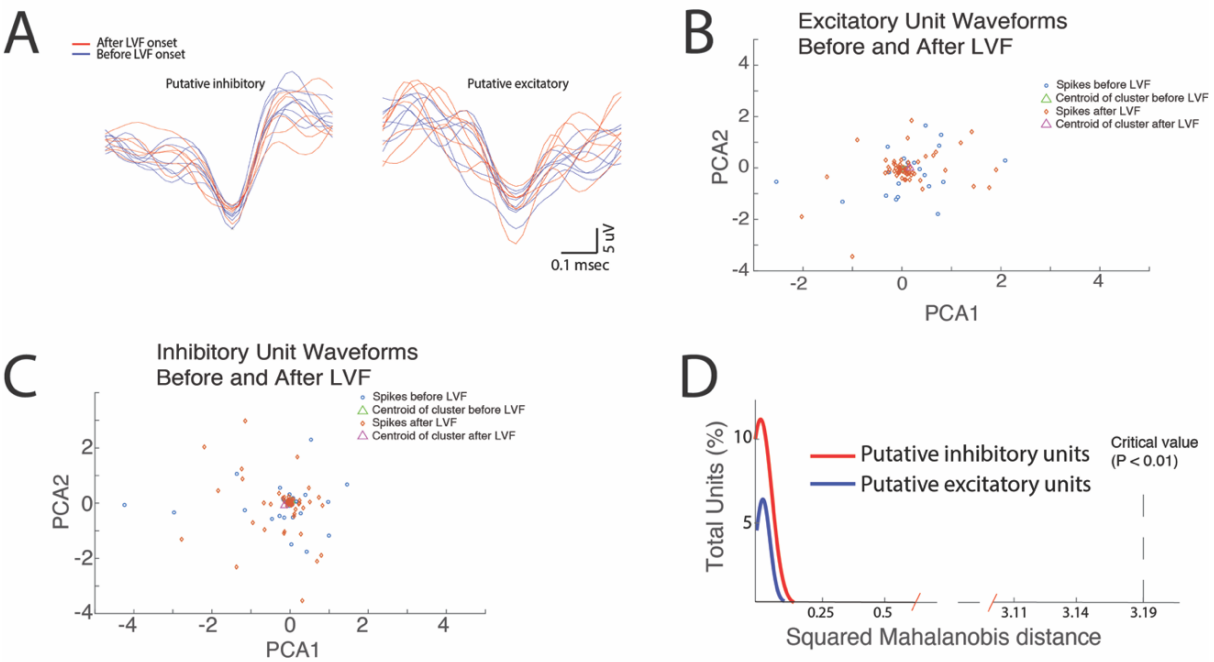

Figure 6.10. Morphalogy of waveform before and after LVF doesn't change . (A) Representative examples of excitatory neuron (left) and inhibitory neuron (right) waveforms before (blue) and after LVF onset (red).(B, C) Principal component analysis of all the spike waveforms for a representative excitatory (B) and inhibitory (C) neuron before (blue) and after LVF onset (red). (D) Normalized histogram of the squared Mahalanobis distance between the centroid of spike clusters prior to LVF onset and after LVF onset for all the excitatory (blue) and inhibitory (red) neurons in the study. The squared Mahalonbis distance was not significant for two distinct clusters.

6.7 Changes in the firing rate of excitatory and inhibitory neurons during LVF seizure-onset

Comparing the firing patterns of putative excitatory and inhibitory neurons during the spontaneous focal seizures often revealed that the firing rate of inhibitory interneurons increased dramatically early during the LVF epoch in the mesial temporal SOZ ($p<0.0001$, Wilcoxon signed-rank, n= 22). Later, during the LVF epoch, and following the initial increase in inhibitory interneuron firing, the excitatory neuron firing rate could also exhibit a dramatic increase or rebound ($p<0.0001$, Wilcoxon signed-rank, n= 50, Figure 6.11).

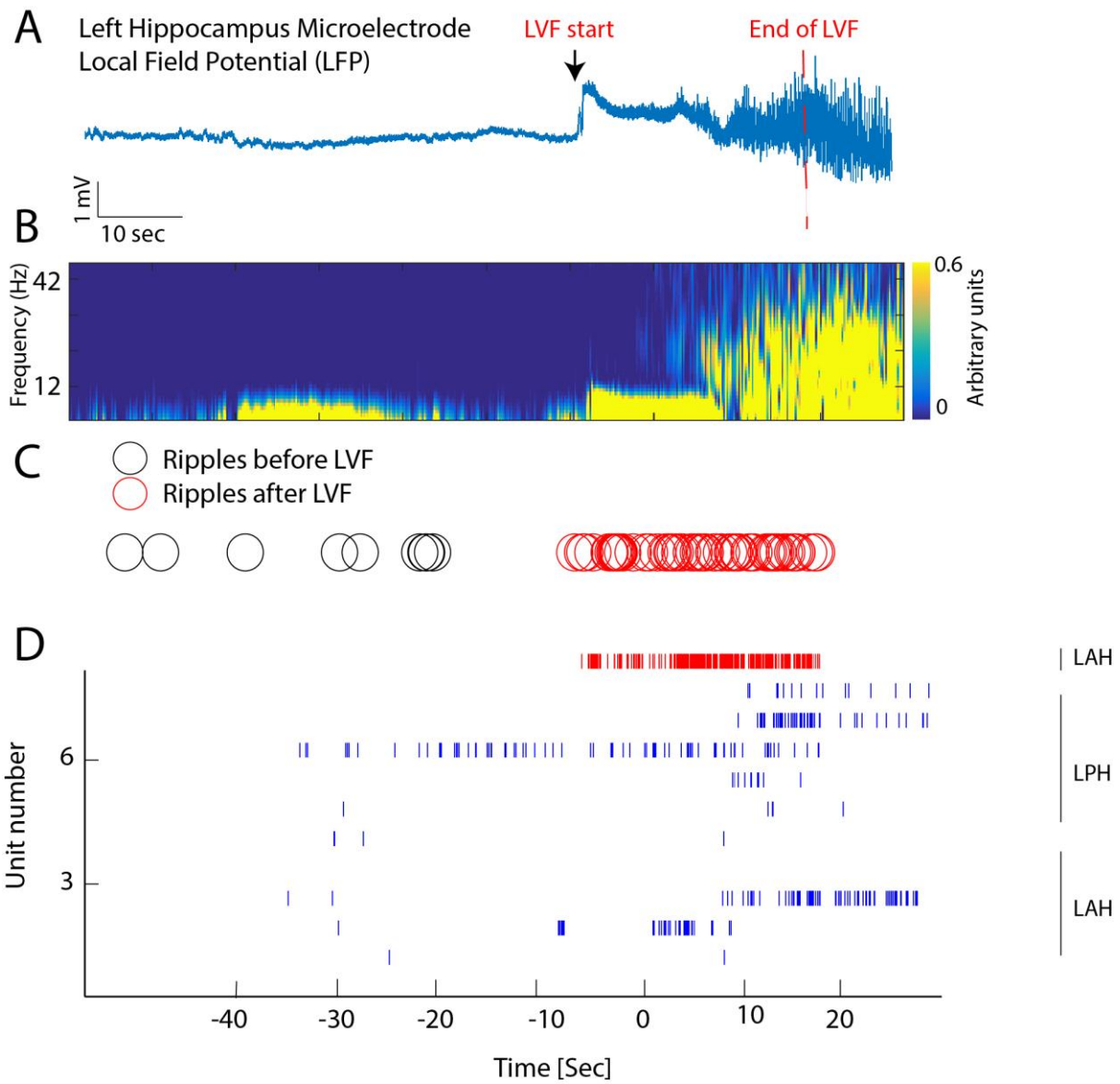

Figure 6.11.. LVF onset is accompanied by an increase in the firing rate of an inhibitory interneuron and an increase in the ripple rate followed by a rebound in the firing rate of excitatory neurons. (A) Aligned LFP recorded from a microelectrode in the left hippocampus in patient TJU049 indicating the beginning and end of LVF when the fast activity fully transitioned to clonic bursts. (B) Corresponding spectrogram, the increase in the power in faster frequencies during LVF onset. (C) Aligned plot of ripple events prior to and during LVF onset. (D) Aligned raster plot of spiking activity of excitatory (blue) and inhibitory neurons (red) prior to and during LVF onset. Note that LVF ended at different times for each microelectrode recording. Abbreviations (LAH: left anterior hippocampus, LPH: left posterior hippocampus).

Across all the seizures, the firing pattern of the excitatory and inhibitory neurons was Heterogeneous; however, for 6 of the analyzed seizures, a change in excitatory and inhibitory balance was evident at the time of LVF onset (Figure 6.12).

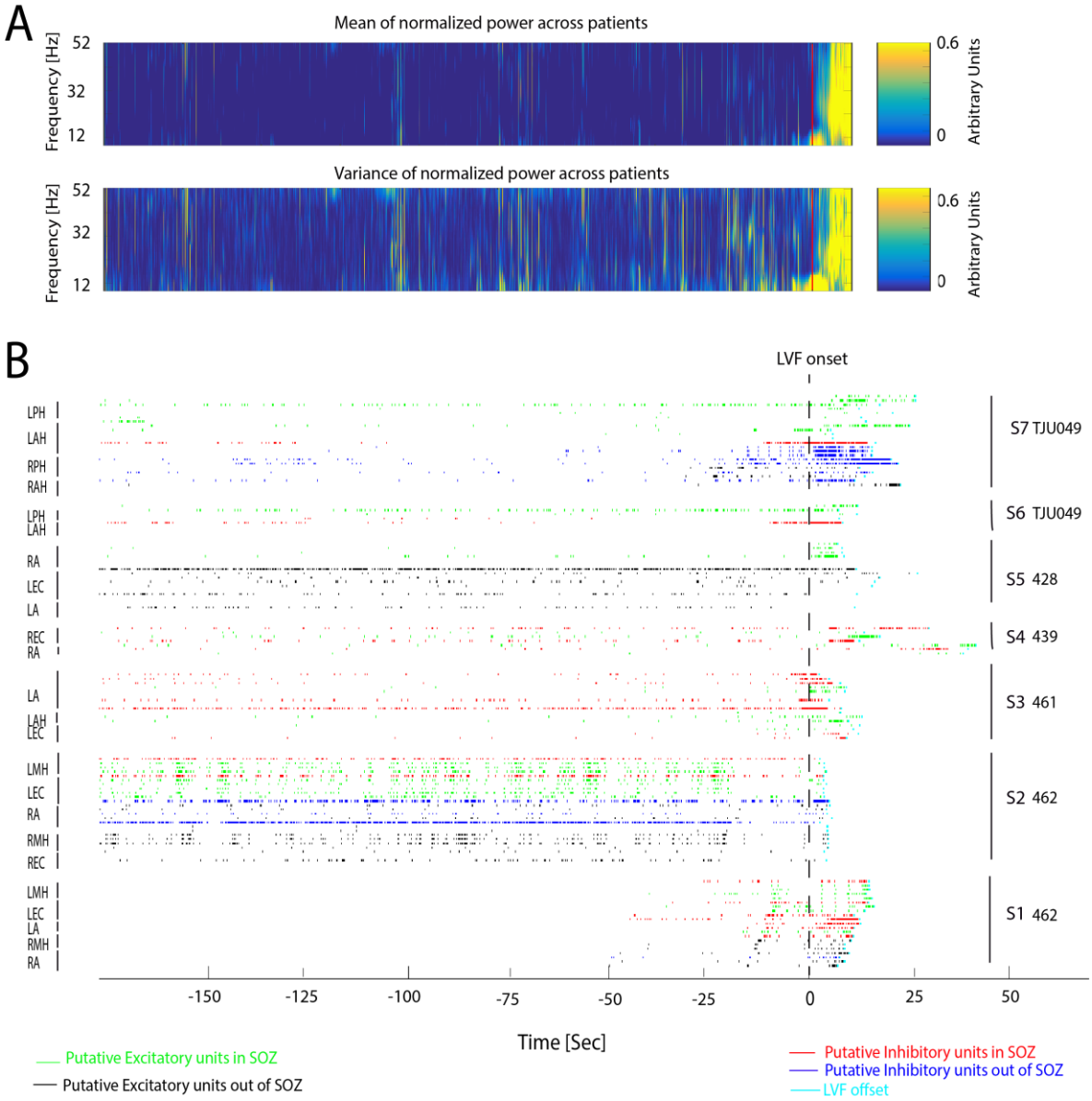

Figure 6.12. Across all seizures excitatory and inhibitory neuron firing is heterogeneous, but changes in excitatory and of LVF. (A) Time-Frequency plot of the mean normalized power (top), and variance (bottom) prior to and during LVF onset in the LFP across all the seizures. (B) Aligned raster plot of 104 units (5 Patients, 7 seizures). The seizures are aligned to the onset of LVF activity (dashed vertical line). Excitatory neurons in the SOZ are shown in green, inhibitory neurons in the SOZ are shown in red, excitatory neurons in the NSOZ are

shown in black, inhibitory neurons in the NSOZ are shown in blue. Abbreviations (REC : Right Entorhinal Cortex, LEC: Left Entorhinal Cortex, LPH: Left Posterior Hippocampus, RPH: Right Posterior Hippocampus, LPH: Left Posterior Hippocampus, RMH: Right Medial Hippocampus, LMH: Left Medial Hippocampus, RA: Right Amygdala, LA: Left Amygdala).

To quantify this change, we measured the average firing rate of putative excitatory and inhibitory neurons. We found that the EC inhibitory neuron firing rates increased at LVF onset ($p<0.05$, Wilcoxon signed-rank, n= 6). During this time, the excitatory neuron firing rate was suppressed comparing to 10 seconds before LVF onset ($p<0.05$, Wilcoxon rank-sum, n= 9). Approximately 10 seconds after LVF onset, a dramatic rebound of the excitatory neuron firing rate was evident ($p<0.05$, Wilcoxon signed-rank, n= 11; Figure 6.13A). In the amygdala (Figure 6.13B), the firing rate of inhibitory interneurons also increased at LVF onset ($p<0.01$, Wilcoxon signed-rank, n= 11, respectively), and the excitatory neuron firing rate rebounded later during LVF ($p<0.01$, Wilcoxon signed-rank, n= 11). In contrast to the EC and amygdala, an increase in the inhibitory firing rate ($p= 0.13$, Wilcoxon signed-rank, n=5) and a rebound in the firing rate of excitatory neurons ($p<0.7$, Wilcoxon signed-rank, n= 30) was not evident in the hippocampus (Figure 6.13C). As discussed in Section 6.2, ripples and fast ripples rate are different for two kinds of seizure onset: LVF and HYP. As stated (Perucca, Dubeau, and Gotman 2014), for LVF seizures, ripples rate increases, which is not the same case for fast ripples. To make sure, we marked the onset of LVF precisely while we also quantified the change in the ripple and fast ripple rate during the pre-ictal epoch as compared with during LVF onset. We found that in the mesial temporal SOZ, the ripple rate increased from 1.2 ± 0.077 (mean ± standard error) ripples/sec to 2.2 ± 0.13 ripples/sec (Wilcoxon signed-rank test, $p<0.001$). In contrast, the fast ripple rate decreased (Wilcoxon signed-rank test, $p<0.001$ Figure 6.14).

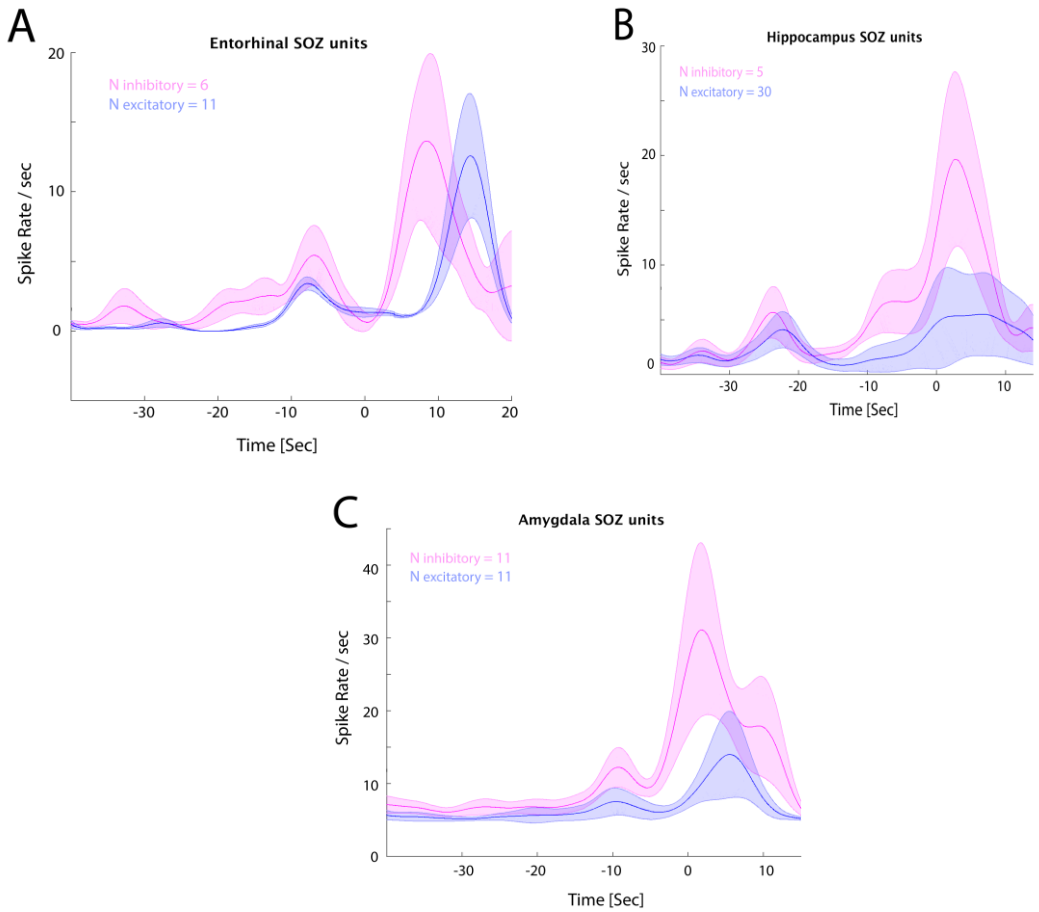

Figure 6.13. In the seizure-onset zone, the firing rate of inhibitory neurons increases during LVF onset and is followed by a rebound in the firing rate of excitatory neurons. Comparison of the mean spike firing rate following smoothing using a Gaussian kernel for excitatory (blue) and inhibitory (red) neurons prior to and during LVF onset in the entorhinal cortex (A), hippocampus (B), and amygdala (C) seizure onset zone. Error bars represent the standard error of the mean (s.e.m).

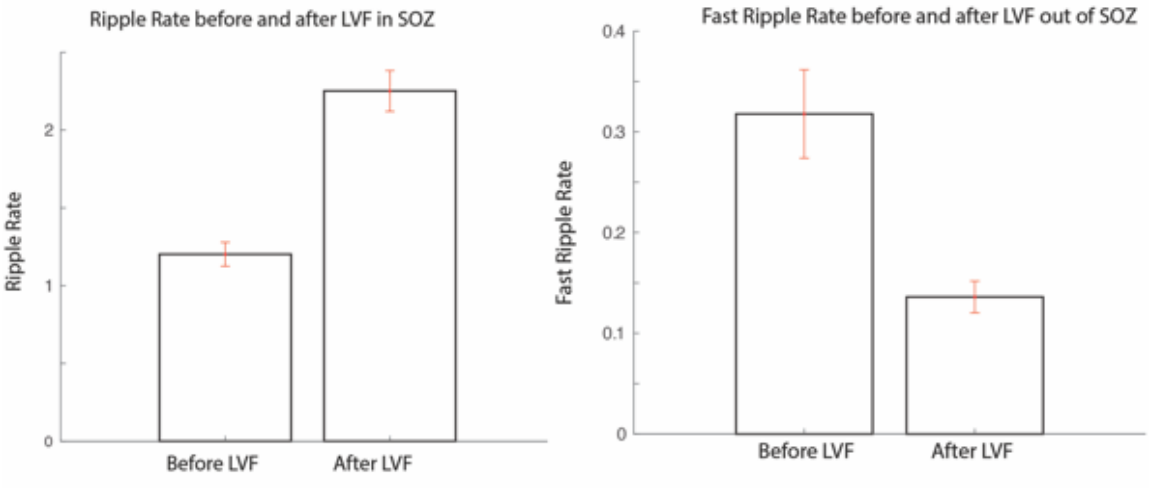

Figure 6.14. During LVF onset in the seizure-onset zone, the ripple rate increased but the fast ripple rate decreased. Error bars show standard error of the mean (s.e.m).

We also examined the changes in excitatory and inhibitory cell firing in recordings from the mesial temporal lobe contralateral to the seizure-onset zone during LVF activity. Surprisingly, we found the same pattern as ipsilateral to seizure onset. During LVF spread, the firing rate of the inhibitory interneurons increased dramatically. This increase in the amygdala was ($p<0.05$, Wilcoxon signed-rank, n= 4) and in the hippocampus ($p<0.05$, Wilcoxon signed-rank, n= 7). As shown in Figure 6.15, following the increase in the firing rate of inhibitory interneurons, and later during the LVF spread, a small increase in the firing rate of excitatory neurons was evident in the amygdala and hippocampus ($p<0.05$, Wilcoxon signed-rank, n= 17).

The ripple rate also increased during LVF spread in the mesial temporal lobe contralateral to the seizure onset zone from 1.06 ± 0.13 (mean ± standard error) ripples/sec to 1.54 ± 0.16 (mean ± standard error) ripples/sec (Wilcoxon signed-rank test, $p<0.05$); the fast ripple rate decreased (Wilcoxon signed-rank test, $p<0.01$, Figure 6.16). Figure 6.11 shows that an increase in the ripple rate was also evident following the LVF spread during the clonic bursting that followed. These results are consistent with animal models (Librizzi et al. 2017; LEvesque et al. 2016) and the definition of LVF type of onset in humans (Perucca, Dubeau, and Gotman 2014).

.

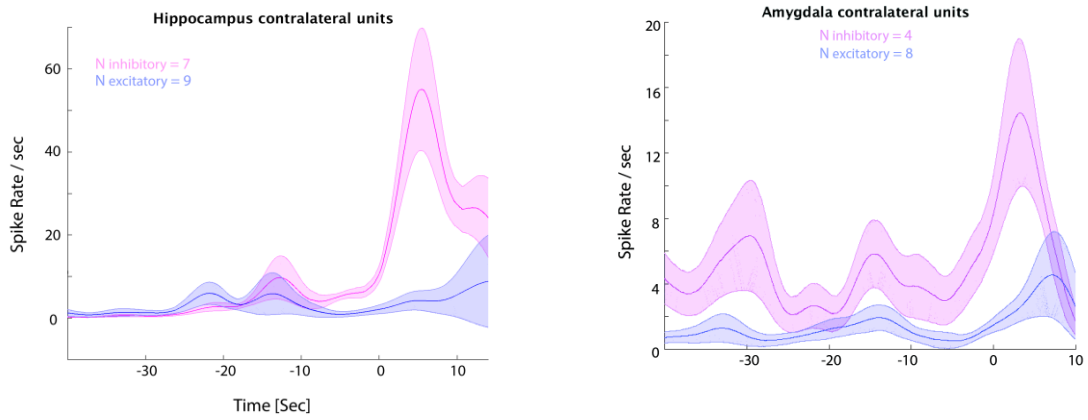

Figure 6.15. Contralateral to the seizure onset zone, the firing rate of inhibitory neurons also increases during LVF activity prior to an increase in the firing rate of excitatory neurons. Comparison of the mean spike firing rate following smoothing using a Gaussian kernel for excitatory (blue) and inhibitory (red) neurons prior to and during LVF onset in the amygdala (A) and hippocampus (B) contralateral to the seizure onset zone. Error bars represent the standard error of the mean (s.e.m).

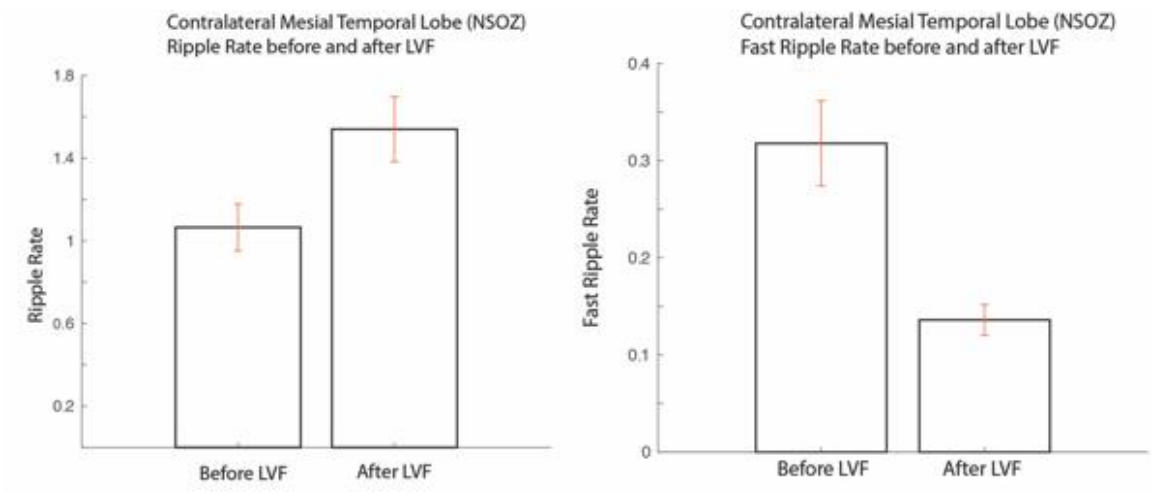

Figure 6.16. During LVF spread in the mesial temporal lobe contralateral to the seizure-onset zone, the ripple rate increased but the fast ripple rate decreased. Error bars show standard error of the mean (s.e.m).

6.8 Phase relationship between single unit firing and LVF activity

From the animal model (LEvesque et al. 2016), we know that inhibitory interneurons are phase-locked with LVF activity, which is not the same case for excitatory neurons. To

reconfirm our putative inhibitory and excitatory neurons, we characterized the firing properties of these interneurons. We examined whether the action potentials of each single unit were phase-locked to the LVF activity. If the answer is positive, we can finally declare that our putative inhibitory and excitatory neurons are correctly categorized. We studied the phase-locking of action potentials to two arbitrary and equal frequencies that compose LVF, a slower band often present at onset between 5-15 Hz, and a faster band often present later between 20-30 Hz. We found that, in the SOZ, the inhibitory interneurons were often phase-locked to the peak of the LVF activity occurring in these two frequency bands (Figure 6.12 Top, $p<0.05$). In contrast, fewer of the excitatory neurons showed phase-locking to the LVF activity (Figure 6.12 bottom, $p<0.05$). Figure 6.17 illustrates that the putative excitatory and inhibitory neurons isolated in the mesial temporal lobe contralateral to the seizure-onset zone exhibited similar properties.

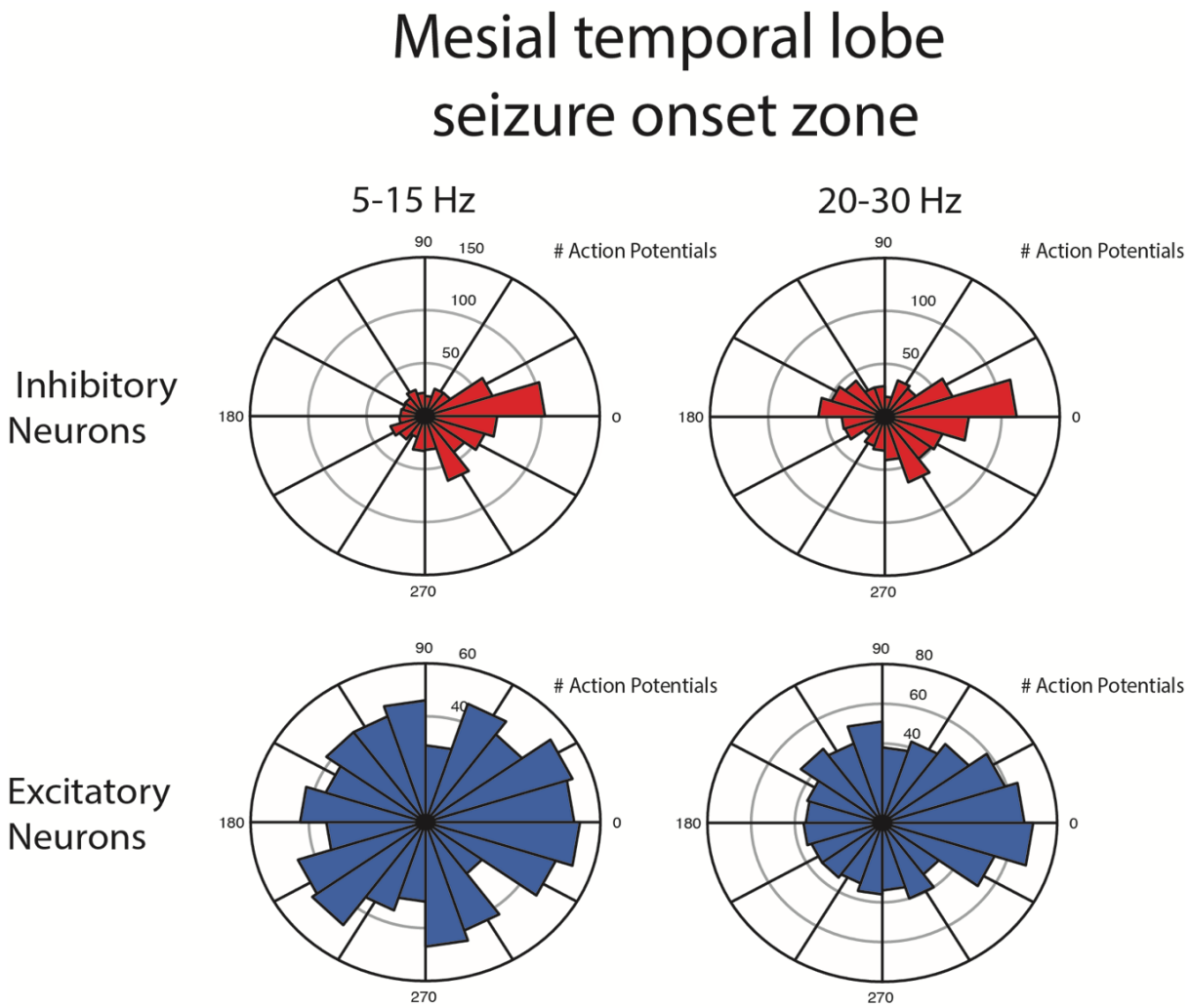

Figure 6.17. The action potentials of inhibitory interneurons are phase-locked to low-voltage fast oscillations during LVF onset, but the action potentials of excitatory neuron are not. Top, Rose plots, i.e., circular histograms of the preferred phase angle of B. Inhibitory interneuron action potentials (red, top), and bottom, excitatory neuron action potentials (blue, bottom) with respect to LVF oscillations between 5-15 Hz (left) and 20-30 Hz (right).

6.9 Discussion

We applied single- and multi-unit analysis to LFP recordings of spontaneous LVF onset seizures in patients with MTLE and found that action potentials do not change morphology during LVF ictal onset, and that the action potentials can be reliably sorted into putative excitatory and inhibitory units. During LVF onset, in the EC onset zone, inhibitory neurons dramatically increase their firing rate prior to a rebound of increased excitatory neuron firing.

Contralateral to the SOZ, during LVF spread, inhibitory neurons also increase their firing rate prior to excitatory neurons. Therefore, these results demonstrate a specific imbalance of excitation and inhibition during spontaneous LVF onset seizures in humans.

6.9.1 Accuracy and validity of single unit spike sorting during seizure onset

Using both single-unit analysis and MUA approaches, we found that the morphology of action potentials remains unaltered during LVF oscillations in the seizure-onset zone or sites of spread. MUA analysis was necessary for this proof because single-unit recordings may introduce a bias towards excluding action potentials with an altered morphology (Quiroga, Nadasdy, and Ben-Shaul 2004). Our results differ from those obtained using microelectrode arrays implanted in the human neocortex, which demonstrated that in the ictal core, single units cannot be discriminated (Merricks et al. 2015). The disparity is not due to electrode placement, since the ictal core encompasses the mesial temporal seizure-onset zone and later some of the sites of spread in patients with MTLE (Weiss Shennan et al. 2015). One reason that we were able to successfully perform SUA in LFP recordings from the ictal core—while a prior study claimed this approach was invalid—is that the prior study analyzed unit activity not just during the ictal onset pattern but rather during onset and the clonic bursting that followed (Merricks et al. 2015). In contrast, in our study, we restricted the analysis of ictal neuronal spiking to the LVF-onset epoch and found that the action potential waveform morphology was stable. Demonstrating this stability was critical to establishing that action potentials from excitatory and inhibitory interneurons could be reliably identified during seizure onset.

We used established criteria to discriminate putative excitatory from inhibitory neurons on the basis of waveform morphology (Jozsef Csicsvari et al. 1998; LEvesque et al. 2016). Other approaches to discriminating excitatory from inhibitory neurons have examined the temporal autocorrelation of the spike train (Grasse, Karunakaran, and Moxon 2013; Shennan Aibel Weiss et al. 2016); however, this approach may be inappropriate for ictal epochs due to

atypical neuronal firing patterns. The validity of our spike-sorting approach was further supported by the fact that the putative inhibitory neurons were phase-locked to the LVF activity, while the putative excitatory neurons were less often phase-locked to it (Grasse, Karunakaran, and Moxon 2013; LEvesque et al. 2016).

6.9.2 Excitatory/Inhibitory imbalance during LVF onset in the seizure-onset zone

Across all the seizures examined in this study, the inhibitory neuron firing that was recorded in the EC-onset zone dramatically increased at LVF onset, presumably suppressing excitatory neuron firing. Approximately 10 seconds after LVF onset, we observed a rebound of excitatory neuron firing. This pattern of excitatory/inhibitory imbalance during LVF onset in the EC recapitulates the firing pattern of excitatory and inhibitory neurons in pharmacologically induced seizures in in vitro models of epileptiform synchronization (LEvesque et al. 2016; Trombin, Gnatkovsky, and de Curtis 2011; Gnatkovsky et al. 2008; Uva et al. 2015). The mechanism by which the specific excitatory/inhibitory imbalance at LVF onset promotes seizure genesis is not yet resolved, but may involve depolarizing GABAergic activity (LEvesque et al. 2016) or potassium and chloride efflux due to the KCC transporter (Hamidi and Massimo 2015). Another similarity between the spontaneous LVF-onset seizures recorded from the patients in this study and the pharmacologically induced LVF seizures in vitro was an increase in the ripple, but not fast ripple, rate that accompanied LVF onset.

In this study, in the amygdala onset zone, LVF onset was also associated with increased inhibitory neuron firing and an increase in the ripple rate. In contrast to the EC and amygdala, in the hippocampus no significant increase in the firing rate of inhibitory and excitatory neuron firing rates was seen during LVF. The role of excitatory/inhibitory balance in the hippocampus and amygdala during LVF seizure genesis has been investigated in pharmacological models of *status epilepticus*. Our findings in patients with medically refractory focal epilepsy suggest that the hippocampus preferentially generates

hypersynchronous seizures (Shennan Aibel Weiss et al. 2016; Memarian et al. 2015) and that the relationship of these events to LVF seizures in EC remain to be elucidated.

6.9.3 Excitatory/Inhibitory imbalance during LVF spread

We found that inhibitory neuron firing also increased during LVF spread in mesial temporal lobe structures contralateral to the seizure-onset zone. Following such an increase, a small increase in excitatory neuron firing was evident. The significance of the increase in inhibitory neuron firing during LVF spread is not yet clear. The inhibitory interneurons in the region of spread were phase-locked to the LVF oscillations, suggesting that they may have been intrinsically involved in the generation of the LVF spread.

It is unlikely that the increase in the firing rate of local inhibitory interneurons in sites of spread reflect an inhibitory restraint mechanism (C. a. Schevon et al. 2012; Shennan Aibel Weiss et al. 2016) because the excitatory neurons at these sites were quiescent prior to and during the appearance of the LVF activity. It is unfortunate that the initial LVF onset and the contralateral propagation both exhibited an increase in the ripple rate and inhibitory interneuron firing rate, because, according to the parameters, the sites of onset and spread cannot be easily differentiated.

An alternative interpretation—at least for mesial temporal onsets—is that LVF may not be a seizure onset pattern at all, but may reflect the propagation of unseen hypersynchronous onsets.

LVF onsets are usually regional while hypersynchronous onsets are usually focal, and the former are associated with a poorer outcome than the latter (Memarian et al. 2015; Ogren, Wilson, et al. 2009), perhaps because the precise site of seizure onset cannot be identified. In a single seizure recording from a patient in a prior study, a hypersynchronous microseizure was present on the microelectrode recordings prior to the LVF onset seen in the clinical macroelectrodes (Shennan Aibel Weiss et al. 2016).

Chapter 7

Conclusion

7.1 Summary of Contributions

The goal of this dissertation was to develop a unified framework for data-driven modeling of neuroimaging signals in order to investigate seizure-onset zones and any biomarker related to seizure-onset from a tissue to single neuron.

Reading the EEG recordings to identify the electrodes whose recordings show seizure activity requires several days of expert analysis; however, some seizure activities are not easy to be detect by eyesight alone; hence, there is a need for more signal processing techniques. Removing any part of the patient's brain is very changeable since each part of the brain is involved in a part of its functioning. The greatest challenge for experts is how to identify the SOZ accurately so that patients are seizure free following the surgery, while using the minimum of his/her brain functionality.

Chapter 3 investigated a newly developed biomarker to localize the seizure-onset zone. Using the Phase Locking Value (PLV)—a measurement to calculate phase amplitude coupling—we studied how the amplitudes of higher frequency rhythms (80-150 Hz) modulate the phase of lower ones (4-30 Hz). By extracting five features (explained in Chapter 5) and using a machine learning algorithm such as Logistic Regression, we were able to build a model. This model was based on the extracted features from PLV signal related to seizure-free patients. As we know that the resected area for these patients was appropriate to make them seizure free, we trained our model on these features. Then, we tested it on those patients who were not seizure free. The results of this study showed that, for those patients who were not seizure free after surgery, the proposed algorithm could find some more electrodes as aSOZ electrodes beyond the resection area. However, the post-surgical results, confirmed that most of these aSOZ electrodes were included in language, motor, visual or memory parts of the cortex. The resection of these areas will decrease the quality of life of

the patients at the price of being seizure free. That is the main reason that those aSOZ electrodes have not been resected. There were some other electrodes that our algorithm could find as putative SOZ electrodes and that were not visible to neurologists while reading EEG recordings.

In Chapter 4, we explored the idea of the rate of HFO and FHFO in different epochs. The first step was make an automate algorithm, which does not need any tuning for each patient. Second, we removed those activities that looked like artifacts and spikes using the physiologic characteristics of these two events. Then, we were able to obtain the HFO/FHFO onset time and duration for each single channel. We investigated these rates for 10 minutes during night, wake, preictal, and 2 minutes of ictal. Having obtained the postsurgical results and resected area along with SOZ, we could analyze the results based on each group of patients (seizure free or not), in/out of SOZ and in/out of the resected area. We showed that, as expected, the ictal period has the highest of HFO/FHFO, and that it is due to propagation of the seizure when more electrodes are engaged with seizure activity. For most cases, the preictal period had a higher HFO/FHFO rate than that of the night rate. This fact is contradictory to common belief that at night the rates of HFO/FHFO are higher. The reason for this opposition is that at night we have fewer artifacts and may be spikes. Without using any signal-processing technics, to remove these cases, it is easier to find HFO/FHFO events; however, by removing unwanted events, we could see higher rates of HFO/FHFO in preictal.

Finally, we then chose to use deep neuron's data to efficiently study the role of neurons at the onset of seizure. In Chapter 6 we focused on those seizures that exhibited LVF at their onset. The rationale behind this choice was that we wanted to study how seizure propagates other regions than on were it initiates. LVF seizure onsets are more defuse than other types of MTLE's common seizure onset, which is HYP. LVF seizure onsets start from the entorhinal cortex and rapidly propagate to the hippocampus. To study the different role of neurons to initiate the seizure, the first step was to detect them. We used Waveclus to detect the action

potentials from each electrodes. Using K-mean clustering and then confirming by phase locking value, we were able to categorize the interneurons into two distinct groups: inhibitory and excitatory. We proved that across all seizures excitatory and inhibitory neuron firing is heterogeneous, but that changes in excitatory and inhibitory balance are evident at the beginning of LVF. Inhibitory neurons started to fire prior to excitatory neurons at the very start of LVF onset, or even prior to that in some cases. However, excitatory neurons fire later, and in some cases are even quiet before LVF onset. This fact was consistent for each region of the brain (hippocampus, entorhinal cortex and amygdala), ipsilateral and surprisingly contralateral to seizure onset. We also showed that the morphology of action potentials never change before and after LVF. It is worth to noting that by saying "after LVF" onset we mean from LVF onset until start of burst activity of the seizure.

7.2 Future Directions

Several interesting problems would be interesting to explore.

Considering the combination of HFO and PAC as a biomarker for localizing the seizure: In this study, we focused on the features extracted from PLV to train our model. We will have more robust model if we can have features that are more meaningful. As the rate of HFO/FHFO has been studied in this study, it would be interesting to combine it with PLV features and feed them into the algorithm.

Study the effect of the seizure generation site to PAC or HFO rates: In this study, we did not separate our patients based on the seizure-onset region. It would be interesting to look at the effect of the seizure-onset site and correlate it with the obtained values from PLV or the rate of HFO/FHFO. In this dissertation, we investigated the effect of time on the rate of HFO/FHFO, but we did not consider the location of seizure initiation.

Exploring the effect of interneurons on the HYP seizure onset: As we mentioned before, for the sake of this study, we only analyzed the seizures with LVF onset. It would also be worth looking at the other onset type (HYP) and comparing the results. From the animal

models, the results are completely reversed, but no study has been done on humans to prove this fact.

Data and software availability

All codes related for analysis in Chapter 4 are available on Github:

https://github.com/babahareh/HighFreq_PLV_ECOG

The codes for analysis in Chapter 5 are available on Github:

https://github.com/babahareh/HFO-and-FHFO-for-different-Epochs

Raw data recordings used for analysis in Chapter 6 are available on the international EEG portal iEEG.org.

The analysis for Waveclus and the database along with all spreadsheets are available on a permanent Zenodo repository: https://www.zenodo.org/record/836286#.WX0Ht9PyuWZ.

Matlab codes used for analysis in Chapter 6 are available: https://github.com/shennanw/lvf_code

Relationship to published works

- Chapter 4:
  - **Bahareh Elahian**, Mohammed Yeasin, Basanagoud Mudigoudar, James Wheless, Abbas Babajani-Feremi, "*Identifying Seizure Onset Zone from Electrocorticographic Recording: A Machine Learning Approach based on Phase Locking Value,*" Journal of Seizure, European Journal of Epilepsy, Accepted July, 20, 2017. European Journal of Epilepsy 51C (2017) pp. 35-42
  - **Bahareh Elahian**, Basanagoud Mudigoudar, Mohammed Yeasin, Andrew Papanicolaou, James Wheless, Abbas Babajani-Feremi, "Identification of Seizure Onset Zone using Electrocorticographic High-frequency Oscillation", American Epilepsy Society, December 2015
  - **Bahareh Elahian**, Mohammed Yeasin, Basanagoud Mudigoudar, James Wheless, Abbas Babajani-Feremi, "*Identification of Seizure Onset Zone Using Phase Locking Value in Electrocorticographic Recording,*" Organization for Human Brain Mapping, June 2016.
  - **Bahareh Elahian**, Mohammed Yeasin, Basanagoud Mudigoudar, James Wheless, Abbas Babajani-Feremi, "*A multivariate approach for seizure localization using high frequency coupling,*" North American Neuromodulation Society, June 2016.
  - **Bahareh Elahian**, Mohammed Yeasin, Basanagoud Mudigoudar, James Wheless, Abbas Babajani-Feremi, "*Localization of seizure onset zone using classification of Electrocorticographic synchronization pattern,*" American Epilepsy Society, December 2016.

- **Bahareh Elahian**, Mohammed Yeasin, Basanagoud Mudigoudar, James Wheless, Abbas Babajani-Feremi, "*Multivariate approach to predict the seizure onset zone and improve the outcome of surgery*," Neuromodulation Symposium, April 2017.

- Chapter 6
  - **Bahareh Elahian**, Nathan Lado, Karen Moxon, Amrit Misra, Ashwini Sharan, Itzhak Fried, Mohammed Yeasin, Jerome Engel Jr., Michael Sperling, Richard Staba, Shennan Aibel Weiss, "*Human Low-Voltage Fast Seizures Are Caused by Inhibitory/Excitatory Imbalance*," Annals of Neurology, Under Revision, Ref: 2017ANA-17-0921.
  - **Bahareh Elahian**, Nathan Lado, Karen Moxon, Amrit Misra, Ashwini Sharan, Itzhak Fried, Mohammed Yeasin, Jerome Engel Jr., Michael Sperling, Richard Staba, Shennan Aibel Weiss, "*Characterizing single unit activity from putative excitatory and inhibitory neurons in limbic structures during spontaneous focal seizures in patients with medically refractory epilepsy*", Society For Neuroscience, November, 2017.
  - **Bahareh Elahian**, Nathan Lado, Amrit Misra, Karen Moxon, Itzhak Fried, Mohammed Yeasin, Ashwini Sharan, Richard Staba, Anatol Bragin, Micheal Sperling, Jerome Engel, Shennan Weiss," *Spontaneous low-voltage fast limbic seizures in humans exhibit a specific excitatory-inhibitory imbalance at seizure onset*", American Epilepsy Society, December 2017.

References

‘t Klooster, Maryse A. van, Nicole E C Van Klink, Frans S. S. Leijten, Rina Zelmann, Tineke A. Gebbink, Peter H Gosselaar, Kees P J Braun, Geertjan J M Huiskamp, and Maeike Zijlmans. 2015. “Residual Fast Ripples in the Intraoperative Corticogram Predict Epilepsy Surgery Outcome,” 120–28.

Adamos, Dimitrios A., Nikolaos A. Laskaris, Efstratios K. Kosmidis, and George Theophilidis. 2010. “NASS: An Empirical Approach to Spike Sorting with Overlap Resolution Based on a Hybrid Noise-Assisted Methodology.” *Journal of Neuroscience Methods* 190 (1):129–42. https://doi.org/10.1016/j.jneumeth.2010.04.018.

Al-Otaibi, Faisal, Saleh S. Baeesa, Andrew G. Parrent, John P. Girvin, and David Steven. 2012. “Surgical Techniques for the Treatment of Temporal Lobe Epilepsy.” *Epilepsy Research and Treatment* 2012:1–13. https://doi.org/10.1155/2012/374848.

Alkawadri, Rafeed, Nicolas Gaspard, Irina I. Goncharova, Dennis D. Spencer, Jason L. Gerrard, Hitten Zaveri, Robert B. Duckrow, Hal Blumenfeld, and Lawrence J. Hirsch. 2014. “The Spatial and Signal Characteristics of Physiologic High Frequency Oscillations.” *Epilepsia* 55 (12):1986–95. https://doi.org/10.1111/epi.12851.

Alvarado-Rojas, C., M. Valderrama, A. Witon, V. Navarro, and M. Le Van Quyen. 2011. “Probing Cortical Excitability Using Cross-Frequency Coupling in Intracranial EEG Recordings: A New Method for Seizure Prediction.” *Proceedings of the Annual International Conference of the IEEE Engineering in Medicine and Biology Society, EMBS*, no. 1:1632–35. https://doi.org/10.1109/IEMBS.2011.6090471.

Alvarado-Rojas, Catalina, Mario Valderrama, A Fouad-Ahmed, H Feldwisch-Drentrup, M Ihle, C A Teixeira, F Sales, et al. 2014. “Slow Modulations of High-Frequency Activity (40-140Hz) Discriminate Preictal Changes in Human Focal Epilepsy.” *Sci. Rep.* 4:4545. https://doi.org/10.1038/srep04545.

Amiri, Mina, Jean-Marc Lina, Francesca Pizzo, and Jean Gotman. 2015. “High Frequency

Oscillations and Spikes: Separating Real HFOs from False Oscillations." *Clinical Neurophysiology*. International Federation of Clinical Neurophysiology. https://doi.org/10.1016/j.clinph.2015.04.290.

Asadi-Pooya, A. A., M. Nei, C. Rostami, and M. R. Sperling. 2016. "Mesial Temporal Lobe Epilepsy with Childhood Febrile Seizure." *Acta Neurologica Scandinavica*, no. 6:88–91. https://doi.org/10.1111/ane.12566.

Avoli, Massimo, Marco De Curtis, Vadym Gnatkovsky, Jean Gotman, Rüdiger Köhling, Maxime Lévesque, Frédéric Manseau, Zahra Shiri, and Sylvain Williams. 2016. "Specific Imbalance of Excitatory/inhibitory Signaling Establishes Seizure Onset Pattern in Temporal Lobe Epilepsy." *Journal of Neurophysiology* 2015 (April):jn.01128.2015. https://doi.org/10.1152/jn.01128.2015.

AYALA, G. F., M. DICHTER*, R. J. GUMNIT, H. MATSUMOTO**, and W. A. SPENCER. 1973. "GENESIS OF EPILEPTIC INTERICTAL SPIKES. NEW KNOWLEDGE OF CORTICAL FEEDBACK SYSTEMS SUGGESTS A NEUROPHYSIOLOGICAL EXPLANATION OF BRIEF PAROXYSMS" 6:303–13.

Baker, Stuart N., Curio Gabriel, and Roger N. Lemon. 2003. "EEG Oscillations at 600 Hz Are Macroscopic Markers for Cortical Spike Bursts." *The Journal of Physiology* 550 (2):529–34. https://doi.org/10.1113/jphysiol.2003.045674.

Banerjee, Poonam Nina, David Filippi, and W. Allen Hauser. 2009. "The Descriptive Epidemiology of Epilepsy-A Review." *Epilepsy Research* 85 (1):31–45. https://doi.org/10.1016/j.eplepsyres.2009.03.003.

Barth, Daniel S. 2003. "Submillisecond Synchronization of Fast Electrical Oscillations in Neocortex." *The Journal of Neuroscience : The Official Journal of the Society for Neuroscience* 23 (6):2502–10. https://doi.org/23/6/2502 [pii].

Benar, C. G., L. Chauviere, F. Bartolomei, and F. Wendling. 2010. "Pitfalls of High-Pass Filtering for Detecting Epileptic Oscillations: A Technical Note On 'false' ripples."

Clinical Neurophysiology 121 (3). International Federation of Clinical Neurophysiology:301–10. https://doi.org/10.1016/j.clinph.2009.10.019.

Blanco, Justin A., Matt Stead, Abba Krieger, William Stacey, Douglas Maus, Eric Marsh, Jonathan Viventi, et al. 2011. "Data Mining Neocortical High-Frequency Oscillations in Epilepsy and Controls." *Brain* 134 (10):2948–59. https://doi.org/10.1093/brain/awr212.

Bower, Mark R., Michal T. Kucewicz, Erik K. St. Louis, Fredric B. Meyer, W. Richard Marsh, Matt Stead, and Gregory A. Worrell. 2017. "Reactivation of Seizure-Related Changes to Interictal Spike Shape and Synchrony during Postseizure Sleep in Patients." *Epilepsia* 58 (1):94–104. https://doi.org/10.1111/epi.13614.

Bragin, a, G Jandó, Z Nádasdy, J Hetke, K Wise, and G Buzsáki. 1995. "Gamma (40-100 Hz) Oscillation in the Hippocampus of the Behaving Rat." *The Journal of Neuroscience : The Official Journal of the Society for Neuroscience* 15 (1 Pt 1):47–60.

Bragin, Anatol, Avetis Azizyan, Joyel Almajano, Charles L. Wilson, and Jerome Engel. 2005. "Analysis of Chronic Seizure Onsets after Intrahippocampal Kainic Acid Injection in Freely Moving Rats." *Epilepsia* 46 (10):1592–98. https://doi.org/10.1111/j.1528-1167.2005.00268.x.

Bragin, Anatol, Simone K. Benassi, and Engel Jr. Kheiri, Farshad, Jerome. 2011. "Further Evidence That Pathological High Frequency Oscillations Are Bursts of Population Spikes Derived from Recordings of Identified Cells in Dentate Gyrus" 52 (1):45–52. https://doi.org/10.1086/498510.Parasitic.

Bragin, Anatol, Jerome Engel, Charles L. Wilson, Elizabeth Vizentin, and Gary W. Mathern. 1999. "Electrophysiologic Analysis of a Chronic Seizure Model after Unilateral Hippocampal KA Injection." *Epilepsia* 40 (9):1210–21. https://doi.org/10.1111/j.1528-1157.1999.tb00849.x.

Bragin, Anatol, Istvan Mody, Charles L Wilson, and Jerome Engel. 2002. "Local Generation of Fast Ripples in Epileptic Brain." *The Journal of Neuroscience : The Official Journal*

of the Society for Neuroscience 22 (5):2012–21. https://doi.org/22/5/2012 [pii].

Bragin, Anatol, Charles L. Wilson, and Jerome Engel. 2007. "Voltage Depth Profiles of High-Frequency Oscillations after Kainic Acid-Induced Status Epilepticus." *Epilepsia* 48 (SUPPL. 5):35–40. https://doi.org/10.1111/j.1528-1167.2007.01287.x.

Bulacio, Juan C., Lara Jehi, Chong Wong, Jorge Gonzalez-Martinez, Prakash Kotagal, Dileep Nair, Imad Najm, and William Bingaman. 2012. "Long-Term Seizure Outcome after Resective Surgery in Patients Evaluated with Intracranial Electrodes." *Epilepsia* 53 (10):1722–30. https://doi.org/10.1111/j.1528-1167.2012.03633.x.

Buzsaki, Gyorgy. 2006. *Rhythms of the Brain*. Oxford University Press. https://doi.org/10.1093/acprof:oso/9780195301069.001.0001.

Buzsáki, György. 2004. "Large-Scale Recording of Neuronal Ensembles." *Nature Neuroscience* 7 (5):446–51. https://doi.org/10.1038/nn1233.

Buzsaki, Gyorgy, Zsolt Horvath, and Ronald Urioste. 1992. "High-Frequency Network Oscillation in the Hippocampus." *Science* 256 (5059):1025–27.

Buzsáki, György, and Xiao-Jing Wang. 2012. "Mechanisms of Gamma Oscillations." *Annual Review of Neuroscience*, no. March:203–25. https://doi.org/10.1146/annurev-neuro-062111-150444.

Canolty, R T, E Edwards, S S Dalal, M Soltani, S S Nagarajan, H E Kirsch, M S Berger, N M Barbaro, and R T Knight. 2006. "High Gamma Power Is Phase-Locked to Theta Oscillations in Human Neocortex." *Science (New York, N.Y.)* 313 (5793):1626–28. https://doi.org/10.1126/science.1128115.

Canolty, Ryan T., Charles F. Cadieu, Kilian Koepsell, Robert T. Knight, and Jose M. Carmena. 2012. "Multivariate Phase-Amplitude Cross-Frequency Coupling in Neurophysiological Signals." *IEEE Transactions on Biomedical Engineering* 59 (1):8–11. https://doi.org/10.1109/TBME.2011.2172439.

Chaibi, Sahbi, Tarek Lajnef, Zied Sakka, Mounir Samet, and Abdennaceur Kachouri. 2014.

"A Reliable Approach to Distinguish between Transient with and without HFOs Using TQWT and MCA." *Journal of Neuroscience Methods* 232:36–46. https://doi.org/10.1016/j.jneumeth.2014.04.025.

Cohen, Michael X. 2008. "Assessing Transient Cross-Frequency Coupling in EEG Data." *Journal of Neuroscience Methods* 168 (2):494–99. https://doi.org/10.1016/j.jneumeth.2007.10.012.

Crépon, Benoît, Vincent Navarro, Dominique Hasboun, Stéphane Clemenceau, Jacques Martinerie, Michel Baulac, Claude Adam, and Michel Le Van Quyen. 2010. "Mapping Interictal Oscillations Greater than 200 Hz Recorded with Intracranial Macroelectrodes in Human Epilepsy." *Brain* 133 (2009):33–45. https://doi.org/10.1093/brain/awp277.

Csicsvari, J, H Hirase, a Czurkó, a Mamiya, and G Buzsáki. 1999. "Oscillatory Coupling of Hippocampal Pyramidal Cells and Interneurons in the Behaving Rat." *The Journal of Neuroscience : The Official Journal of the Society for Neuroscience* 19 (1):274–87.

Csicsvari, Jozsef, Hajime Hirase, Andras Czurko, and György Buzsáki. 1998. "Reliability and State Dependence of Pyramidal Cell-Interneuron Synapses in the Hippocampus: An Ensemble Approach in the Behaving Rat." *Neuron* 21 (1):179–89. https://doi.org/10.1016/S0896-6273(00)80525-5.

Curtis, Marco De, and Massimo Avoli. 2015. "Initiation, Propagation, and Termination of Partial (Focal) Seizures," 1–16.

Dichter, Marc A., and G. F. Ayala. 1987. "Cellular Mechanisms of Epilepsy: A Status Report." *American Association for the Advancement of Science Is Collaborating with JSTOR to Digitize, Preserve and Extend Access to Science* 237 (4811):157–64. https://doi.org/10.1007/sl0551-010-0729-l.

Diessen, Eric Van, Judith I. Hanemaaijer, Willem M. Otte, Rina Zelmann, Julia Jacobs, Floor E. Jansen, François Dubeau, Cornelis J. Stam, Jean Gotman, and Maeike Zijlmans. 2013. "Are High Frequency Oscillations Associated with Altered Network Topology in

Partial Epilepsy?" *NeuroImage* 82. Elsevier Inc.:564–73. https://doi.org/10.1016/j.neuroimage.2013.06.031.

Durnford, Andrew J., William Rodgers, Fenella J. Kirkham, Mark A. Mullee, Andrea Whitney, Martin Prevett, Lucy Kinton, Matthew Harris, and William P. Gray. 2011. "Very Good Inter-Rater Reliability of Engel and ILAE Epilepsy Surgery Outcome Classifications in a Series of 76 Patients." *Seizure* 20 (10). BEA Trading Ltd:809–12. https://doi.org/10.1016/j.seizure.2011.08.004.

Eadie, Mervyn J. 2005. "Victor Horsley's Contribution to Jacksonian Epileptology." *Epilepsia* 46 (11):1836–40. https://doi.org/10.1111/j.1528-1167.2005.00290.x.

Edelman, Jay a, and Michael E Goldberg. 2003. "Saccade-Related Activity in the Primate Superior Colliculus Depends on the Presence of Local Landmarks at the Saccade Endpoint." *Journal of Neurophysiology* 90 (3):1728–36. https://doi.org/10.1152/jn.00016.2003.

Eisenschenk, Stephan, Robin L. Gilmore, Jean E. Cibula, and Steven N. Roper. 2001. "Lateralization of Temporal Lobe Foci: Depth versus Subdural Electrodes." *Clinical Neurophysiology* 112 (5):836–44. https://doi.org/10.1016/S1388-2457(01)00517-X.

Engel, Jerome, Anatol Bragin, Richard Staba, and Istvan Mody. 2009. "High-Frequency Oscillations: What Is Normal and What Is Not?" *Epilepsia* 50 (4):598–604. https://doi.org/10.1111/j.1528-1167.2008.01917.x.

Engel, Jerome, and Fernando Lopes da Silva. 2012. "High-Frequency Oscillations - Where We Are and Where We Need to Go." *Progress in Neurobiology* 98 (3). Elsevier Ltd:316–18. https://doi.org/10.1016/j.pneurobio.2012.02.001.

Fee, Michale S., Partha P. Mitra, and David Kleinfeld. 1996. "Automatic Sorting of Multiple Unit Neuronal Signals in the Presence of Anisotropic and Non-Gaussian Variability." *Journal of Neuroscience Methods* 69 (2):175–88. https://doi.org/10.1016/S0165-0270(96)00050-7.

Ferastraoaru, Victor, Andreas Schulze-Bonhage, Richard B. Lipton, Matthias Dümpelmann, Alan D. Legatt, Julie Blumberg, and Sheryl R. Haut. 2016. "Termination of Seizure Clusters Is Related to the Duration of Focal Seizures." *Epilepsia*, n/a-n/a. https://doi.org/10.1111/epi.13375.

Fisher, Robert S., Carlos Acevedo, Alexis Arzimanoglou, Alicia Bogacz, J. Helen Cross, Christian E. Elger, Jerome Engel, et al. 2014. "ILAE Official Report: A Practical Clinical Definition of Epilepsy." *Epilepsia* 55 (4):475–82. https://doi.org/10.1111/epi.12550.

Foffani, Guglielmo, Yoryani G. Uzcategui, Beatriz Gal, and Liset Menendez de la Prida. 2007. "Reduced Spike-Timing Reliability Correlates with the Emergence of Fast Ripples in the Rat Epileptic Hippocampus." *Neuron* 55 (6):930–41. https://doi.org/10.1016/j.neuron.2007.07.040.

Foster, David J., and Matthew A. Wilson. 2006. "Reverse Replay of Behavioural Sequences in Hippocampal Place Cells during the Awake State" 440:680–83.

Freedman, David A. 2009. *Statistical Models: Theory and Practice*. 2nd ed. cambridge university press.

Fujiwara, Hisako, Hansel M. Greiner, Ki Hyeong Lee, Katherine D. Holland-Bouley, Joo Hee Seo, Todd Arthur, Francesco T. Mangano, James L. Leach, and Douglas F. Rose. 2012. "Resection of Ictal High-Frequency Oscillations Leads to Favorable Surgical Outcome in Pediatric Epilepsy." *Epilepsia* 53 (9):1607–17. https://doi.org/10.1111/j.1528-1167.2012.03629.x.

Geertsema, Evelien E., Gerhard H. Visser, Demetrios N. Velis, Steven P. Claus, Maeike Zijlmans, and Stiliyan N. Kalitzin. 2015. "Automated Seizure Onset Zone Approximation Based on Nonharmonic High-Frequency Oscillations in Human Interictal Intracranial EEGs." *International Journal of Neural Systems* 25 (5):1550015. https://doi.org/10.1142/S012906571550015X.

Gliske, Stephen V., Irwin Zachary T., Davis Kathryn A., Sahaya Kinshuk, Chestek Cynthia, and Stacey William C. 2016. “Universal Automated High Frequency Oscillation Detector for Real-Time, Long Term EEG.” *Clinical Neurophysiology Journal* 127:1057–66.

Gloss, David, Sarah J Nolan, and Richard Staba. 2015. “The Role of High-Frequency Oscillations in Epilepsy Surgery.” *Cochrane Database Syst Rev*, 1–33. https://doi.org/10.1002/14651858.CD010235.pub2.The.

Gnatkovsky, Vadym, Laura Librizzi, Federica Trombin, and Marco De Curtis. 2008. “Fast Activity at Seizure Onset Is Mediated by Inhibitory Circuits in the Entorhinal Cortex in Vitro.” *Annals of Neurology* 64 (6):674–86. https://doi.org/10.1002/ana.21519.

Gompel, Jamie J. Van, Gregory A. Worrell, Michael L. Bell, Todd A. Patrick, Gregory D. Cascino, Corey Raffel, W. Richard Marsh, and Fredric B. Meyer. 2008. “Intracranial Electroencephalography with Subdural Grid Electrodes: Techniques, Complications, and Outcomes.” *Neurosurgery* 63 (3):498–505. https://doi.org/10.1227/01.NEU.0000324996.37228.F8.

Grasse, Dane W., Suganya Karunakaran, and Karen A. Moxon. 2013. “Neuronal Synchrony and the Transition to Spontaneous Seizures.” *Experimental Neurology* 248. Elsevier Inc.:72–84. https://doi.org/10.1016/j.expneurol.2013.05.004.

Grenier, F, I Timofeev, and M Steriade. 2001. “Focal Synchronization of Ripples (80-200 Hz) in Neocortex and Their Neuronal Correlates.” *Journal of Neurophysiology* 86 (4):1884–98.

Guirgis, Mirna, Yotin Chinvarun, Martin del Campo, Peter L Carlen, and Berj L Bardakjian. 2015. “Defining Regions of Interest Using Cross-Frequency Coupling in Extratemporal Lobe Epilepsy Patients.” *Journal of Neural Engineering* 12 (2):26011. http://stacks.iop.org/1741-2552/12/i=2/a=026011.

Gump, William C, Karen L Skjei, and Shefali N Karkare. 2013. “Seizure Control after

Subtotal Lesional Resection." *Neurosurgical Focus* 34 (6):E1. https://doi.org/10.3171/2013.3.FOCUS1348.

Haegelen, Claire, Piero Perucca, Claude Edouard Châtillon, Luciana Andrade-Valença, Rina Zelmann, Julia Jacobs, D. Louis Collins, François Dubeau, André Olivier, and Jean Gotman. 2013. "High-Frequency Oscillations, Extent of Surgical Resection, and Surgical Outcome in Drug-Resistant Focal Epilepsy." *Epilepsia* 54 (5):848–57. https://doi.org/10.1111/epi.12075.

Hamidi, Shabnam, and Avoli* Massimo. 2015. "KCC2 Function Modulates in Vitro Ictogenesis." *Neurobiology of Disease* 79 (2):51–58. https://doi.org/10.1167/iovs.07-1072.Complement-Associated.

Harris, K.D. Kenneth D, D.A. Darrell A Henze, Jozsef Csicsvari, Hajime Hirase, G. Buzsaki, and G Buzsáki. 2000. "Accuracy of Tetrode Spike Separation as Determined by Simultaneous Intracellular and Extracellular Measurements." *Journal of Neurophysiology* 84 (1):401. https://doi.org/http://jn.physiology.org/cgi/content/abstract/84/1/401.

Hill, Daniel N., Samar B. Mehta, and David Kleinfeld. 2011. "Quality Metrics to Accompany Spike Sorting of Extracellular Signals." *The Journal of Neuroscience : The Official Journal of the Society for Neuroscience* 31 (24):8699–8705. https://doi.org/10.1523/JNEUROSCI.0971-11.2011.

Höller, Yvonne, Raoul Kutil, Lukas Klaffenböck, Aljoscha Thomschewski, Peter M. Höller, Arne C. Bathke, Julia Jacobs, Alexandra C. Taylor, Raffaele Nardone, and Eugen Trinka. 2015. "High-Frequency Oscillations in Epilepsy and Surgical Outcome. A Meta-Analysis." *Frontiers in Human Neuroscience* 9 (October):1–14. https://doi.org/10.3389/fnhum.2015.00574.

Hu, Wen-Han, Chao Zhang, Kai Zhang, Fan-Gang Meng, Ning Chen, and Jian-Guo Zhang. 2013. "Selective Amygdalohippocampectomy versus Anterior Temporal Lobectomy in

the Management of Mesial Temporal Lobe Epilepsy: A Meta-Analysis of Comparative Studies." *Journal of Neurosurgery* 119 (5):1089–97. https://doi.org/10.3171/2013.8.JNS121854.

Ibrahim, George M., Simeon M. Wong, Ryan a. Anderson, Gabrielle Singh-Cadieux, Tomoyuki Akiyama, Ayako Ochi, Hiroshi Otsubo, et al. 2014. "Dynamic Modulation of Epileptic High Frequency Oscillations by the Phase of Slower Cortical Rhythms." *Experimental Neurology* 251:30–38. https://doi.org/10.1016/j.expneurol.2013.10.019.

Ikeda, Akio, Waro Taki, Takeharu Kunieda, Kiyohito Terada, Nobuhiro Mikuni, Takashi Nagamine, Shogo Yazawa, et al. 1999. "Focal Ictal Direct Current Shifts in Human Epilepsy as Studied by Subdural and Scalp Recording." *Brain* 122 (5):827–38. https://doi.org/10.1093/brain/122.5.827.

Jacobs, J., R. Staba, E. Asano, H. Otsubo, J. Y. Wu, M. Zijlmans, I. Mohamed, et al. 2012. "High-Frequency Oscillations (HFOs) in Clinical Epilepsy." *Progress in Neurobiology* 98:302–15. https://doi.org/10.1016/j.pneurobio.2012.03.001.

Jacobs, Julia, Pierre LeVan, Rahul Chander, Jeffery Hall, François Dubeau, and Jean Gotman. 2008. "Interictal High-Frequency Oscillations (80–500 Hz) Are an Indicator of Seizure Onset Areas Independent of Spikes in the Human Epileptic Brain." *Clinical Neurophysiology* 49 (11):1893–1907. https://doi.org/10.1016/j.clinph.2011.06.006.A.

Jacobs, Julia, Pierre LeVan, Claude Édouard Chatillon, André Olivier, F Dubeau, and J Gotman. 2009. "High Frequency Oscillations in Intracranial EEGs Mark Epileptogenicity rather than Lesion Type." *Clinical Neurophysiology* 132 (4):1022–37. https://doi.org/10.1016/j.clinph.2011.06.006.A.

Jacobs, Julia, Christina Vogt, Pierre LeVan, Rina Zelmann, Jean Gotman, and Katsuhiro Kobayashi. 2016. "The Identification of Distinct High-Frequency Oscillations during Spikes Delineates the Seizure Onset Zone Better than High-Frequency Spectral Power Changes." *Clinical Neurophysiology*. https://doi.org/10.1016/j.clinph.2015.04.053.

Jacobs, Julia, Maeike Zijlmans, Rina Zelmann, Claude Édouard Chatillon, Jeffrey Hall, André Olivier, François Dubeau, and Jean Gotman. 2010. "High-Frequency Electroencephalographic Oscillations Correlate with Outcome of Epilepsy Surgery." *Annals of Neurology* 67:209–20. https://doi.org/10.1002/ana.21847.

Jehi, Lara, Elaine Wyllie, and Orrin Devinsky. 2015. "Epileptic Encephalopathies: Optimizing Seizure Control and Developmental Outcome." *Epilepsia* 56 (10):1486–89. https://doi.org/10.1111/epi.13107.

Jirsch, J. D., E. Urrestarazu, P. LeVan, A. Olivier, F. Dubeau, and J. Gotman. 2006. "High-Frequency Oscillations during Human Focal Seizures." *Brain* 129 (6):1593–1608. https://doi.org/10.1093/brain/awl085.

Joo, Eun Yeon, Seung Bong Hong, Hyun Jung Han, Woo Suk Tae, Jee Hyun Kim, Sun Jung Han, Dae Won Seo, et al. 2005. "Postoperative Alteration of Cerebral Glucose Metabolism in Mesial Temporal Lobe Epilepsy." *Brain : A Journal of Neurology* 128 (Pt 8):1802–10. https://doi.org/10.1093/brain/awh534.

Kajikawa, Yoshinao, and Charles E. Schroeder. 2011. "How Local Is the Local Field Potential?" *Neuron* 72 (5). Elsevier Inc.:847–58. https://doi.org/10.1016/j.neuron.2011.09.029.

Kelvin, Elizabeth A., Dale C. Hesdorffer, Emilia Bagiella, Howard Andrews, Timothy A. Pedley, Tina T. Shih, Linda Leary, David J. Thurman, and W. Allen Hauser. 2007. "Prevalence of Self-Reported Epilepsy in a Multiracial and Multiethnic Community in New York City." *Epilepsy Research* 77 (2–3). Elsevier B.V.:141–50. https://doi.org/10.1016/j.eplepsyres.2007.09.012.

Kerber, Karolin, Matthias Dumpelmann, Bjorn Schelter, Pierre Le Van, Rudolf Korinthenberg, Andreas Schulze-Bonhage, and Julia Jacobs. 2014. "Differentiation of Specific Ripple Patterns Helps to Identify Epileptogenic Areas for Surgical Procedures." *Clinical Neurophysiology* 125 (7). International Federation of Clinical

Neurophysiology:1339–45. https://doi.org/10.1016/j.clinph.2013.11.030.

Khosravani, Houman, Nikhil Mehrotra, Michael Rigby, Walter J. Hader, C. Robert Pinnegar, Neelan Pillay, Samuel Wiebe, and Paolo Federico. 2009. "Spatial Localization and Time-Dependant Changes of Electrographic High Frequency Oscillations in Human Temporal Lobe Epilepsy." *Epilepsia* 50 (4):605–16. https://doi.org/10.1111/j.1528-1167.2008.01761.x.

Kim, Dong Wook, Sunghun Kim, Sung-Hye Park, Chun-Kee Chung, and Sang Kun Lee. 2012. "Comparison of MRI Features and Surgical Outcome among the Subtypes of Focal Cortical Dysplasia." *Seizure* 21 (10). BEA Trading Ltd:789–94. https://doi.org/10.1016/j.seizure.2012.09.006.

Klausberger, Thomas, Peter J Magill, Philip M Cobden, and Peter Somogyi. 2003. "Firing of Hippocampal Interneurons in Vivo." *Nature* 421 (February):844–48. https://doi.org/10.1038/nature01374.

Kohtaroh Edakawa, Takufumi Yanagisawa, Haruhiko Kishima, Ryohei Fukuma, Masataka Tanaka& Satoru Oshino, Hui Ming Khoo, Maki Kobayashi, and Toshiki Yoshimine. 2016. "Detection of Epileptic Seizures Using Phase–Amplitude Coupling in Intracranial Electroencephalography." *Nature Reviews. Neuroscience*.

Krendl, R., S. Lurger, and C. Baumgartner. 2008. "Absolute Spike Frequency Predicts Surgical Outcome in TLE with Unilateral Hippocampal Atrophy." *Neurology* 71 (6):413–18. https://doi.org/10.1212/01.wnl.0000310775.87331.90.

Kucewicz, Michal T., Jan Cimbalnik, Joseph Y. Matsumoto, Benjamin H. Brinkmann, Mark R. Bower, Vincent Vasoli, Vlastimil Sulc, et al. 2014. "High Frequency Oscillations Are Associated with Cognitive Processing in Human Recognition Memory." *Brain* 137 (8):2231–44. https://doi.org/10.1093/brain/awu149.

Kucewicz, Michal T, B Michael Berry, Mark R Bower, Jan Cimbalnik, Vojtech Svehlik, S Matt Stead, and Gregory A Worrell. 2015. "Combined Single Neuron Unit Activity and

Local Field Potential Oscillations in a Human Visual Recognition Memory Task" 0 (0):67–75. https://doi.org/10.1109/TBME.2015.2451596.

Lachaux, J P, E Rodriguez, J Martinerie, and F J Varela. 1999. "Measuring Phase Synchrony in Brain Signals." *Human Brain Mapping* 8 (4):194–208. http://www.ncbi.nlm.nih.gov/pubmed/10619414.

Leppik, Ilo. 2010. "Epilepsy in the Elderly." *Annals of Teh New York Academy of Science* 1184 (4):208–24. https://doi.org/10.3238/arztebl.2009.0135.

Levesque, M., P. Salami, J. Gotman, and M. Avoli. 2012. "Two Seizure-Onset Types Reveal Specific Patterns of High-Frequency Oscillations in a Model of Temporal Lobe Epilepsy." *Journal of Neuroscience* 32 (38):13264–72. https://doi.org/10.1523/JNEUROSCI.5086-11.2012.

LEvesque, Maxime, Herrington Rochelle, Shabnam Hamidi, and Massimo Avoli*. 2016. "Interneurons Spark Seizure-like Activity in the Entorhinal Cortex." *Neurobiology of Disease* 87 (2):91–101. https://doi.org/10.1167/iovs.07-1072.Complement-Associated.

Librizzi, Laura, Gabriele Losi, Iacopo Marcon, Michele Sessolo, Paolo Scalmani, Giorgio Carmignoto, and Marco de Curtis. 2017. "Interneuronal Network Activity at the Onset of Seizure-like Events in Entorhinal Cortex Slices." *The Journal of Neuroscience*, 3906–16. https://doi.org/10.1523/JNEUROSCI.3906-16.2017.

Loo, Pieter, Van, Evelien Carrette, Alfred Meurs, Dirk GOOSSENS, LUTGARD , Van Roost, and Kristl Vonck. 2011. "Surgical Successes and Failures of Invasive Video-EEG Monitoring in the Presurgical Evaluation of Epilepsy." *PANMINERVA MEDICA* 53 (4):227–40.

Lopantsev, V, and M Avoli. 1998. "Participation of GABAA-Mediated Inhibition in Ictallike Discharges in the Rat Entorhinal Cortex." *J Neurophysiol* 79 (1):352–60. http://www.ncbi.nlm.nih.gov/pubmed/9425204%5Cnhttp://jn.physiology.org/content/jn/79/1/352.full.pdf.

Lüders, Hans O., Imad Najm, Dileep Nair, Peter Widdess-Walsh, and William Bingman. 2006. “The Epileptogenic Zone: General Principles.” *Epileptic Disorders* 8 (SUPPL. 2):1–9.

Malinowska, Urszula, Gregory K. Bergey, Jaroslaw Harezlak, and Christophe C. Jouny. 2015. “Identification of Seizure Onset Zone and Preictal State Based on Characteristics of High Frequency Oscillations.” *Clinical Neurophysiology* 126 (8). International Federation of Clinical Neurophysiology:1505–13. https://doi.org/10.1016/j.clinph.2014.11.007.

Mansouri, Alireza, Abdulrahman Aldakkan, Magda J. Kosicka, Jean-Eric Tarride, and Taufik A. Valiante. 2015. “Bridging the Gap between Evidence and Practice for Adults with Medically Refractory Temporal Lobe Epilepsy: Is a Change in Funding Policy Needed to Stimulate a Shift in Practice?” *Epilepsy Research and Treatment* 2015:1–10. https://doi.org/10.1155/2015/675071.

Maris, Eric, Marieke van Vugt, and Michael Kahana. 2011. “Spatially Distributed Patterns of Oscillatory Coupling between High-Frequency Amplitudes and Low-Frequency Phases in Human iEEG.” *NeuroImage* 54 (2). Elsevier Inc.:836–50. https://doi.org/10.1016/j.neuroimage.2010.09.029.

Marks, William J. 2002. “Temporal Lobe Epilepsy in Patients Older Than 50 Years.” *Epilepsy Currents* 2 (3):74. https://doi.org/10.1046/j.1535-7597.2002.t01-1-00027.x.

Matsumoto, Andrew, Benjamin H Brinkmann, S Matthew Stead, Joseph Y Matsumoto, Michal T Kucewicz, W Richard Marsh, Frederic Meyer, and Gregory Worrell. 2013. “Pathological and Physiological High-Frequency Oscillations in Focal Human Epilepsy.” *Journal of Neurophysiology* 110 (8):1958–64. https://doi.org/10.1152/jn.00341.2013.

McKhann, G M, J Schoenfeld-McNeill, D E Born, M M Haglund, and G A Ojemann. 2000. “Intraoperative Hippocampal Electrocorticography to Predict the Extent of Hippocampal

Resection in Temporal Lobe Epilepsy Surgery." *Journal of Neurosurgery* 93 (1):44–52. https://doi.org/10.3171/jns.2000.93.1.0044.

Melani, Federico, Rina Zelmann, Francesco Mari, and Jean Gotman. 2013. "Continuous High Frequency Activity: A Peculiar SEEG Pattern Related to Specific Brain Regions." *Clinical Neurophysiology* 124 (8). International Federation of Clinical Neurophysiology:1507–16. https://doi.org/10.1016/j.clinph.2012.11.016.

Memarian, Negar, Sarah K. Madsen, Paul M. Macey, Itzhak Fried, Jerome Engel, Paul M. Thompson, and Richard J. Staba. 2015. "Ictal Depth EEG and MRI Structural Evidence for Two Different Epileptogenic Networks in Mesial Temporal Lobe Epilepsy." *PLoS ONE* 10 (4):1–16. https://doi.org/10.1371/journal.pone.0123588.

Menendez de la Prida, Liset, Richard J. Staba, and Joshua A. Dian. 2015. "Conundrums of High-Frequency Oscillations (80-800 Hz) in the Epileptic Brain" 32 (3):207–19. https://doi.org/10.1016/bs.mcb.2015.01.016.Observing.

Menendez de la Prida, Liset, and Andrew J. Trevelyan. 2011. "Cellular Mechanisms of High Frequency Oscillations in Epilepsy: On the Diverse Sources of Pathological Activities." *Epilepsy Research* 97 (3). Elsevier B.V.:308–17. https://doi.org/10.1016/j.eplepsyres.2011.02.009.

Merricks, Edward M., Elliot H. Smith, Guy M. McKhann, Robert R. Goodman, Lisa M. Bateman, Ronald G. Emerson, Catherine A. Schevon, and Andrew J. Trevelyan. 2015. "Single Unit Action Potentials in Humans and the Effect of Seizure Activity." *Brain* 138 (10):2891–2906. https://doi.org/10.1093/brain/awv208.

Mirowski, Piotr, Deepak Madhavan, Yann LeCun, and Ruben Kuzniecky. 2009. "Classification of Patterns of EEG Synchronization for Seizure Prediction." *Clinical Neurophysiology* 120 (11):1927–40. https://doi.org/10.1016/j.clinph.2009.09.002.

Mormann, Florian, Juergen Fell, Nikolai Axmacher, Bernd Weber, Klaus Lehnertz, Christian E. Elger, and Guillén Fernández. 2005. "Phase/amplitude Reset and Theta-Gamma

Interaction in the Human Medial Temporal Lobe during a Continuous Word Recognition Memory Task." *Hippocampus* 15 (7):890–900. https://doi.org/10.1002/hipo.20117.

Nadasdy, Zoltan, T. Peter Nguyen, Ágoston Török, Jason Y. Shen, Deborah E. Briggs, Pradeep N. Modur, and Robert J. Buchanan. 2017. "Context-Dependent Spatially Periodic Activity in the Human Entorhinal Cortex." *Proceedings of the National Academy of Sciences* 114 (17):E3516–25. https://doi.org/10.1073/pnas.1701352114.

Niedermeyer, Ernst, and FH Lopes da Silva. 2005. *Electroencephalography: Basic Principles, Clinical Applications, and Related Fields*. 5th ed.

Noe, Katherine, Vlastimil Sulc, Lily Wong-Kisiel, Elaine Wirrell FRCPC, Jamie J. Van Gompel, Nicholas Wetjen, Britton Jeffrey, et al. 2014. "Long-Term Outcomes After Nonlesional Extratemporal Lobe Epilepsy Surgery" 70 (8):1–20. https://doi.org/10.1158/2326-6066.CIR-13-0034.PD-L1.

Novak, Jennifer L., Patrick R. Miller, Daniela Markovic, Sheba K. Meymandi, and Christopher M. DeGiorgio. 2015. "Risk Assessment for Sudden Death in Epilepsy: The SUDEP-7 Inventory." *Frontiers in Neurology* 6 (DEC):1–5. https://doi.org/10.3389/fneur.2015.00252.

Nunez, Paul L, and Ramesh . 2006. Srinivasan. 2006. *Electric Fields of the Brain: The Neurophysics of EEG.* Oxford University Press,USA.

Ochi, Ayako, Hiroshi Otsubo, Elizabeth J. Donner, Irene Elliott, Ryoichi Iwata, Takanori Funaki, Yoko Akizuki, et al. 2007. "Dynamic Changes of Ictal High-Frequency Oscillations in Neocortical Epilepsy: Using Multiple Band Frequency Analysis." *Epilepsia* 48 (2):286–96. https://doi.org/10.1111/j.1528-1167.2007.00923.x.

Ogren, Jennifer A., Anatol Bragin, Charles L. Wilson, Gil D. Hoftman, Jack J. Lin, Rebecca A. Dutton, Tony A. Fields, et al. 2009. "Three-Dimensional Hippocampal Atrophy Maps Distinguish Two Common Temporal Lobe Seizure-Onset Patterns." *Epilepsia* 50

(6):1361–70. https://doi.org/10.1111/j.1528-1167.2008.01881.x.

Ogren, Jennifer A., Charles L. Wilson, Anatol Bragin, Jack J. Lin, Noriko Salamon, Rebecca A. Dutton, Eileen Luders, et al. 2009. "Three-Dimensional Surface Maps Link Local Atrophy and Fast Ripples in Human Epileptic Hippocampus." *Annals of Neurology* 66 (6):783–91. https://doi.org/10.1002/ana.21703.

Okanishi, Tohru, Tomoyuki Akiyama, Shin Ichi Tanaka, Ellen Mayo, Ayu Mitsutake, Cyrus Boelman, Cristina Go, et al. 2014. "Interictal High Frequency Oscillations Correlating with Seizure Outcome in Patients with Widespread Epileptic Networks in Tuberous Sclerosis Complex." *Epilepsia* 55 (10):1602–10. https://doi.org/10.1111/epi.12761.

Önal, Çagatay, Hiroshi Otsubo, Takashi Araki, Shiro Chitoku, Ayako Ochi, Shelly Weiss, William Logan, Irene Elliott, O. Carter Snead, and James T. Rutka. 2003. "Complications of Invasive Subdural Grid Monitoring in Children with Epilepsy." *Journal of Neurosurgery* 98 (5):1017–26. https://doi.org/10.3171/jns.2003.98.5.1017.

Osipova, Daria, Dora Hermes, and Ole Jensen. 2008. "Gamma Power Is Phase-Locked to Posterior Alpha Activity." *PLoS ONE* 3 (12):1–7. https://doi.org/10.1371/journal.pone.0003990.

Penfield, W.G., and H.H. Jasper. 1954. "Epilepsy and the Functional Anatomy of the Human Brain."

Penny, W. D., E. Duzel, K. J. Miller, and J. G. Ojemann. 2008. "Testing for Nested Oscillation." *Journal of Neuroscience Methods* 174 (1). Elsevier B.V.:50–61. https://doi.org/10.1016/j.jneumeth.2008.06.035.

Perucca, Piero, François Dubeau, and Jean Gotman. 2014. "Intracranial Electroencephalographic Seizure-Onset Patterns: Effect of Underlying Pathology." *Brain* 137 (1):183–96. https://doi.org/10.1093/brain/awt299.

Quiroga, R Quian, Z Nadasdy, and Y Ben-Shaul. 2004. "Unsupervised Spike Detection and Sorting with Wavelets and Superparamagnetic Clustering." *Neural Computation* 16

(8):1661–87. https://doi.org/10.1162/089976604774201631.

Rosenow, Felix, and Hans Luders. 2001. “Presurgical Evaluation of Epilepsy Patients.” *Brain : A Journal of Neurology* 124:1683–1700. https://doi.org/10.4103/1817-1745.40593.

Rutishauser, Ueli, Erin M. Schuman, and Adam N. Mamelak. 2006. “Online Detection and Sorting of Extracellularly Recorded Action Potentials in Human Medial Temporal Lobe Recordings, in Vivo.” *Journal of Neuroscience Methods* 154 (1–2):204–24. https://doi.org/10.1016/j.jneumeth.2005.12.033.

Schevon, Catherine A., A. J. Trevelyan, C. E. Schroeder, R. R. Goodman, G. McKhann, and R. G. Emerson. 2009. “Spatial Characterization of Interictal High Frequency Oscillations in Epileptic Neocortex.” *Brain* 132 (11):3047–59. https://doi.org/10.1093/brain/awp222.

Schevon, Catherine a., Shennan a. Weiss, Guy McKhann, Robert R. Goodman, Rafael Yuste, Ronald G. Emerson, and Andrew J. Trevelyan. 2012. “Evidence of an Inhibitory Restraint of Seizure Activity in Humans.” *Nature Communications* 3. Nature Publishing Group:1060. https://doi.org/10.1038/ncomms2056.

Schwartz, T H, C W Bazil, M Forgione, J N Bruce, and R R Goodman. 2000. “Do Reactive Post-Resection ‘injury’ spikes Exist?” *Epilepsia* 41 (11):1463–68. https://doi.org/10.1111/j.1528-1157.2000.tb00123.x.

Schwartz, T H, and T Bonhoeffer. 2001. “In Vivo Optical Mapping of Epileptic Foci and Surround Inhibition in Ferret Cerebral Cortex.” *Nat Med* 7 (9):1063–67. https://doi.org/10.1038/nm0901-1063.

Shiri, Zahra, Frederic Manseau, Maxime Levesque, Sylvain Williams, and Massimo Avoli. 2016. “Activation of Specific Neuronal Networks Leads to Different Seizure Onset Types.” *Annals of Neurology* 79 (3):354–65. https://doi.org/10.1002/ana.24570.

Singer, Wolf. 1999. “Neuronal Synchrony : A Versatile Code for the Definition of Relations ?

Most of Our Knowledge about the Functional Organization" 24:49–65.

Smith, M. L., and K. Puka. 2016. "Epilepsy and Cognition." *Epilepsy and Intellectual Disabilities* 7 (1):281–301. https://doi.org/10.1007/978-3-319-39144-1_13.

Spanedda, F., F. Cendes, and J. Gotman. 1997. "Relations between EEG Seizure Morphology, Interhemispheric Spread, and Mesial Temporal Atrophy in Bitemporal Epilepsy." *Epilepsia* 38 (12):1300–1314. https://doi.org/10.1111/j.1528-1157.1997.tb00068.x.

Spencer, Susan S. 2002. "When Should Temporal-Lobe Epilepsy Be Treated Surgically?" *Lancet Neurology* 1 (6):375–82. https://doi.org/10.1016/S1474-4422(02)00163-1.

Spencer, Susan S, Jung Kim, and Dennis D Spencer. 1992. "Ictal Spikes: A Marker of Specific Hippocampal Cell Loss." *Electroencephalography and Clinical Neurophysiology* 83:104–11.

Spencer, Susan S, Peter D Williamson, Samuel L Bridgers, Richard H Mattson, Domenic V Cicchetti, and Dennis D Spencer. 1985. "Reliability and Accuracy of Localization by Scalp Ictal EEG." *Neurology* 35 (November):1567–75.

Sperling Michael R. 2015. "Mortality after Epilepsy Surgery." *Long-Term Outcomes of Epilepsy Surgery in Adults and Children* 46:125–33. https://doi.org/10.1007/978-3-319-17783-0_9.

Srikijvilaikul, Teeradej, Sukulya Lerdlum, Supatporn Tepmongkol, Shanop Shuangshoti, and Chaichon Locharernkul. 2011. "Outcome of Temporal Lobectomy for Hippocampal Sclerosis in Older Patients." *Seizure* 20 (4). BEA Trading Ltd:276–79. https://doi.org/10.1016/j.seizure.2010.12.008.

Staba, Richard J. 2010. "Normal and Pathologic High-Frequency Oscillations." *Jasper's Basic Mechanisms of the Epilepsies [Internet]*, no. Md:1–17. https://www.ncbi.nlm.nih.gov/books/NBK98191/.

Staba, Richard J. 2012. "Normal and Pathologic High-Frequency Oscillations" 1 (Figure

1):1–28. www.pubmed.com.

Staba, Richard J., Charles L. Wilson, Anatol Bragin, Donald Jhung, Itzhak Fried, and Jerome Engel. 2004. "High-Frequency Oscillations Recorded in Human Medial Temporal Lobe during Sleep." *Annals of Neurology* 56 (1):108–15. https://doi.org/10.1002/ana.20164.

Staba, Richard J, Charles L Wilson, Anatol Bragin, Itzhak Fried, and Jerome Engel. 2002. "Quantitative Analysis of High-Frequency Oscillations (80-500 Hz) Recorded in Human Epileptic Hippocampus and Entorhinal Cortex." *Journal of Neurophysiology* 88 (4):1743–52. https://doi.org/10.1152/jn.00322.2002.

Takahashi, S., Yuichiro Anzai, and Yoshio Sakurai. 2003. "Automatic Sorting for Multi-Neuronal Activity Recorded With Tetrodes in the Presence of Overlapping Spikes." *Journal of Neurophysiology* 89 (4):2245–58. https://doi.org/10.1152/jn.00827.2002.

Takahashi, Susumu, Yuichiro Anzai, and Yoshio Sakurai. 2003. "A New Approach to Spike Sorting for Multi-Neuronal Activities Recorded with a Tetrode - How ICA Can Be Practical." *Neuroscience Research* 46 (3):265–72. https://doi.org/10.1016/S0168-0102(03)00103-2.

Tasker, Jeffrey G., and F. Edward Dudek. 1991. "Electrophysiology of GABA-Mediated Synaptic Transmission and Possible Roles in Epilepsy." *Neurochemical Research* 16 (3):251–62. https://doi.org/10.1007/BF00966088.

Toyoda, I., S. Fujita, A. K. Thamattoor, and P. S. Buckmaster. 2015. "Unit Activity of Hippocampal Interneurons before Spontaneous Seizures in an Animal Model of Temporal Lobe Epilepsy." *Journal of Neuroscience* 35 (16):6600–6618. https://doi.org/10.1523/JNEUROSCI.4786-14.2015.

Trevelyan, A. J. 2009. "The Direct Relationship between Inhibitory Currents and Local Field Potentials." *Journal of Neuroscience* 29 (48):15299–307. https://doi.org/10.1523/JNEUROSCI.2019-09.2009.

Trevelyan, A. J., D. Sussillo, B. O. Watson, and R. Yuste. 2006. "Modular Propagation of

Epileptiform Activity: Evidence for an Inhibitory Veto in Neocortex." *Journal of Neuroscience* 26 (48):12447–55. https://doi.org/10.1523/JNEUROSCI.2787-06.2006.

Trevelyan, A. J., D. Sussillo, and R. Yuste. 2007. "Feedforward Inhibition Contributes to the Control of Epileptiform Propagation Speed." *Journal of Neuroscience* 27 (13):3383–87. https://doi.org/10.1523/JNEUROSCI.0145-07.2007.

Trombin, F., V. Gnatkovsky, and M. de Curtis. 2011. "Changes in Action Potential Features during Focal Seizure Discharges in the Entorhinal Cortex of the in Vitro Isolated Guinea Pig Brain." *Journal of Neurophysiology* 106 (3):1411–23. https://doi.org/10.1152/jn.00207.2011.

Truccolo, Wilson, Jacob A Donoghue, Leigh R Hochberg, Emad N Eskandar, Joseph R Madsen, William S Anderson, Emery N Brown, Eric Halgren, and Sydney S Cash. 2011. "Single-Neuron Dynamics in Human Focal Epilepsy." *Nature Neuroscience* 14 (5). Nature Publishing Group:635–41. https://doi.org/10.1038/nn.2782.

Urrestarazu, Elena, Rahul Chander, François Dubeau, and Jean Gotman. 2007. "Interictal High-Frequency Oscillations (10-500 Hz) in the Intracerebral EEG of Epileptic Patients." *Brain* 130 (9):2354–66. https://doi.org/10.1093/brain/awm149.

Uva, L., G. L. Breschi, V. Gnatkovsky, S. Taverna, and M. de Curtis. 2015. "Synchronous Inhibitory Potentials Precede Seizure-Like Events in Acute Models of Focal Limbic Seizures." *Journal of Neuroscience* 35 (7):3048–55. https://doi.org/10.1523/JNEUROSCI.3692-14.2015.

Van Quyen, Michel Le, and Anatol Bragin. 2007. "Analysis of Dynamic Brain Oscillations: Methodological Advances." *Trends in Neurosciences* 30 (7):365–73. https://doi.org/10.1016/j.tins.2007.05.006.

Vanhatalo, S, J M Palva, M D Holmes, J W Miller, J Voipio, and K Kaila. 2004. "Infraslow Oscillations Modulate Excitability and Interictal Epileptic Activity in the Human Cortex during Sleep." *Proceedings of the National Academy of Sciences of the USA* 101

(14):5053–57. https://doi.org/10.1073/pnas.0305375101.

Varatharajah, Yogatheesan, Ravishankar K. Iyer, Brent M. Berry, Gregory A. Worrell, and Benjamin H. Brinkmann. 2017. "Seizure Forecasting and the Preictal State in Canine Epilepsy." *International Journal of Neural Systems* 27 (1):1650046. https://doi.org/10.1142/S0129065716500465.

Velasco, a L, C L Wilson, T L Babb, and J Engel. 2000. "Functional and Anatomic Correlates of Two Frequently Observed Temporal Lobe Seizure-Onset Patterns." *Neural Plasticity* 7:49–63. https://doi.org/10.1155/NP.2000.49.

Voorhies, Jason M., and Aaron Cohen-Gadol. 2013. "Techniques for Placement of Grid and Strip Electrodes for Intracranial Epilepsy Surgery Monitoring: Pearls and Pitfalls." *Surgical Neurology International* 98.

Waziri, A, Catherine A Schevon, J Cappell, Ronald G. Emerson, Guy M. McKhann, and Robert R. Goodman. 2009. "Initial Surgical Experience with a Dense Cortical Microarray in Epileptic Patients Undergoing Craniotomy for Subdural Electrode Implantation" 64 (3):540–45. https://doi.org/10.1086/498510.Parasitic.

Weiss, Shennan A, Garrett P Banks, Guy M McKhann, Robert R Goodman, Ronald G Emerson, Andrew J Trevelyan, and Catherine A Schevon. 2013. "Ictal High Frequency Oscillations Distinguish Two Types of Seizure Territories in Humans." *Brain : A Journal of Neurology* 136 (Pt 12):3796–3808. https://doi.org/10.1093/brain/awt276.

Weiss, Shennan A, Iren Orosz, Noriko Salamon, Stephanie Moy, Linqing Wei, Maryse A Van't Klooster, Robert T Knight, et al. 2016. "Ripples on Spikes Show Increased Phase-Amplitude Coupling in Mesial Temporal Lobe Epilepsy Seizure-Onset Zones." *Epilepsia*, 1–15. https://doi.org/10.1111/epi.13572.

Weiss, Shennan Aibel, Catalina Alvarado-Rojas, Anatol Bragin, Eric Behnke, Tony Fields, Itzhak Fried, Jerome Engel, and Richard Staba. 2016. "Ictal Onset Patterns of Local Field Potentials, High Frequency Oscillations, and Unit Activity in Human Mesial

Temporal Lobe Epilepsy." *Epilepsia* 57 (1):111–21. https://doi.org/10.1111/epi.13251.

Weiss Shennan, Athena Lemesiou, Robert Connors, Garrett P Banks, Guy M Mckhann, Robert R Goodman, Binsheng Zhao, et al. 2015. "Seizure Localization Using Ictal Phase-Locked High Gamma A Retrospective Surgical Outcome Study." *Neurology* 84(23):2320–28.

Werz, Mary Ann, and Ignacio Pita. 2010. *Epilepsy Syndromes*. 1st ed. Philadelphia: Elsevier.

Widdess-Walsh, P., L. Jeha, D. Nair, P. Kotagal, W. Bingaman, and I. Najm. 2007. "Subdural Electrode Analysis in Focal Cortical Dysplasia: Predictors of Surgical Outcome." *Neurology* 69 (7):660–67. https://doi.org/10.1212/01.wnl.0000267427.91987.21.

Wiebe, Samuel, and Warren B. 2001. "A Randomized , Controlled Trial of Surgery" 345 (5):311–18.

Wild, Jiri, Zoltan Prekopcsak, Tomas Sieger, Daniel Novak, and Robert Jech. 2012. "Performance Comparison of Extracellular Spike Sorting Algorithms for Single-Channel Recordings." *Journal of Neuroscience Methods* 203 (2). Elsevier B.V.:369–76. https://doi.org/10.1016/j.jneumeth.2011.10.013.

Worrell, G. a., K. Jerbi, K. Kobayashi, J. M. Lina, R. Zelmann, and M. Le Van Quyen. 2012. "Recording and Analysis Techniques for High-Frequency Oscillations." *Progress in Neurobiology* 98 (3). Elsevier Ltd:265–78. https://doi.org/10.1016/j.pneurobio.2012.02.006.

Worrell, Greg A., Landi Parish, Stephen D. Cranstoun, Rachel Jonas, Gordon Baltuch, and Brian Litt. 2004. "High-Frequency Oscillations and Seizure Generation in Neocortical Epilepsy." *Brain* 127 (7):1496–1506. https://doi.org/10.1093/brain/awh149.

Worrell, Greg A, Andrew B Gardner, S Matt Stead, Sanqing Hu, Steve Goerss, Gregory J Cascino, Fredric B Meyer, Richard Marsh, and Brian Litt. 2008. "High-Frequency Oscillations in Human Temporal Lobe: Simultaneous Microwire and Clinical Macroelectrode Recordings Greg" 131 (Pt 4):928–37.

https://doi.org/10.1093/brain/awn006.High-frequency.

Worrell, Gregory a, and J Gotman. 2011. “High-Frequency Oscillations and Other Electrophysiological Biomarkers of Epilepsy: Clinical Studies.” *Biomark Med.* 5 (5):557–66. https://doi.org/10.2217/bmm.11.74.High-frequency.

Ylinen, A, A Bragin, Z Nádasdy, G Jandó, I Szabó, A Sik, and G Buzsáki. 1995. “Sharp Wave-Associated High-Frequency Oscillation (200 Hz) in the Intact Hippocampus: Network and Intracellular Mechanisms.” *The Journal of Neuroscience : The Official Journal of the Society for Neuroscience* 15 (1 Pt 1):30–46. http://www.ncbi.nlm.nih.gov/pubmed/7823136.

Yun, Chang Ho, Sang Kun Lee, Seo Young Lee, Kwang Ki Kim, Sang Wook Jeong, and Chun Ki Chung. 2006. “Prognostic Factors in Neocortical Epilepsy Surgery: Multivariate Analysis.” *Epilepsia* 47 (3):574–79. https://doi.org/10.1111/j.1528-1167.2006.00470.x.

Zelmann, R., F. Mari, J. Jacobs, M. Zijlmans, R. Chander, and J. Gotman. 2010. “Automatic Detector of High Frequency Oscillations for Human Recordings with Macroelectrodes.” *2010 Annual International Conference of the IEEE Engineering in Medicine and Biology Society, EMBC’10*, 2329–33. https://doi.org/10.1109/IEMBS.2010.5627464.

Zelmann, Rina, Maeike Zijlmans, Julia Jacobs, Claude E. Châtillon, and Jean Gotman. 2009. “Improving the Identification of High Frequency Oscillations.” *Clinical Neurophysiology* 120 (8). International Federation of Clinical Neurophysiology:1457–64. https://doi.org/10.1016/j.clinph.2009.05.029.

Žiburkus1, Jokūbas, John R. Cressman1, Ernest Barreto, and Steven J. Schiff. 2006. “Interneuron and Pyramidal Cell Interplay during in Vitro Seizure- like Events.” *Neurophysiology* 98 (4):3948–54. https://doi.org/10.1002/ana.22528.Toll-like.